Deltares

DCSM-FM 0.5nm: a sixth-generation model for the NW European Shelf

2022 release

DCSM-FM 0.5nm: a sixth-generation model for the NW European Shelf
2022 release

Auteur(s)
Firmijn Zijl
Tammo Zijlker
Stendert Laan
Julien Groenenboom

DCSM-FM 0.5nm: a sixth-generation model for the NW European Shelf
2022 release

Opdrachtgever	Rijkswaterstaat Water, Verkeer en Leefomgeving
Contactpersoon	de heer M. Scholten
Referenties	
Trefwoorden	D-HYDRO, D-Flow Flexible Mesh, North Sea, NW European Continental Shelf, DCSM-FM, hydrodynamic model

Documentgegevens	
Versie	1.0
Datum	19-12-2022
Projectnummer	11208054-000
Document ID	11208054-000-ZKS-0010
Pagina's	105
Classificatie	
Status	definitief

Auteur(s)		
	Firmijn Zijl	
	Tammo Zijlker	
	Stendert Laan	
	Julien Groenenboom	

Onderstaande tabel is niet voor publicatie

Doc. Versie	Auteur	Controle	Akkoord
1.0	Firmijn Zijl	Tony Minns	Toon Segeren
	Tammo Zijlker		
	Stendert Laan		
	Julien Groenenboom		

Summary

Upon request of Rijkswaterstaat (RWS), Deltares has developed a sixth-generation hydrodynamic model of the Northwest European Shelf: the Dutch Continental Shelf Model – Flexible Mesh (DCSM-FM). This model is the latest in a line of DCSM models developed by RWS and Deltares and a successor to the fifth-generation WAQUA model DCSMv6. Specifically, this model covers the North Sea and adjacent shallow seas and estuaries in the Netherlands, such as the Wadden Sea, the Ems-Dollard estuary, the Western Scheldt and the Eastern Scheldt.

The development of the present model is part of a more comprehensive project in which sixth-generation models have been developed for all waters managed and maintained by RWS. An important difference with the previous fifth-generation models is the use of the D-HYDRO Suite, the new software framework for modelling free surface flows, which was first released in 2015 and allows for the use of unstructured grids.

Since the proposed applications on the North Sea pose a wide range of sometimes mutually exclusive demands on a model, two horizontal schematizations were proposed: a relatively coarse two-dimensional model (DCSM-FM 0.5nm) and a relatively fine schematization (DCSM-FM 100m) with further refinement in most Dutch coastal waters. DCSM-FM 0.5nm is primarily aimed at ensemble forecasting, but also forms a sound basis for a subsequent 3D model development, including temperature and salinity as state parameters. DCSM-FM 100m is primarily aimed at deterministic water level forecasting at HMC and WMCN-kust.

The present report describes the model setup, calibration and validation of the relatively coarse, two-dimensional model DCSM-FM 0.5nm. A first version of this model was released in 2019. In 2022, this model was updated with respect to model bathymetry, tidal boundary forcing and meteorological forcing and numerous other adjustments and improvements. These changes, including a recalibration and revalidation are reflected in this current report.

Contents

1 Introduction

1.1 Background

Upon request of Rijkswaterstaat (RWS), Deltares has developed a sixth-generation hydrodynamic model of the Northwest European Shelf. Specifically, this model should cover the North Sea and adjacent shallow seas and estuaries in the Netherlands, such as the Wadden Sea, the Ems-Dollard estuary, the Western Scheldt and the Eastern Scheldt.

The development of this model is part of a more comprehensive project in which sixth-generation models have been developed for all waters maintained by RWS. An important difference with the previous fifth-generation models is the use of the D-HYDRO Suite (known internationally as the Delft3D Flexible Mesh Suite), the new software framework for modelling free surface flows, which was first released in 2015 and allows for the use of unstructured grids.

While the previous generation model (DCSMv6 and DCSMv6-ZUNOv4, see Zijl et al. (2013)) for the same area were specifically aimed at an optimal representation of water levels for operational forecasting under daily and storm surge conditions, for the sixth-generation model(s) the scope is wider. The model should, for example, also be suitable to use for water quality and ecology studies, oil spill modelling, search and rescue and to provide three-dimensional (3D) boundary conditions (including temperature and salinity) for detailed models of the Western Scheldt, Haringvliet, Rhine-Meuse Delta (RMM) and Wadden Sea.

The above applications pose a wide range of sometimes mutually exclusive demands on a model. This is because both the relative importance of representing certain phenomena as well as the allowed computational time varies per application. Since the demands are impossible to meet with one model, three model schematizations (consisting of two horizontal schematizations) were proposed:

1. DCSM-FM 0.5nm: a relatively coarse schematization (minimum grid size of 800-900 m in Dutch waters), which a computational time that is feasible for water level probability forecasts with a 2 to 10-day lead-time. These forecasts are based on meteorology of the ECMWF Ensemble Prediction System (EPS) with 51 members.
2. 3D DCSM-FM: a three-dimensional model that uses the same horizontal schematization as the above DCSM-FM 0.5nm and additionally includes temperature and salinity as state variables.
3. DCSM-FM 100m: a relatively fine schematization with a minimum resolution of around 100 m in most Dutch waters (including the entire Wadden Sea and all Dutch coastlines) to be used for accurate (operational) water level forecasting. This model will be a based on the schematization in item 1, but with refinement in the southern North Sea.

1.2 The present report

The present report describes a new release of the relatively coarse two-dimensional DCSM-FM 0.5nm model (item 1 above). The first version of this model has been released in 2019 (Zijl & Groenenboom, 2019) and is externally also referred to as dflowfm2d-noordzee_0_5nm-j17_6-v1. In the present report it will be referred to as the *2019 release* of DCSM-FM 0.5nm. The updated version described in this report is the second release of this model and will be referred to as the *2022 release* in this report. For external reference purposes, the name *dflowfm2d-noordzee_0_5nm-j22_6-v1a* is used.

The 2022 release of this model was updated with respect to model bathymetry, tidal boundary forcing and meteorological forcing and numerous other adjustments and improvements. These changes, including a recalibration and revalidation are reflected in this current report. Changes compared to the 2019 release are separately summarized in a grey text box at the end of the relevant paragraphs.

1.3 Guide to this report

The next chapter describes the setup of DCSM-FM 0.5nm (Chapter 2), while in Chapter 3 and Chapter 4 the calibration and the validation are presented, respectively. The report ends with conclusions and recommendations in Chapter 5.

2 Model setup

2.1 Network

2.1.1 Network coverage, horizontal extent

The model network of DCSM-FM 0.5nm covers the northwest European continental shelf, specifically the area between 15° W to 13° E and 43° N to 64° N (Figure 2.1). This means that the open boundary locations are the same as in the fifth-generation model DCSMv6 (Zijl et al., 2013).

During the development of the model, a possible extension of the model domain was considered as this might have a beneficial impact on the surge representation, since a larger part of the surge signal would then be generated inside the model by means of wind stress and atmospheric pressure gradients. Consequently, a smaller part would enter the domain through an approximated surge boundary condition based on air pressure alone. Even though tests computations showed an improvement during the highest storm surge events, this was considered too limited to justify the additional computations cost of an extended domain. The results of these test computations are described in Appendix A of Zijl & Groenenboom (2019).

2.1.2 Grid size

The computational grid of the previous generation WAQUA-DCSMv6 model has rectangular cells with a uniform resolution. One of the advantages of D-HYDRO Flexible Mesh above WAQUA is the enhanced possibility to better match resolution with relevant local spatial scales. In Zijl et al. (2016), a test is reported where, starting from a grid with uniform resolution, the deep areas off the shelf were refined by a factor of up to 4 x 4. The advantage of coarsening in deep areas in particular is twofold: firstly, it reduces the number of cells in areas where local spatial scales allow it and secondly it eases the numerical time step restriction. The combination of both leads to a reduction in computational time with a factor of approximately 4, while – crucially – maintaining accuracy. On the other hand, in shallow areas, resolution plays an important role in accurately representing tide and surge, including its enhanced non-linear interaction (Zijl, 2016a).

Given the above considerations, the DCSM-FM network was designed to have a resolution that increases with decreasing water depth. The starting point was a network with a uniform cell size of 1/10° in east-west direction and 1/15° in north-south direction. This course network was refined in three steps with a factor of 2 by 2. The areas of refinement were specified with smooth polygons that were approximately aligned with the 800 m, 200 m, 50 m and 12.5 m isobaths (i.e. lines with equal depth). Areas with different resolution are connected with triangles. The choice of isobaths ensures that the cell size scales with the square root of the depth, resulting in relatively limited variations of wave Courant number within the model domain.

Apart from applying the refinements based on local bathymetry, another consideration in positioning the refinements was the necessity to have at least a few cells between transitions. Also, it was ensured that all coastlines, except very small islands, were covered by several rows of the highest resolution cells. This implies that in areas with steep coasts the transition to the highest resolution takes place in deeper water. Another exception was made for the southern North Sea, where the area of highest resolution was expanded. This was done to ensure that the highly variable features in the bathymetry can properly be represented on the computational network. Furthermore, it ensures that the areas where steep salinity gradients can be expected are within the area with the highest resolution.

The resulting network is shown in Figure 2.1 and has approximately 630,000 cells with a variable resolution. The largest cells (shown in yellow) have a size of 1/10° in east-west direction and 1/15° in north-south direction, which corresponds to about 4 x 4 nautical miles (nm) or 4.9 - 8.1 km by 7.4 km, depending on the latitude. The smallest cells (shown in red) have a size of 2/3' in east-west direction and 1/2' in north-south direction. This corresponds to about 0.5 nm x 0.5 nm or 840 m x 930 m in the vicinity of the Dutch waters.

The network is specified in geographical coordinates (WGS84).

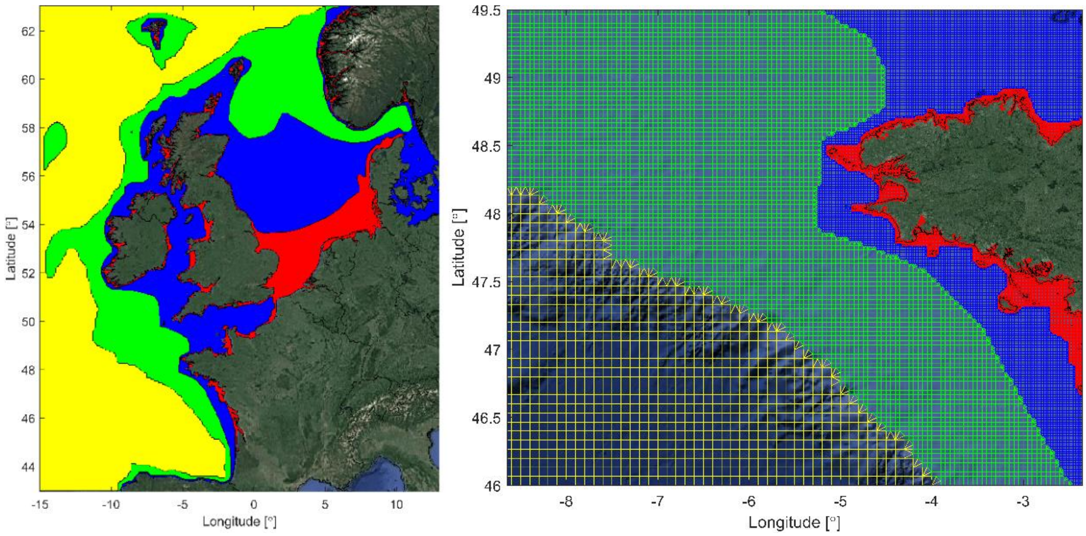

Figure 2.1 Overview (left) and detail (right) of the DCSM-FM model network with the colours indicating the grid size (yellow: ~4 nm; green: ~2 nm; blue: ~1nm; red: ~0.5 nm).

Differences with 2019 release

- Compared to the previous release, the model network has only changed in the Ems river. By coincidence, it was found that removing some cells in this coarsely schematized river improved results with respect to water levels in the already calibrated 2019 release. Therefore, it was decided to discard these cells in the network used in the 2022 release.

2.2 Network optimization

The computational time step used is automatically limited by D-FLOW Flexible Mesh (the hydrodynamic module of the D-HYDRO Suite) based on a Courant criterium. This means that parts of the network with a combination of small flow links and high velocities are most likely to restrict the time-varying computational time step and consequently increase the overall computational time. Figure 2.2 displays an example of the maximum occurring flow velocity during an arbitrary neap-spring cycle (in colour), whereas the black dots indicate the locations of computational cells that are responsible for limiting the time step at least once during this period. From the example in Figure 2.2, it also becomes clear that the time step restricting cells are located in areas with high flow velocities and mostly at the triangles used for the transition in resolution. These triangles have flow links (the connection between two circumcentres or so-called water level points) that are shorter than in the highest resolution rectangles.

To allow for a larger time step and consequently a faster computation, the grid was improved at the locations of the restricting cells. By extending the refinement of the grid more offshore, the transition of the two resolutions is moved outside of the region of high flow velocities. Even though this measure slightly increases the number of computational cells, the net effect is a decrease in overall computational time (see paragraph 2.9.9), because of the increase in the average time step.

After a few repetitions of manually changing the transition of resolution to eliminate restricting cells and therewith improving the computation time, all restricting cells within the transition of resolution were resolved (see right of Figure 2.2). The remaining restricting cells are located in the area of the Pentland Firth (see Figure 2.3). These restricting cells are not on the transition of resolution but are within the area covered by the higher resolution rectangles. This means that removing these restrictions is not possible with the above described method.

Another way to eliminate the restricting cells in this region would be to locally coarsen the grid. However, since an accurate schematization of this narrow area is deemed to be important for a correct representation of tide propagation towards the North Sea, it was decided to retain the highest resolution cells there.

Note that the above described network optimization was performed during the development of the first release of DCSM-FM 0.5nm. Many of the changes made in the 2022 release will affect flow velocities and as a result could in principle have an impact on restricting cells. However, because the impact on the computational time is expected to be limited, the procedure has not been repeated for the 2022 release.

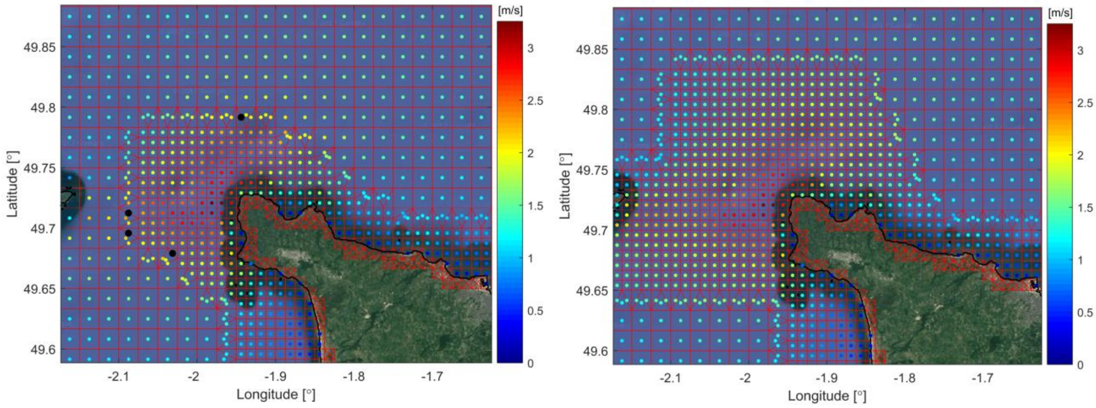

Figure 2.2 Maximum flow velocities in flow element centre during a neap-spring cycle near the Normandy coast. The black line displays the sea-land boundary and the permanently dry cells are indicated by red crosses. The black dots represent computational cells that are limiting the time step (left: before optimization; right: after optimization)

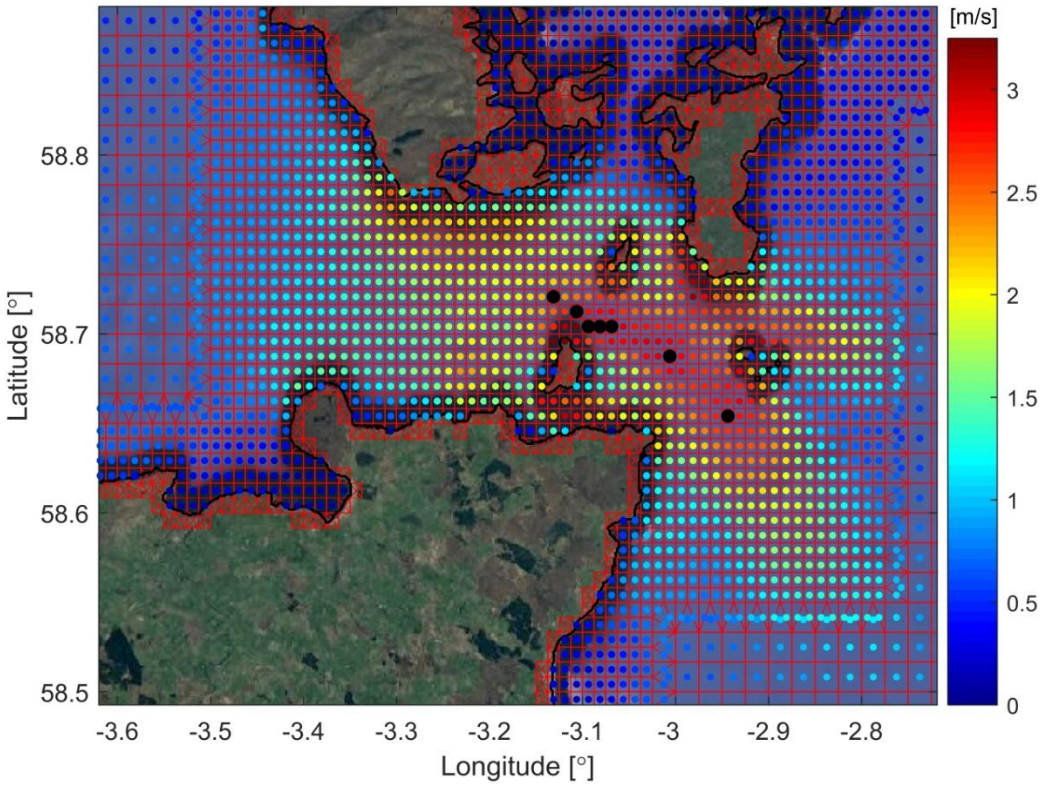

Figure 2.3 Maximum flow velocities in flow element centre during a spring-neap cycle in the Pentland Firth. The black line displays the sea-land boundary and the permanently dry cells are indicated by red crosses. The black dots represent computational cells that are limiting the time step.

2.3 Land-sea boundary, dry points and thin dams

After the local refinement of the network, the cells that covered land were removed from the computational domain. The first step was to interpolate the bathymetric data to the grid and to delete all cells that do not have data in its vicinity. Subsequently, a land-sea boundary obtained from the World Vector Shoreline (https://shoreline.noaa.gov/) was used to distinguish between land and water. All cells that, according to this land-sea boundary, were covered by more than 40% land were made inactive by specifying so-called dry points. The creation of these dry points was done automatically by a MATLAB-script. Figure 2.4 shows an overview of the resulting computational domain in the southwestern part of the Netherlands. The black line indicates the land-sea boundary and the red crosses within the grid illustrate the dry points.

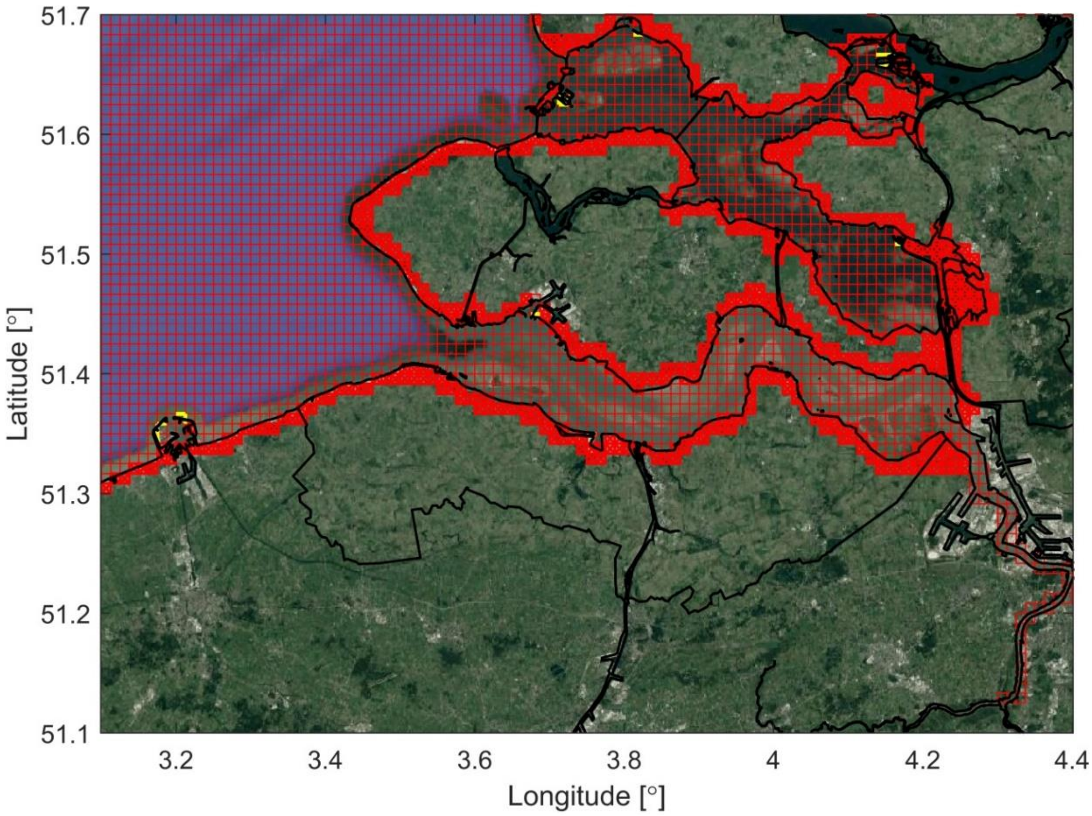

Figure 2.4 Overview of the computational grid (red), land-sea boundary (black), dry points (red crosses) and thin dams (yellow) in the Southwest Delta.

After this automated creation of a first set of dry points, manual work was required to get to the final version of the model geometry. During visual inspection of the shorelines dry cells were added or removed where necessary. In addition, features that are relatively small compared to the area of a cell, are captured in the model schematisation by specifying so-called thin dams. These thin dams prohibit flow exchange through cell edges. The thick, yellow lines in Figure 2.5 illustrate how the entrance to the Humber Estuary (in which tide gauge station Immingham is located) and the breakwaters of the port of Ijmuiden are represented by thin dams.

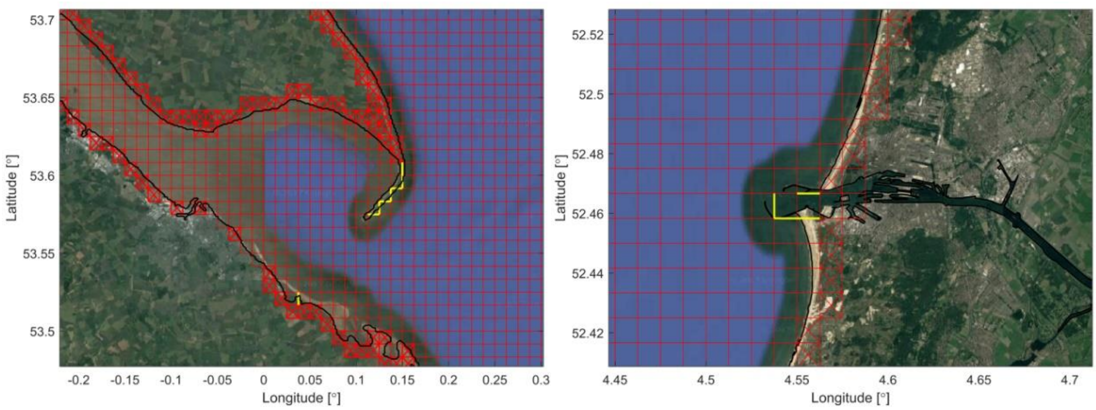

Figure 2.5 Overview of the computational grid (red), land-sea boundary (black), dry points (red crosses) and thin dams (yellow) in the Humber Estuary (left) and around the harbour of Ijmuiden (right).

Another example of manual adjustments is at the Scheldt river (entrance to the port of Antwerp). There, the river was too thin to be retained in the automated dry point creation. At some location in the river a dry point was added since the threshold of 40% land was exceeded and this resulted in blockage of the upstream river. The dry point was removed to allow for a tidal flow up to the upstream part of the model domain. Even larger bodies of water were excluded from the model in a couple of fjords in Norway. Some fjords consist of very small inlets that are connected to relatively large upstream basins. Also, these erroneously created dry points were removed from the model schematisation. The resulting geometry near one of the many fjords in Norway is shown in Figure 2.6.

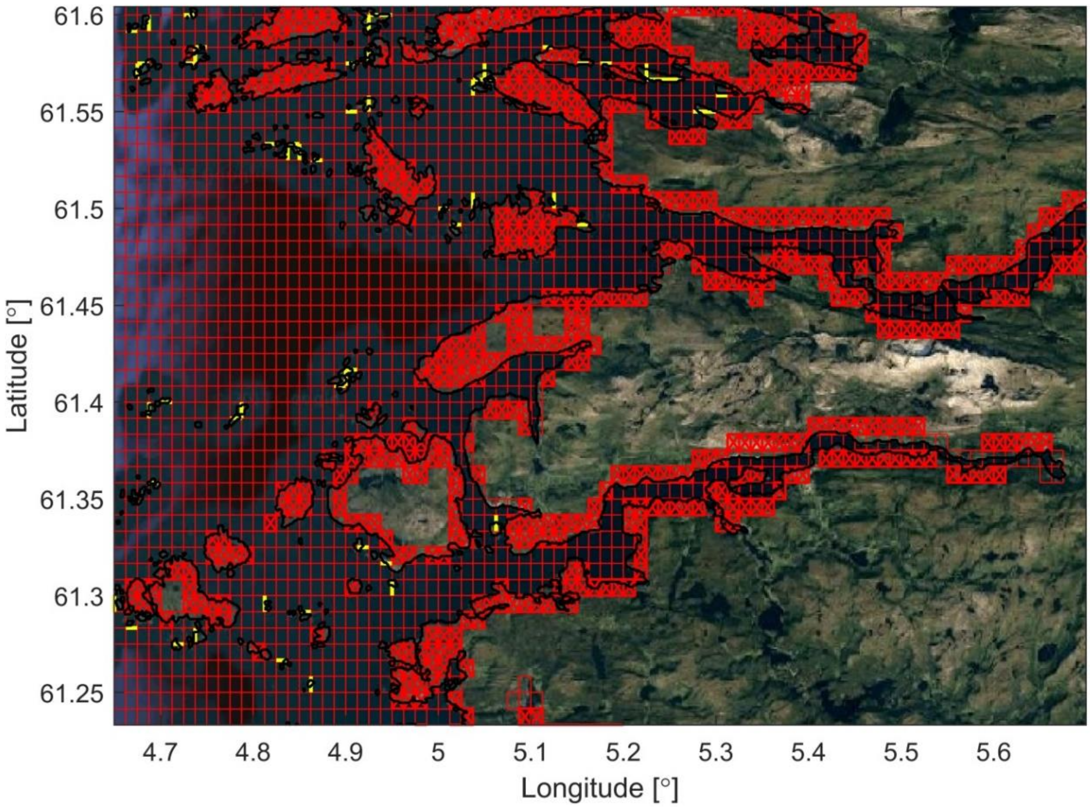

Figure 2.6 Overview of the computational grid (red), land-sea boundary (black), dry points (red crosses) and thin dams (yellow) in Norway.

In order to simulate the correct effect of estuaries on the hydrodynamics, not only did some automatically created dry points need to be removed but also additional grid cells were added to the model domain. Since the removal of grid cells was based on the availability of EMODnet data in the vicinity of the grid cell, some estuaries were not included in the model domain as no bathymetry data was available at these locations. Based on the land-sea boundary and Google Earth, the computational grid at the largest and most important estuaries that were not automatically incorporated in the model domain were manually added.

Differences with 2019 release

- During an investigation on the quality and shape of modelled high waters in tide gauge station Hoek van Holland, it was found that the coarsely schematized harbour basins in Maasvlakte 2 resulted in erroneous amplification of 16-, 18- and 20-times daily frequencies. An experiment where these harbour basins were removed with additional dry points yielded a significant improvement in the quality of both the tide and surge representation in Hoek van Holland, even though the model was not calibrated with these dry points. It was therefore decided to include these additional dry points in the 2022 release of DCSM-FM 0.5nm.

2.4 Bathymetry

The underlying bathymetry information used in this version of DCSM-FM was first collected and merged in the Baseline-NL, which is an ArcGIS database used for hydrodynamic model development at Rijkswaterstaat. Within the Rijkswaterstaat management area, bathymetric data referenced to NAP is available at a spatial resolution of several meters.

EMODnet
For areas outside the Rijkswaterstaat management area, bathymetry has been derived from a gridded bathymetric dataset (December 2020 version) from the European Marine Observation and Data Network (EMODnet; EMODnet Bathymetry Consortium, 2020), a consortium of organisations assembling European marine data, metadata and data products from diverse sources. The data are compounded from selected bathymetric survey data sets (single and multi-beam surveys) and composite DTMs, while gaps with no data coverage are completed by integrating the GEBCO 30'' gridded bathymetry. The resolution of this gridded EMODnet dataset is 1/16' x 1/16' (approx. 75 x 115 m).

The EMODnet data is referred to Mean Sea Level (MSL), while Baseline assumes NAP as a reference level. In addition, MSL is not an equipotential plane, which is inconsistent with the assumptions implicit in D-HYDRO. To convert from MSL to NAP, or European Vertical Reference Frame (EVRF) outside Dutch waters, a reduction matrix has been constructed based on results from 3D DCSM-FM (for the years 2013-2016), which aims to compute water levels relative to NAP/EVRS (Zijl & Groenenboon, 2021; Laan & Zijl, 2021). This reduction matrix has been implemented in Baseline.

Bathymetry interpolation procedure (using Baseline)
The bed levels in the model are based on gridded bathymetry samples in the merged Baseline datasets of *baseline-nl_land-j22_6-w1* and *baseline-nl_zee-j22_6-w1*. The z-coordinate in the net nodes is calculated by the Baseline 6.3.1 plug-in within ArcMap 10.6.1. The procedure follows the steps below:

1) The two Baseline datasets mentioned above are merged into one Baseline tree for DCSM-FM. During this operation the coordinate system of the land data is converted from Amersfoort RD New to WGS84. Furthermore, bathymetry data for Dutch waters is interpolated to a gridded dataset with a resolution of approximately 5 x 5 m. The rest of the model domain stays at the original resolution of the EMODnet bathymetry data. There is a small overlap of approximately 150 m between the two gridded datasets.
2) Based on the DCSM-FM network a geodatabase with polygons is generated. For every grid node a Thiessen polygon is calculated of roughly the size of the surrounding grid cells. The polygon approximates a line through the surrounding cell centres and flow links.
3) The bathymetry data is projected on the net nodes by grid-cell averaging of the gridded data within the polygons.
4) If no z-coordinate is found, the surrounding data is extrapolated over a distance of 250 m outside the enclosure.
5) All net nodes that are still missing a z-coordinate are assigned the value prescribed with the keyword *Bedlevuni*, in this case 5m.

The model bathymetry is provided on the net nodes. Depths at the middle of the cell edges (the velocity points) are set to be determined as the mean value of the depth at the adjacent nodes. Depths at the location of the cell face (the water level points) are specified to be determined as the minimum of the depth in the surrounding cell edges. These bathymetry interpolations options are prescribed by setting *BedlevType=3*.

An overview of the resulting DCSM-FM model bathymetry is presented in Figure 2.7. This shows that depths of more than 2000 m occur in the northern parts of the model domain, with depths exceeding 5000 m in the south-western part. The North Sea is much shallower with depths rarely exceeding 100m in the central part (Figure 2.8). In the southern North Sea, depths are generally less than 50 m. In Figure 2.9 a detail of the DCSM-FM model bathymetry is shown focusing on the South-western Delta, whereas Figure 2.10 shows the model bathymetry in the Dutch Wadden Sea.

Differences with 2019 release

- In the 2022 release, the version of the EMODnet bathymetry dataset has been updated from the 2016 version to the December 2020 version.
- In contrast to the previously used EMODnet 2016 release, which was only provided relative to Lowest Astronomical Tide (LAT), the December 2020 version is also available relative to Mean Sea Level (MSL). Earlier, a LAT-MSL reduction matrix was constructed based on a 19-year computation with the previous generation model DCSMv6 (Zijl et al., 2013). This conversion step has now become obsolete.
- In the 2022 release, a MSL-NAP conversion has been added to the underlying EMODnet bathymetry.
- Previously the interpolation of bathymetry samples was done through the D-HYDRO software, using a ‘grid cell averaging’ method. For the 2022 release, the interpolation was done through Baseline. To achieve this, the same averaging procedure has been implemented in the Baseline software.
- In the 2019 release, some depths at or very close to tide gauge locations were manually adjusted to prevent erroneous drying. As the bathymetry procedure now works through Baseline and manual adjustments are undesirable, this might deteriorate results in some locations, in particular tide gauge location Vlielandhaven. The option of shifting the observation location to an adjacent cell has been considered, but was rejected because this would result in a significantly worsening phase of the M2 tidal constituent.
- The differences in model bathymetry compared to the previous release is presented in Figure 2.11. The updated bathymetry shows the largest changes in the central and Danish North Sea. Furthermore, compared to the previous release, an increase of the bed level of about 2 m is present in a large area off the Zeeland coast.

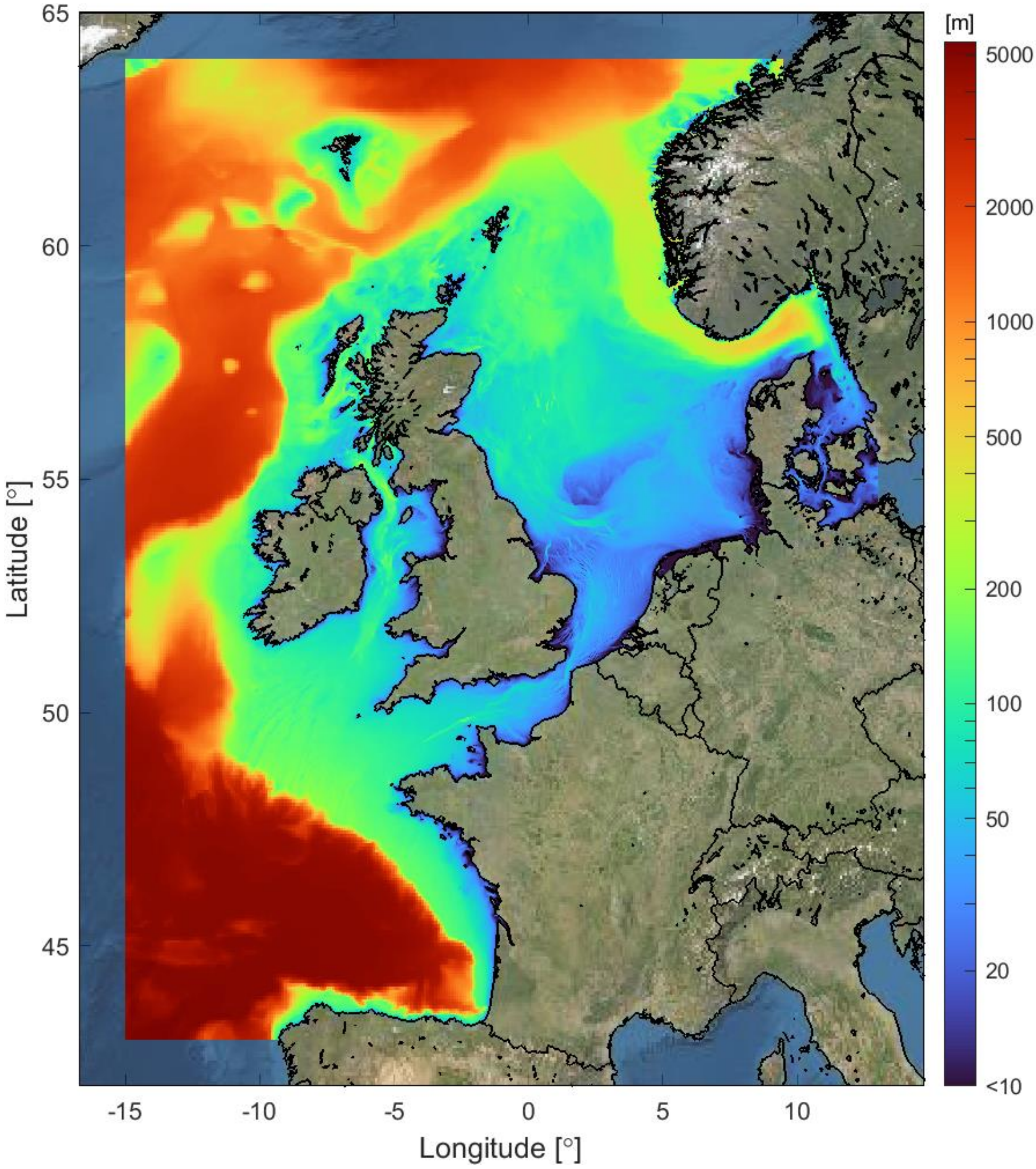

Figure 2.7 Overview of the DCSM-FM model bathymetry (depths relative to NAP, on a logarithmic scale).

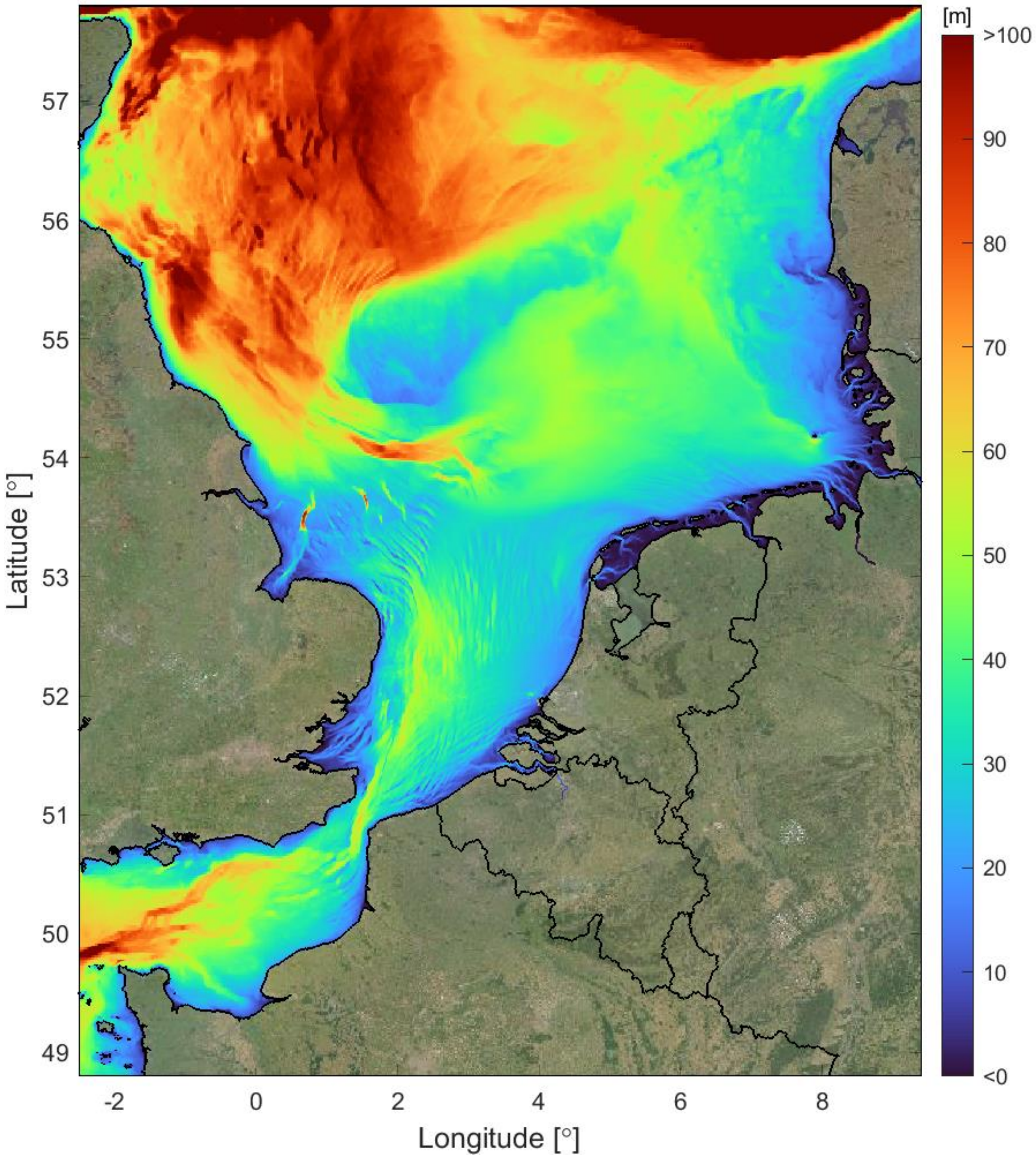

Figure 2.8 DCSM-FM model bathymetry in the central and southern North Sea (depths relative to NAP).

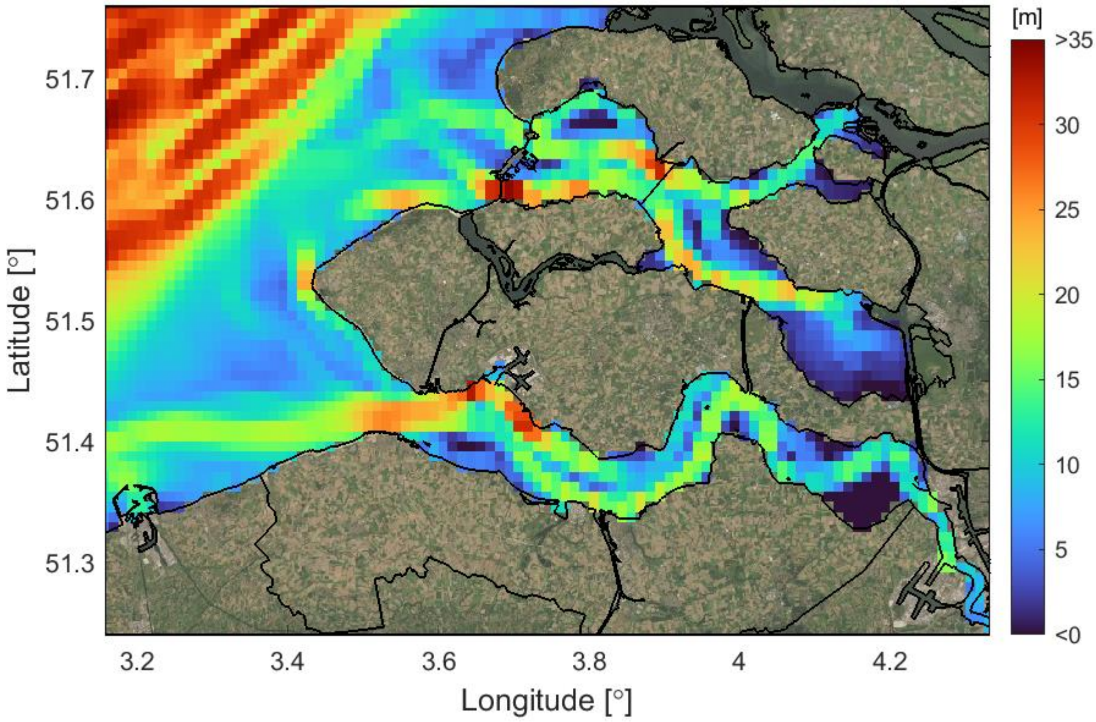

Figure 2.9 DCSM-FM model bathymetry in the South-western Delta (depths relative to NAP).

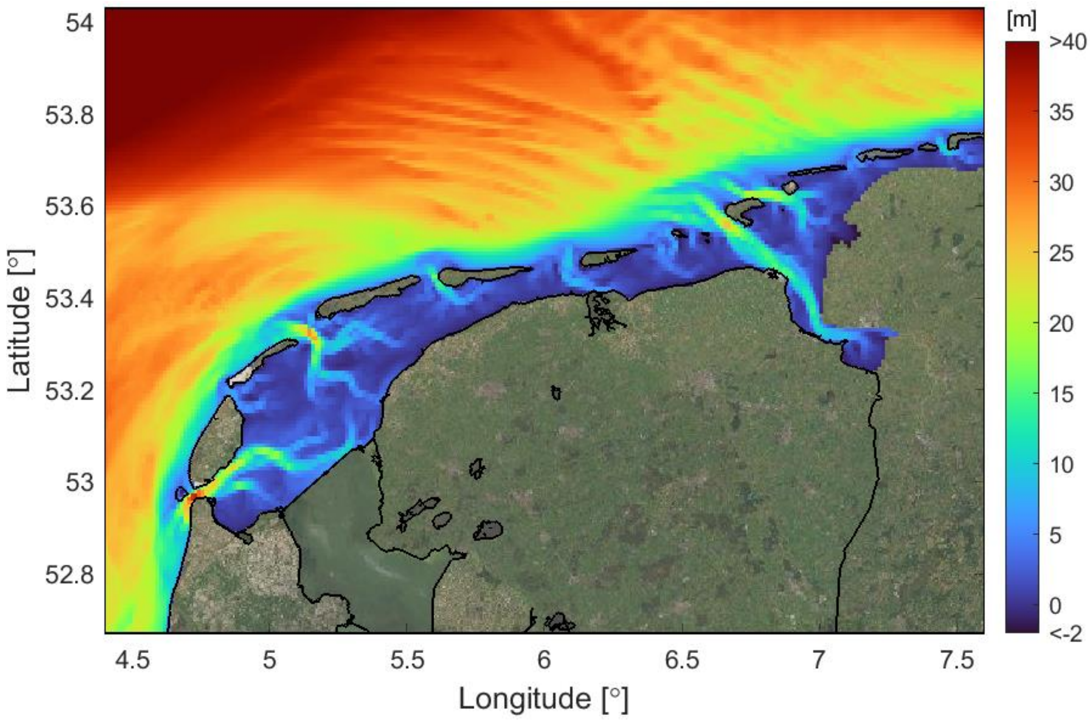

Figure 2.10 DCSM-FM model bathymetry in the Wadden Sea and Ems-Dollard (depths relative to NAP).

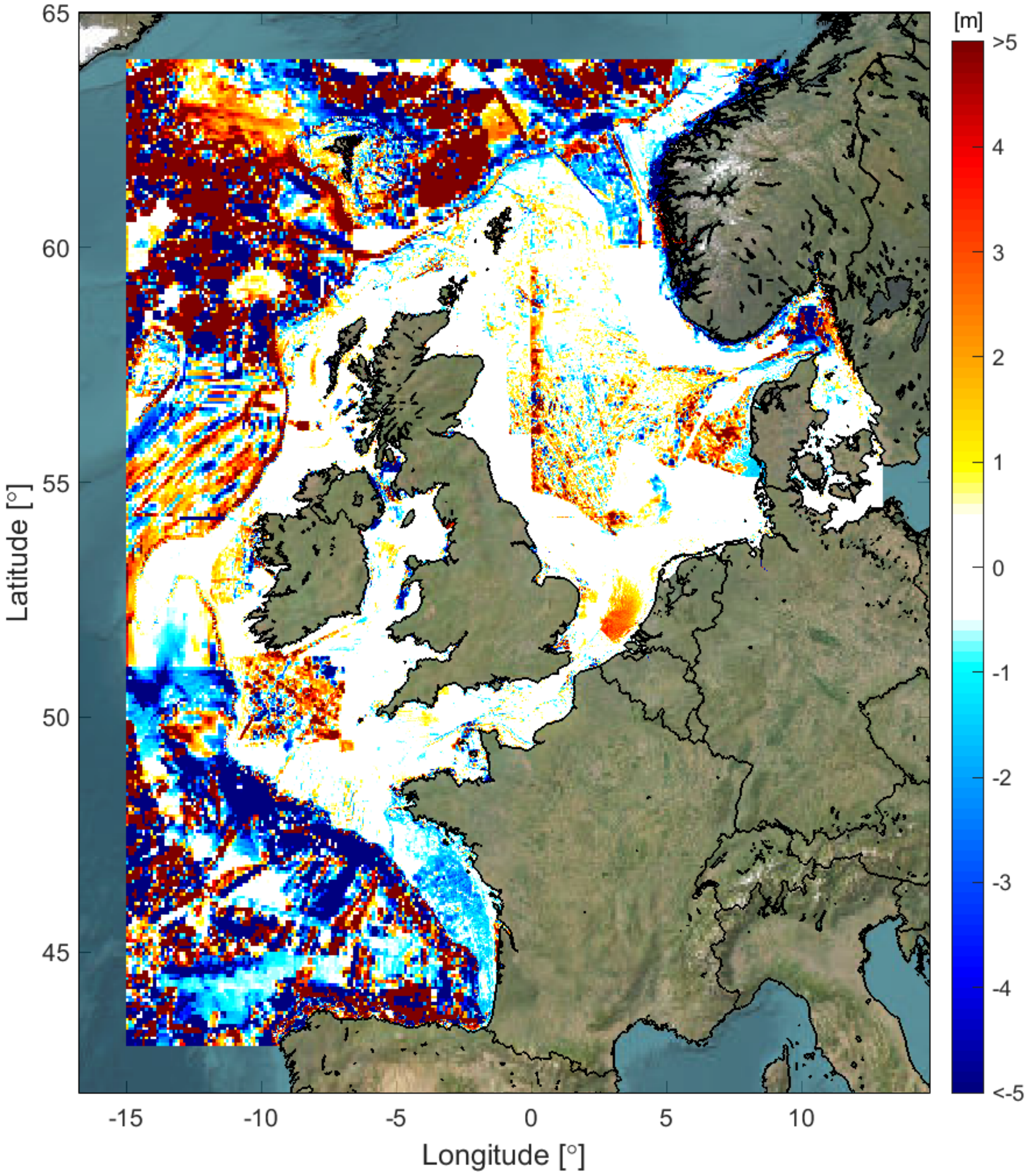

Figure 2.11 Overview of the difference in DCSM-FM model bathymetry (2022 release minus 2019 release).

2.5 Bottom roughness

To account for the effect of bottom friction, a uniform Manning roughness coefficient of 0.028 $s/m^{1/3}$ was initially applied. During the model (re-)calibration (see Chapter 3) this value was adjusted to obtain optimal water level representation. The resulting roughness fields are presented in Figure 2.12 and Figure 2.13. The minimum and maximum bottom roughness values applied are 0.012 $s/m^{1/3}$ and 0.050 $s/m^{1/3}$, respectively.

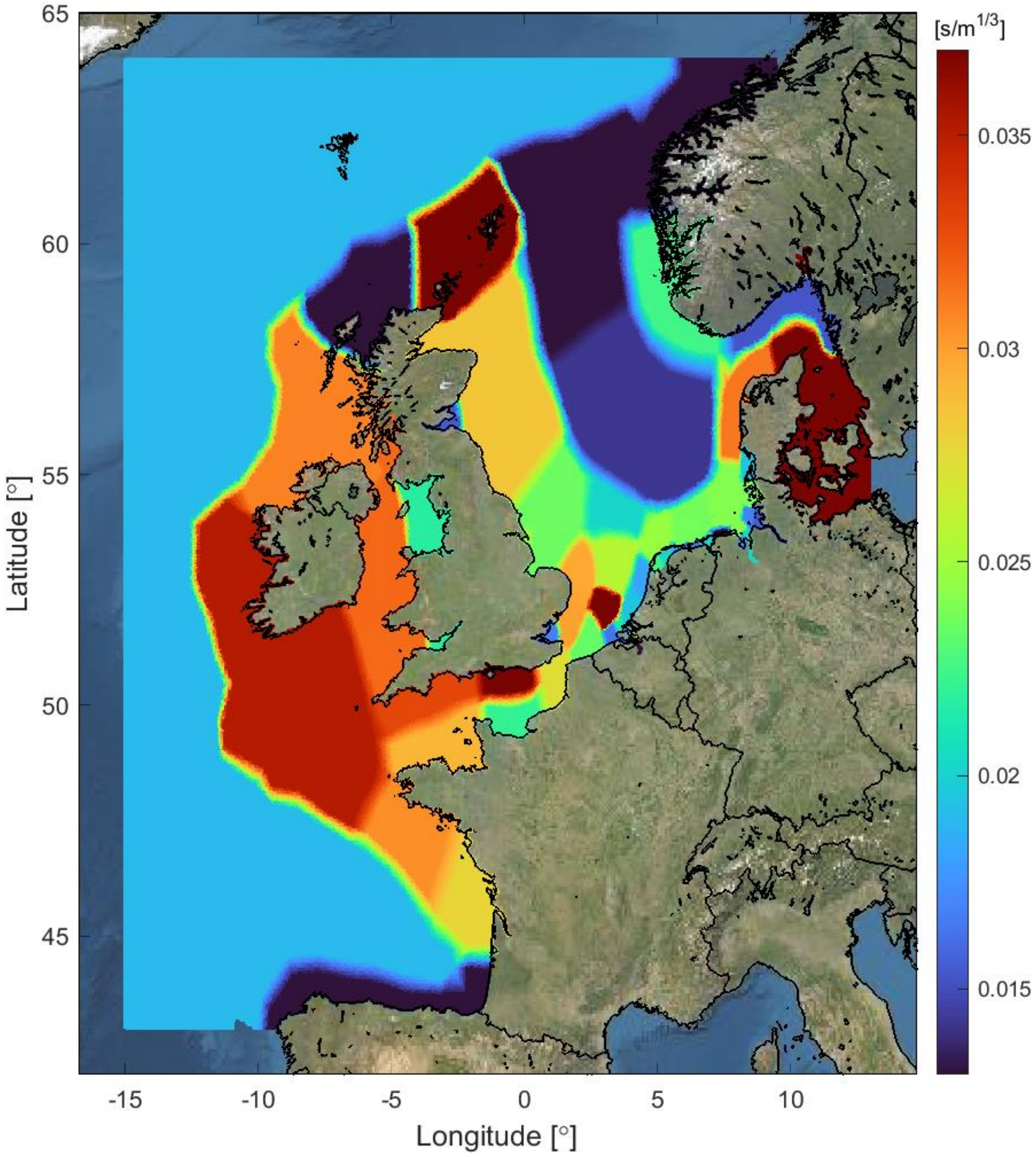

Figure 2.12 Overview of the space-varying Manning bottom roughness field of DCSM-FM.

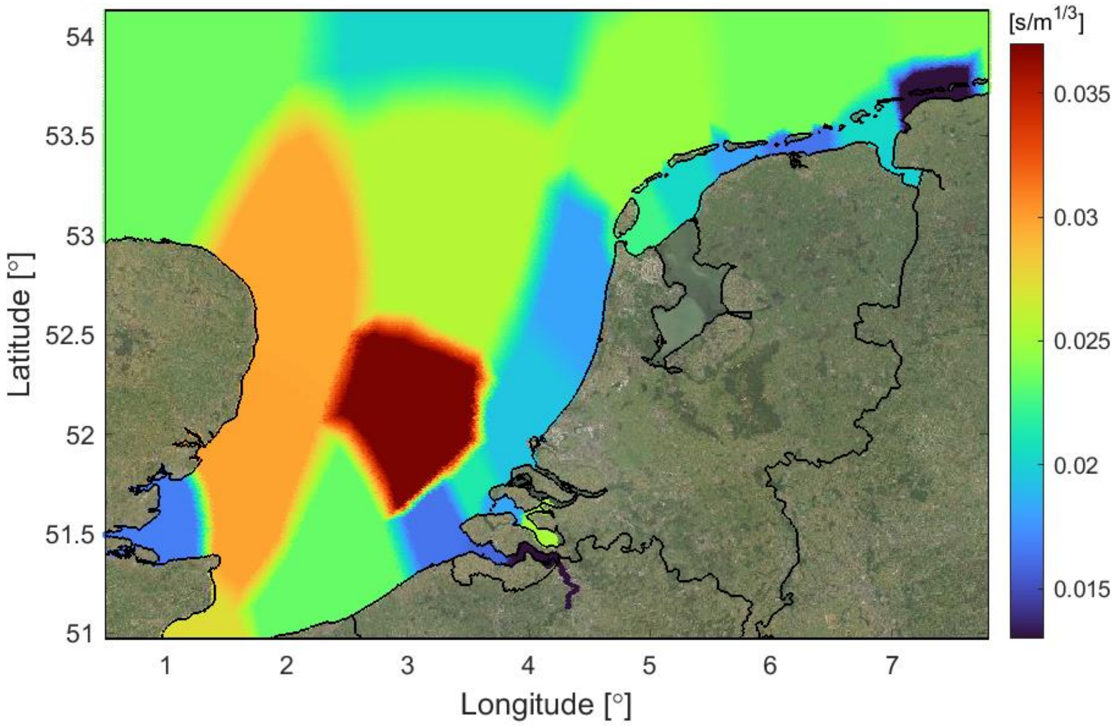

Figure 2.13 Detail of the space-varying Manning bottom roughness field of DCSM-FM in Dutch waters.

Differences with 2019 release

- Because of the many changes to the schematisation in the 2022 release, in particular the significant differences in bathymetry, the Manning bottom roughness coefficient has been recalibrated, see Chapter 3.
- The locations of the roughness areas (each with uniform values) has mostly remained the same, except the addition of a separate roughness section in the deep (>800m), oceanic areas of the model domain.

2.6 Open boundary conditions

At the northern, western and southern sides of the model domain, open water level boundaries are defined. Water levels are specified at 209 different locations along those boundaries. In between these locations the imposed water levels are interpolated linearly.

2.6.1 Tide

The tidal water levels at the open boundaries are derived by harmonic expansion using the amplitudes and phases of 39 harmonic constituents (Table 2.1). These constituents are based on a blend of three different global sources, namely FES2014 (Lyard et al., 2021), GTSMv4.1 (Muis et al., 2016) and EOT20 (Hart-Davis et al., 2021).

FES2014 provides amplitudes and phases of 34 constituents on a 1/16° grid of which 25 are used in DCSM-FM. Seven constituents available in FES2014 have been replaced by constituents calculated by nesting in a purely astronomical simulation of GTSMv4. Additionally, five GTSM-derived constituents that are not available in the FES2014 product, but add value to the quality of the tide representation in DCSM-FM, have been added. In total 12 constituents are taken from GTSMv4. The method to derive constituents from GTSM and come up with an optimal combination of FES2014 and GTSM constituents is further elaborated in Laan & Zijl (2021).

The solar diurnal constituent *S1* is available in FES2014, but also contains a contribution due to the diurnal cycle in air pressure. Since we already include this contribution in the surge (section 2.6.2), adding this constituent from FES2014 would introduce double-counting. (Note that the other constituents in FES2014 do not include an air-pressure contribution.) Amplitudes and phases for the S1 constituent have therefore been taken from EOT20, which only includes the gravitational contribution.

The solar annual constituent *Sa* in FES2014 only contains the gravitational contribution to the annual cycle, even though in the ocean *Sa* is much less gravitational than meteorological and baroclinic in nature. Therefore, *Sa* has been based on what was used in DCSMv6 (see Figure 2.14). In the absence of baroclinic forcing in DCSM-FM this is required to reproduce the observed residual annual cycle, i.e. the signal not captured by annual mean sea-level pressure and wind variations and notably the seasonal temperature cycle.

In the D-HYDRO software the specified amplitudes and phases are converted into timeseries covering the required period by means of harmonic prediction. Implicitly it is assumed that the nodal cycle at the location of the open boundaries can be obtained from the equilibrium tide. The validity of this assumption is corroborated in Zijl (2016b).

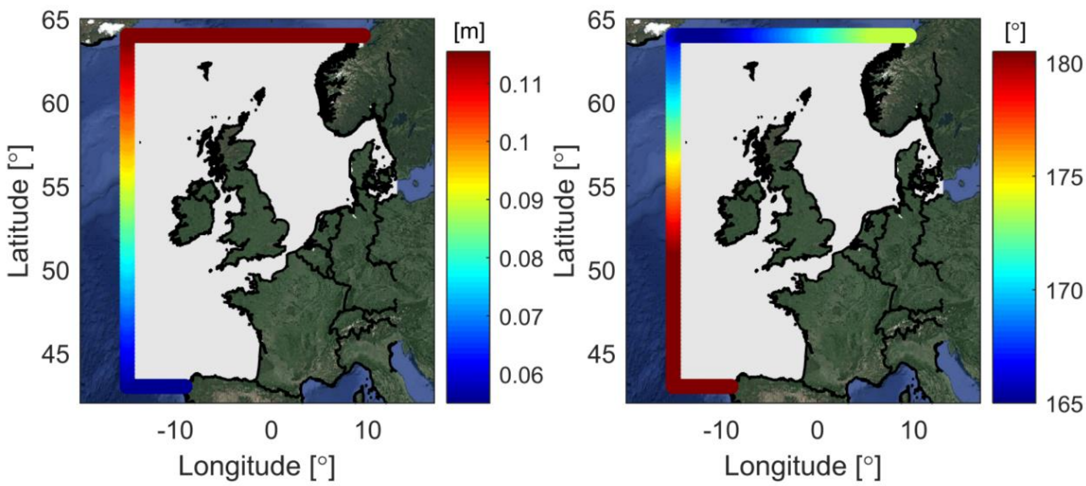

Figure 2.14 Amplitude (left) and phase (right) of the Sa-component along the open boundaries of the model domain

Table 2.1 Overview of the 39 tidal components prescribed at the open boundaries of DCSM-FM, including their angular frequency (°/h) and source.

Constituent	Angular frequency [°/h]	Source	Constituent	Angular frequency [°/h]	Source
SA	0.041069	DCSMv6	**MU2**	27.96821	FES2014
SSA	0.082137	FES2014	**N2**	28.43973	GTSMv4
MM	0.544375	FES2014	**NU2**	28.51258	FES2014
MSF	1.015896	FES2014	**M2**	28.98410	GTSMv4

Constituent	Angular frequency [°/h]	Source	Constituent	Angular frequency [°/h]	Source
MF	1.098033	FES2014	**MKS2**	29.06624	FES2014
MFM	1.642408	FES2014	**L2**	29.52848	FES2014
MSQM	2.113929	FES2014	**T2**	29.95893	FES2014
2Q1	12.85429	GTSMv4	**S2**	30.00000	FES2014
SIGMA1	12.92714	GTSMv4	**R2**	30.04107	FES2014
Q1	13.39866	FES2014	**K2**	30.08214	GTSMv4
O1	13.94304	FES2014	**ETA2**	30.62651	GTSMv4
NO1	14.49669	GTSMv4	**M3**	43.47616	GTSMv4
PI1	14.91786	GTSMv4	**N4**	56.87946	FES2014
P1	14.95893	FES2014	**MN4**	57.42383	GTSMv4
S1	15.00000	EOT20	**M4**	57.96821	FES2014
K1	15.04107	GTSMv4	**MS4**	58.98410	GTSMv4
LABDA2	15.51259	FES2014	**S4**	60.00000	FES2014
J1	15.58544	FES2014	**M6**	86.95231	FES2014
EPSILON2	27.42383	FES2014	**M8**	115.9364	FES2014
2N2	27.89535	FES2014			

Differences with 2019 release

- The previous model release made use of FES2012 (Carrère et al., 2012) tidal constituents, with only Sa added based on DCSMv6. Some FES2012 constituents have been replaced with FES2014, while the others are replaced with GTSM and EOT20 values. In addition, new constituents have been added. The total number of constituents prescribed has increased from 32 to 39.

2.6.2 Surge

While wind setup at the open boundary can arguably be neglected because of the deep water locally (except near the shoreline), the effect of local pressure will be significant. The impact of this is approximated by adding an Inverse Barometer Correction (IBC) to the water levels prescribed at the open boundaries. This correction η_{IBC} is a function of the time- and space-varying local air atmospheric pressure, following

$$\eta_{IBC} = -\frac{1}{g\rho_0}(P_{atm} - P_0)$$

where P_{atm} is the atmospheric pressure and P_0 is a reference atmospheric pressure set to 101,330 N/m^2 to represent the mean pressure over the global ocean. The gravitational acceleration g is set to 9.813 m/s^2, whereas the reference sea water density ρ_0 is set to be 1023 kg/m^3.

One can could also consider nesting in a model with a larger domain, e.g. a global model. This would also account for the differences due to temporal variations in the mean pressure over the global ocean, which is now assumed to be constant, but in reality, varies with the weather.

2.7 Meteorological forcing

There are various options available for meteorological surface forcing of DCSM-FM. The calibration of the 2022 model version has been performed with forcing fields from the Integrated Forecasting System (IFS) of the European Centre for Medium-Range Weather Forecasts (ECMWF). These forcing fields have a horizontal resolution of 1/8° and an hourly temporal resolution. The following time-and space-varying quantities are prescribed:

- Neutral wind speed (at 10 m height, in zonal and meridional direction)
- Air pressure (at MSL)
- Charnock coefficient

The neutral wind speed is calculated from the surface stress under the assumption that the air is neutrally stratified. This implies that in stable conditions, the neutral wind speed is lower than the actual wind speed, and in unstable conditions the neutral wind speed is higher than the actual wind speed. The advantage of specifying the neutral wind speed is that a much simpler wind-drag relation can be used to convert to stress.

While the calibration and validation as presented in the present report have been performed with ECMWF IFS meteorological forcing, the model can be forced with different meteorological model output. The previous (2019) release of DCSM-FM was calibrated and validated with time- and space-varying wind speed (at 10 m height) and air pressure (at MSL) from the Numerical Weather Prediction (NWP) high-resolution limited area model (HiRLAM; version 7.2). This meteorological model has a spatial resolution of approximately 11 km by 11 km, and a temporal output interval of 1 hour.

The wind stress at the surface, associated with the air-sea momentum flux, depends on the square of the local U10 wind speed and the wind drag coefficient, which is a measure of the surface roughness. To translate wind speed to surface stresses, the local wind speed dependent wind drag coefficient is calculated using the Charnock formulation (Charnock, 1955). In the operational ECMWF meteorological model (IFS), the Charnock coefficient is dependent on wind waves (as forecast with the dynamically coupled ECWMF WAM model) and consequently time and space dependent. Consequently, when using ECWMF IFS forcing, the Charnock coefficient also has to be prescribed in a time-and space dependent manner. When using Hirlam, the dimensionless Charnock coefficient has been set to a constant value of 0.025, which corresponds to the value used in the HiRLAM meteorological model. The resulting wind drag coefficient is shown in Figure 2.15 as a function of the 10 m wind speed.

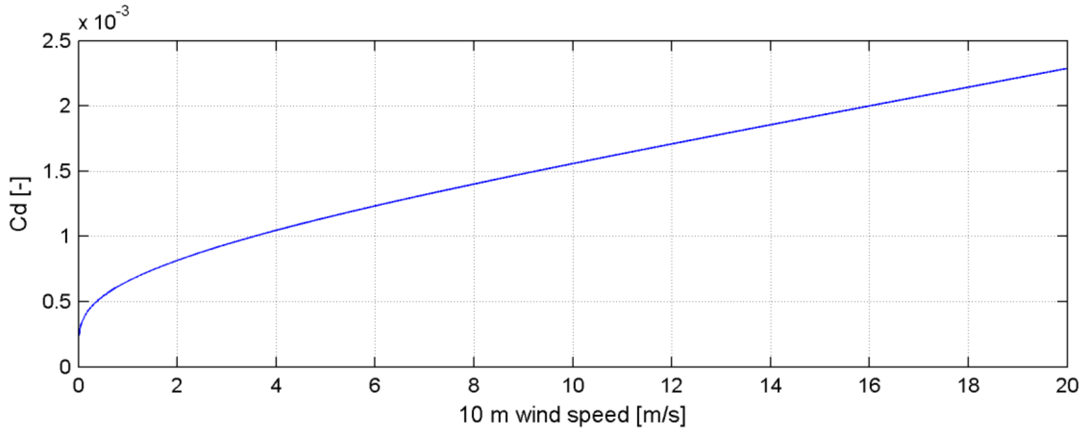

Figure 2.15 Wind drag coefficient (Cd) as a function of the 10 m wind speed, using a Charnock relation with a Charnock parameter of 0.025.

Relative wind effect

In many wind-drag formulations the flow velocity at the water surface is not taken into account in determining the wind shear stress (i.e., the water is assumed to be stagnant). Even though the assumption of a stagnant water surface is common because it makes computing stresses easier, from a physical perspective the use of relative wind speed makes more sense since all physical laws deal with relative changes. In case the flow of water is in opposite direction to the wind speed, this would contribute to higher wind stresses (and vice-versa). The impact of the water velocity on the wind stress at the surface, and consequently also on computed water levels, is denoted with the name 'Relative Wind Effect' (RWE).

In general, including RWE leads to a meaningful improvement in (skew) surge quality during calm conditions (Appendix C of Zijl & Groenenboom, 2019; Zijl, 2021; Groenenboom & Zijl, 2021). Apparently, RWE adds an effect that cannot be fully incorporated by adjusting the bottom roughness instead. Even though inclusion comes at a cost of an increased systematic underestimation during the two most extreme skew surge events of 1-3 cm, it was decided to include RWE. In this 2022 release, an additional factor has been introduced to account for the fact that the wind speeds applied are not taken from a two-way coupled ocean–atmosphere system. In a two-way coupled system, the lowest layers of air would tend to move along with surface currents, reducing the relative wind effect. Following e.g. Lellouche et al. (2018) we therefore pragmatically consider a reduction of the model currents in the wind stress computation of 50% with an additional correction factor of 0.8 to account for the fact that the depth-averaged current is taken into account instead of the surface current. This yields a total reduction of (0.8 * 50% =) 40% (i.e. 60% of the current velocity is taken into account in the wind stress computation).

Note that in earlier versions of the D-HYDRO software, the direct prescription of wind stress required switching off the RWE, which would have an adverse effect on the quality of both the surge and tide representation. In more recent versions of D-HYDRO, RWE also works in combination with the prescription of wind stress.

Differences with 2019 release

- The previous release of DCSM-FM was calibrated using Hirlam meteorological forcing, whereas for the 2022 release use was made of ECMWF IFS.
- In the 2019 release, the entire depth-averaged current velocity was taken into account in the computation of the wind stress. In the current 2022 release, this has been reduced to 60% of the computed current velocity.

2.8 Numerical settings

2.8.1 Theta0

The implicitness of the numerical time integration is specified with the parameter *Teta0*, with *Teta0=1* being fully implicit and *Teta0=0* fully explicit. In accordance with Minns et al. (2022) the value of Theta0 is set to 0.55.

2.8.2 Time step

D-Flow FM automatically limits the time step to prevent numerical instabilities. Since the computation of the advective term is done explicitly in D-Flow FM, the time step limitation is related to the Courant criterion. In accordance with Minns et al. (2022) the maximum Courant number is set to 0.7. The maximum computational time step has been set to 2 minutes (120 s).

2.8.3 Differences with sixth-generation standard settings

While most geometric, numerical and physical model settings of DCSM-FM 0.5nm are in accordance with the current specifications for sixth-generation models as described in Minns et al. (2022), there are some settings that deviate from the standard. These parameters are listed in Table 2.2.

Table 2.2 Overview of settings of the 2022 release that differ from the standard settings

Keyword	Standard setting	Setting 2022 release
Dxwuimin2D	0	0.1
BedlevUni	-5	5
OpenBoundaryTolerance	3	0.1
Izbndpos	0	1
Tlfsmo	0	86400
Rhomean	1000	1023
TidalForcing	0	1
ICdtyp	2 (Smith & Banke)	4 (Charnock)
Relativewind	0	0.6
Rhoair	1.2	1.2265
PavBnd	0	101330
DtUser	300	600
DtMax	30	120
DtInit	1	60

2.8.4 Numerical and physical settings that have been changed in 2022 release

During the development of the 2022 release of DCSM-FM, some numerical and physical settings have been changed compared to the 2019 release, see Table 2.3. For some of the changed settings, this reflects a change in the recommended standard settings that occurred between the two releases, notably for the keywords *Newcorio* and *Corioadamsbashfordfac*. Using the new settings for these keywords affects the tidal propagation in DCSM-FM, with a reduction in M2 amplitude and phase along the Dutch coast of 0.6 cm and 0.4°, respectively. The change in keywords implies improved consistency with the 3D version of this model.

Table 2.3 Overview of settings that have changed compared to the 2019 release, together with the current sixth generation standard setting (Minns et al., 2022).

Keyword	Standard setting	Setting 2019 release	Setting 2022 release
Newcorio	1	0	1
Corioadamsbashfordfac	0.5	-	0.5
Zerozbndinflowadvection	0	1	2
MinTimestepBreak	0	0	0.1
jasfer3D	1	0	1
Relativewind	0	1	0.6
DtInit	1	30	60

Differences with 2019 release

- An overview of changes in numerical and physical settings is given in Table 2.3.
- The change in keywords *Newcorio* and *Corioadamsbashfordfac* affects the tidal propagation in DCSM-FM, with a reduction in M2 amplitude and phase along the Dutch coast of 0.6 cm and 0.4°, respectively.

2.9 Miscellaneous

2.9.1 Tidal potential

The tidal potential representing the direct body force of the gravitational attraction of the moon and sun on the mass of water has been switched on. It is estimated that the effect of these Tide Generating Forces (TGF) has an amplitude in the order of 10 cm throughout the model domain. Components of the tide with a Doodson number from 55.565 to 375.575 have been included.

2.9.2 Mean Dynamic Topography correction

DCSM-FM 0.5nm is a 2D model without spatially varying salinity and temperature and thus it cannot resolve baroclinic processes. These processes do have an important contribution to the modelled water levels, specifically to the calculated mean water level. To account for these processes an additional water level difference field is forced on the model. With this addition, the modelled mean water level approaches the Mean Dynamic Topography (MDT), the long-term difference between the mean sea surface and its geoid. The difference field is based on the mean water level for the period 2013-2017 from a simulation with DCSM-FM 0.5nm and 3D DCSM-FM, which includes baroclinic processes.

When a cell becomes dry, the bed level is written as the water level. This influences the calculated mean water level. To account for this, a drying criterium of 75 cm is set. If the water level is below this value at any point in the simulation, the data is ignored.

The calculated water level difference is interpolated to a structured grid of 2/3’ in east-west direction and 1/2’ in north-south direction, which corresponds with the highest resolution in the DCSM-FM network. A triangulation-based natural neighbour interpolation is used for a smooth result. Subsequently, the water level difference field is converted to an additional atmospheric pressure field with:

$$P_{MSL}\ [N/m^2] = MDT\ [m] * g\ [m/s^2] * \rho_{water}\ [kg/m^3]$$

The water level difference field and the corresponding additional atmospheric pressure field are shown in Figure 2.16. A further description of the method can be found in Zijl & Laan (2021).

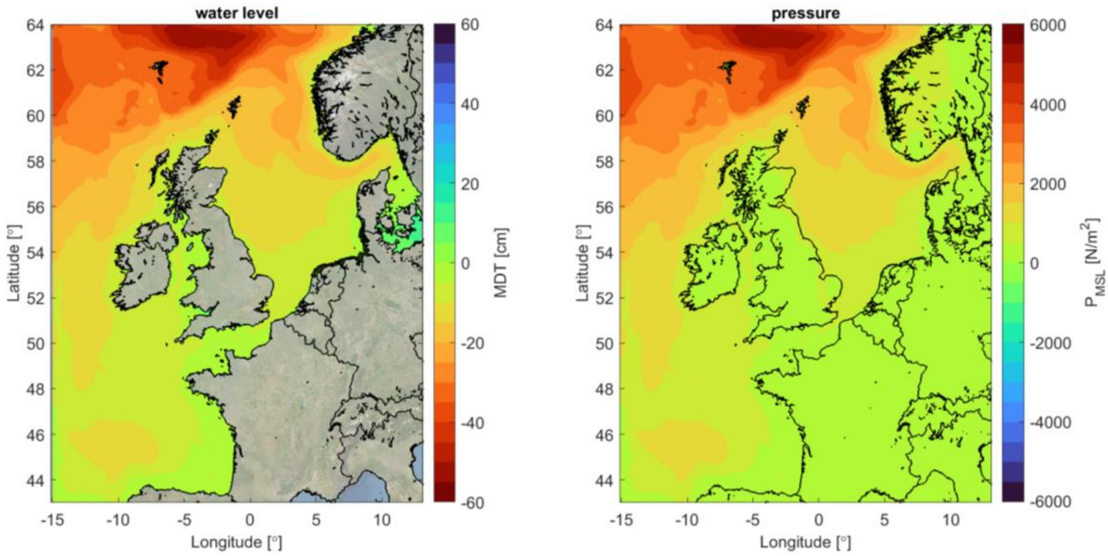

Figure 2.16 Additional water level (left) and corresponding atmospheric pressure field (right) to force the MDT

> **Differences with 2019 release**
> - The Mean Dynamic Topography correction is a new addition to the 2022 release of DCSM-FM.

2.9.3 Horizontal viscosity

The horizontal viscosity is computed with the Smagorinsky sub-grid model, with the coefficient set to 0.20. The use of a Smagorinsky model implies that the viscosity varies in time and space and is dependent on the local cell size. With the exception of a two nodes wide strip along the open boundaries, a background value of 0.1 m^2/s is specified. Along the open boundaries a background value of 2000 m^2/s, gradually reducing to 0.1 m^2/s, has been used (see Appendix D of Zijl & Groenenboom, 2019).

In (Zijl, Irazoqui and Groenenboom 2016) it was concluded that the computed water levels in the North Sea are hardly affected by the use of the Smagorinsky sub-grid model. It is therefore expected that the sensitivity of the water level for the Smagorinsky coefficient is negligible. The impact on currents or the salinity distribution can be larger. The latter is not taken into account in the 2022 model setup.

> **Differences with 2019 release**
> - Smoother transition from increased values along open boundaries to background values. The spatial field is now consistent with what is applied in 3D DCSM-FM.

2.9.4 Movable barriers

There are several movable barriers in the model area, such as the Thames Barrier, the Ems Barrier, the Eastern Scheldt Barrier and the Maeslant Barrier. These barriers protect the hinterland from flooding by closing in case high water is forecast. The only barrier currently implemented in the model is the Eastern Scheldt Barrier (see Figure 2.17). The other barriers either have a negligible effect on water levels in the Netherlands (Thames Barrier) or do not have the area upstream of the barrier sufficiently included in this model (Ems Barrier and Maeslant Barrier).

The Eastern Scheldt Barrier consists of 62 separate gates divided over three sections (from north to south: Hammen, Schaar van Roggenplaat and Roompot). These sections are separately schematized in the model. The modelled sill height in each of these three sections is taken to be the average of the sill heights within this section: NAP -6.32 m, NAP -5.75 m and NAP -8.60m. Next to the crest level, additional vertical levels are needed for the general structure description (keywords Upstream1Level, Upstream2Level, Downstream1Level and Downstream2Level). Directly upstream/downstream of the structure, a level of “crest level minus 5 cm” is applied. One step further upstream/downstream a level of “crest level minus 10 cm” is used.

The energy loss coefficients are taken from the sixth generation Oosterschelde model (Tiessen et al., 2019) and have a value of 0.93 and 1.03 for ebb and flood currents, respectively. Furthermore, all gates are assumed to have an infinite height. While in reality this is obviously not the case, this will not affect the calibration and validation, since in these periods, flow over the gates has not occurred.

During sensitivity tests, the modelled and measured *M2* phase and amplitude difference over the Eastern Scheldt barrier were assessed by comparing Roompot Binnen and Roompot Buiten. This has resulted in an increase of the barrier width by 37% compared to the actual width. This was only implemented after making sure, with OpenDA-DUD experiments, that the desired results could not be obtained by adjusting bottom friction. Furthermore, the adjustment of the barrier width could not be avoided by adjusting the energy loss coefficients. Presumably, the need for adjusting the width is related to the coarseness of the model schematization in this area.

The schematization of the three sections of the Eastern Scheldt Barrier on the model grid, are shown in blue in Figure 2.17. In this figure, the red lines show the computational network, the red crosses illustrate the dry points (permanently inactive cells) and the thin dams are shown in yellow. The cross-sectional area of the barriers follows from a prescribed gate door height and width. These values are listed in Table 2.4. The width of each of the sections is the summed width of the individual gates in each section.

Table 2.4 Gate door height, width and sill height of the three sections of the Eastern Scheldt Barrier

Section	Gate door height [m]	Width [m]	Sill height [m MSL]
Schaar	11.27	856.84	-5.75
Hammen	11.63	811.73	-6.32
Roompot	14.11	1677.57	-8.6

The effect of the structures on the cross-sectional area at each of the structures is controlled by a timeseries of the gate lower edge level of the three sections (data provided by Rijkswaterstaat). These timeseries are corrected for the presence of a horizontal concrete beam at 1.0 m (Roompot en Schaar) and 0.8m (Hammen) above NAP. As the water level at this location sometimes exceeds this vertical level, the flow is partially blocked near the surface. During a closure, see Figure 2.18, the gate lower edge level is almost lowered to the sill height. The timeseries of the gate lower edge level are averaged over the individual gates in each section. The data is corrected for leakage of the hydraulic structure and therefore the gate lower edge level remains above the sill height.

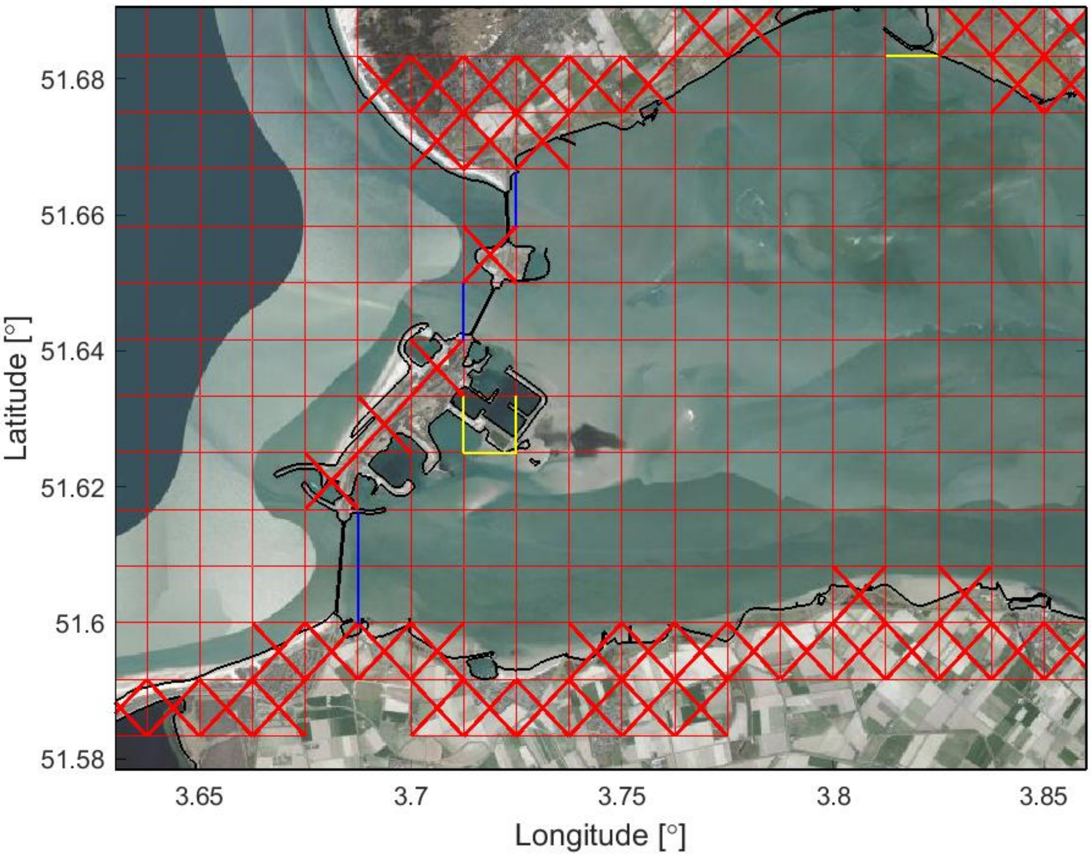

Figure 2.17 Implementation of the Eastern Scheldt Barrier in DCSM-FM (red lines: computational network; red crosses: dry points; yellow lines: thin dams; blue lines: movable barriers).

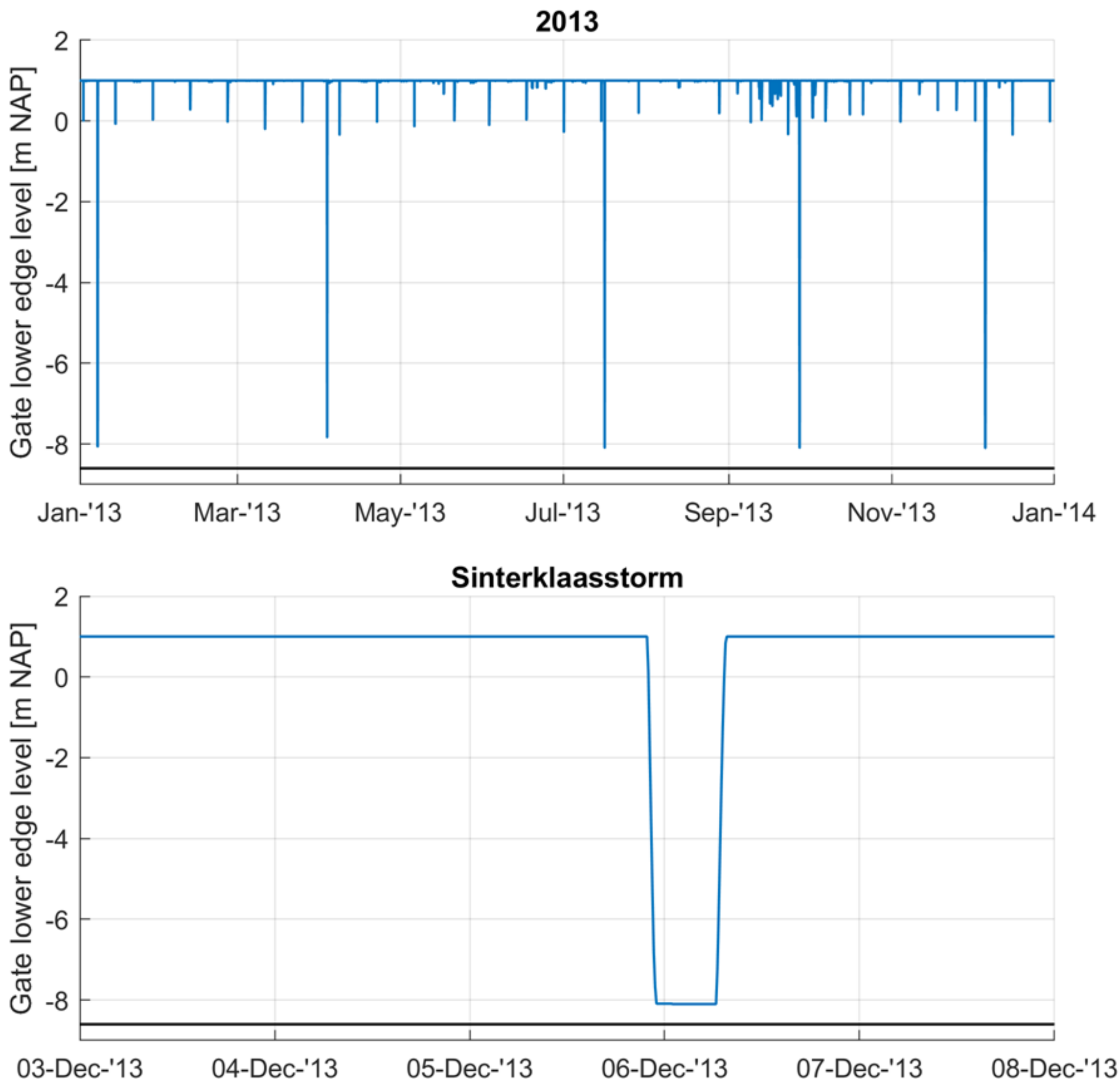

Figure 2.18 Timeseries of the gate lower edge level (in m NAP) of the Eastern Scheldt Barrier section Roompot for year 2013 (top panel) and during the so-called Sinterklaasstorm (lower panel). The black line indicates the sill height of the structure (-8.6 m NAP)

Differences with 2019 release

- Before recalibrating the model, the width of the Eastern Scheldt Barrier has been decreased from a value of 145% to 137% of the actual width. This was done based on an assessment of the modelled and measured M2 phase and amplitude difference over the Eastern Scheldt barrier using tide gauge stations Roompot Binnen and Roompot Buiten.
- Next to the crest level, additional vertical levels are needed for the general structure description (keywords *Upstream1Level*, *Upstream2Level*, *Downstream1Level* and *Downstream2Level*). In the 2019 release the levels were set to be the same as the crest level. In the 2022 release, a level of “crest level minus 5 cm” is applied directly upstream/downstream of the structure. One step further upstream/downstream a level of “crest level minus 10 cm” is used. This is in accordance with the generic technical and functional specifications described in Minns et al. (2022).

2.9.5 Initial conditions and spin-up period

As the spin-up period for tidal models of this scale are not prohibitively large (10 days is assumed to be sufficient), a uniform initial water level of zero elevation has been specified for the calibration and validation computations. For the initial velocity, stagnant flow conditions have been prescribed. Operationally, the initial model state will be taken from previous hindcast computations (i.e., a so-called warm state).

2.9.6 Time zone

The time zone of DCSM-FM 0.5nm is GMT+0 hr. This means that the phases of the harmonic boundary conditions, the tidal potential and the meteorological forcing are prescribed relative to GMT+0 hr. As a result, the model output is in the same time zone. This time zone is the same as in the previous generation DCSMv6 and DCSMv6-ZUNOv4 models.

2.9.7 Observation points

Since the North Sea is one of the most intensively monitored seas in the world, water level observations are readily available. An overview of the more than 200 tide gauge stations available for calibration and validation are presented in Figure 2.19 (for the entire domain) and Figure 2.20 (Dutch and Belgian stations). Model output is generated at 317 locations.
If locations are just outside the model grid, they are manually placed in the closest cell with sufficient depth. One exception is tide gauge location Delfzijl, which is moved to the opening of the harbour breakwater further upstream in the Ems Estuary.

Differences with 2019 release

- Some observation locations have been adjusted to prevent erroneous drying. In the previous release this was done in some locations by locally deepening the bathymetry.

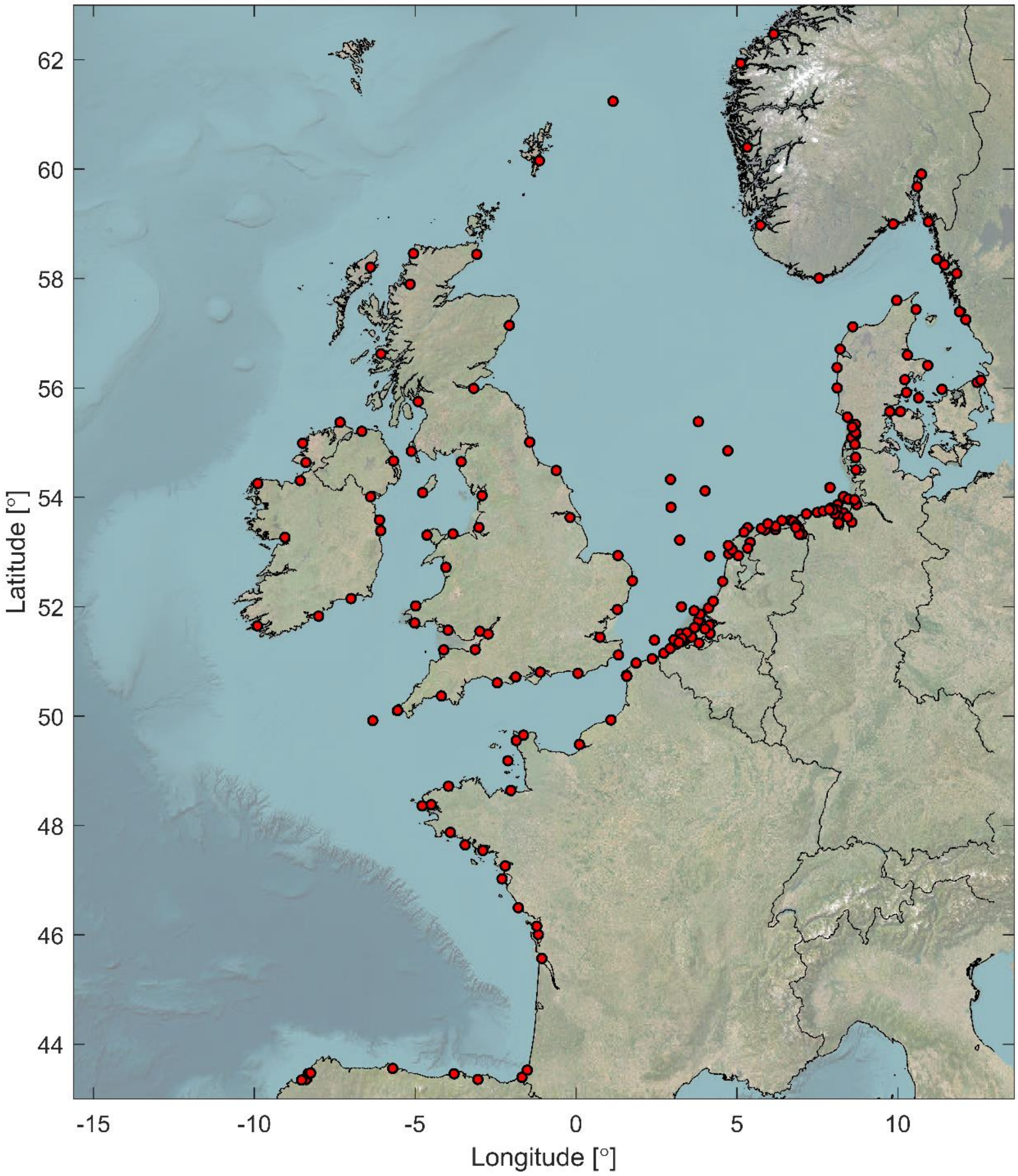

Figure 2.19 Overview of the tide gauge locations at which water level data are available and used for calibration and validation purposes. See Figure 3.3 for stations used for calibration.

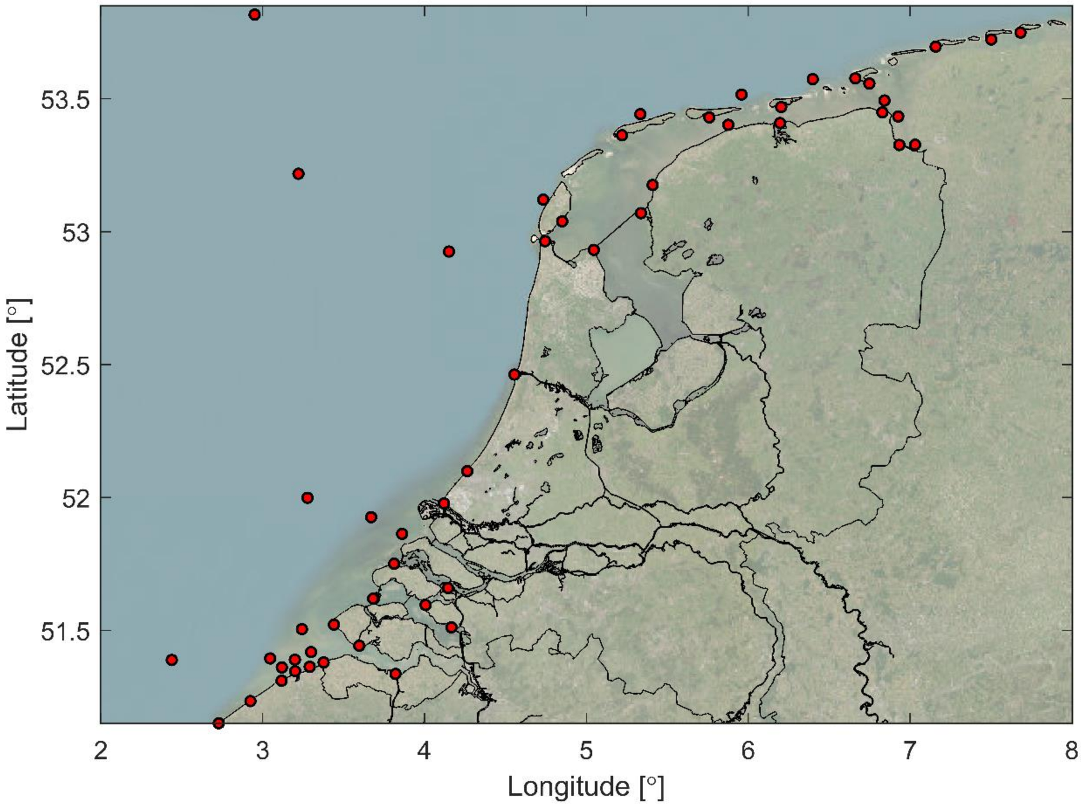

Figure 2.20 Overview of the tide gauge locations at which water level data are available and used for calibration and validation purposes in Dutch waters. See Figure 3.4 for stations used for calibration.

2.9.8 Dissipation by generation of internal waves

The generation of internal waves on the slope towards the continental shelf precipitates barotropic energy dissipation. Even though the 2D barotropic DCSM-FM model cannot explicitly model internal waves, the energy dissipation this causes can be taken into account through a parametrization that is dependent on the local bathymetry gradient, the local flow velocity perpendicular to the continental slope and the local depth-averaged Brunt–Väisälä frequency. The latter quantity is computed as a pre-processing step on the basis of monthly-averaged 3D temperature and salinity fields taken from CMEMS.

During the development of the first model release the impact of taking energy dissipation at the shelf edge into account was quantified, with models that were calibrated separately including and excluding the internal wave generation parameterization (cf. Appendix B of Zijl & Groenenboom, 2019). Considering the general improvement in surge quality, also after calibration, it was decided to include the parametrization of energy dissipation by generation of internal waves into the DCSM-FM model schematization.

Differences with 2019 release

- Adjusted internal tide dissipation forcing field in accordance with what is used in the latest version of Deltares' Global Tide and Surge Model (GTSM).

2.9.9 Software version

DCSM-FM has been developed as an application of the D-Flow Flexible Mesh module (D-Flow FM) module of the D-HYDRO Suite. This module is suitable for one-, two-, and three-dimensional hydrodynamic modelling of free surface flows on unstructured grids. Various versions of D-Flow FM have been used during the development of DCSM-FM. For the final validation presented in this report, use has been made of D-Flow FM version 1.2.162.141597, (August 18, 2022) within DIMRset 2.21.10.76437. This is the version that will be part of D-HYDRO Suite 2022.04.

> **Differences with 2019 release**
> - The 2019 release was calibrated and validated with D-Flow FM version 1.2.54.64101 (June 12, 2019). This version has been updated to 2.21.10.76437, (August 18, 2022) for the 2022 release.

2.9.10 Computational time

In Table 2.5 the computational time of the DCSM-FM is presented together with the (average) time step and cell size and the number of network nodes. This is done for a number of configurations of the model (including a 3D version and a test version with a maximum resolution of 1nm), with all computations performed on Deltares' h6 cluster using 5 nodes with 4 cores each. Note that this comparison was made based on variations of the 2019 release of DCSM-FM.

During the development of DCSM-FM network the minimum size of the network nodes was an important decision since this has a substantial impact on the resulting computational time through the average time step and the number of cells. These results show that halving the minimum cell size more than doubles the computational time. Nonetheless, because of the beneficial impact on the quality of water levels in shallow areas such as the Wadden Sea this is considered acceptable. Even though DCSM-FM (with a minimum cell size of 0.5 nm) has smaller grid cells in the relevant areas, it is still 15% faster than DCSMv6 (1.36 min/day vs. 1.6 min/day).

It can also be observed that the preliminary calibration has increased the average time step and decreased the computational time. This is presumably caused by the higher roughness in the Pentland Firth (i.e., between the north of Scotland and the Orkney Islands), where the remaining restricting cells were located in the uncalibrated model (cf. Figure 2.3).

Three-dimensional configurations

Since (2D) DCSM-FM should also be a sound basis for the subsequent development of a 3D baroclinic transport model of the North Sea, the computational time is also assessed using 20 equidistant sigma-layers (Table 2.6)

In 3D barotropic mode (i.e., without temperature and salinity) the model is approximately 7 times slower than the 2D configuration. Additionally, adding salinity and temperature as state parameters makes it 10 times slower than the 2D model. This amounts to 3.4 days per simulated year, which is considered acceptable. Note that the 2022 release of 3D DCSM-FM will have up to 50 vertical layers and a smaller time step, leading to a larger computational time.

One computational core

An important criterion for DCSM-FM is that it should be fast enough to produce probability forecasts with a 2 – 10 day lead-time within roughly 2 hours. These forecasts will be based on meteorology of the ECMWF Ensemble Prediction System (EPS) and consist of one control run and 50 perturbed members. It is considered most efficient to run as many of these 51 runs at the same time in sequential mode (i.e., on one computational core), instead of consecutively in parallel. Therefore, the computational time on one core is also determined (Table 2.7). These results show a computational time of 10.9 min/day, which means that running 10 days is possible in 109 minutes, less than the maximum of 120 minutes. Note however, that these results are hardware-dependent and that running multiple computations on one node (on one core each) could increase the required computational time.

Table 2.5 Overview of grid cell size, number of net nodes, maximum and average numerical time step and computational time for various 2D models. The computations were performed on Deltares' h6 cluster using 5 nodes with 4 cores each.

Model	cell size (nm)	# nodes	Maximum time step (s)	Average time step (s)	Comp. time (min/day)	Comp. time (hr/year)
5th generation						
DCSMv6	1 nm	859,217	120	120.0	1.6	10.0
DCSMv6-ZUNOv4	4nm – 0.15nm	1,119,106	60	60.0	6.5	40.2
Before calibration						
DCSM-FM (1nm)	4nm-1nm	373,522	200	198.8	0.60	3.7
DCSM-FM (0.5 nm)	4nm-0.5nm	629,187	120	113.8	1.41	8.6
After calibration						
DCSM-FM (1nm)	4nm-1nm	373,522	200	199.8	0.58	3.6
DCSM-FM (0.5 nm)	4nm-0.5nm	629,187	120	118.7	1.36	8.3

Table 2.6 Overview of grid cell size, number of net nodes, maximum and average numerical time step and computational time for various three-dimensional configurations of the model, all using 20 equidistant sigma-layers. The computations were performed on Deltares' h6 cluster using 5 nodes with 4 cores each.

Model	cell size (nm)	# nodes	Maximum time step (s)	Average time step (s)	Comp. time (min/day)	Comp. time (hr/year)
3D (excl S and T)						
3D DCSM-FM (0.5nm)	4nm-0.5nm	629,187	120	114.1	9.4	57
3D (incl S and T)						
3D DCSM-FM (1nm)	4nm-1nm	373,522	200	198.7	4.9	30
3D DCSM-FM (0.5nm)	4nm-0.5nm	629,187	120	113.4	13.5	82

Table 2.7 Overview of grid cell size, number of net nodes, maximum and average numerical time step and computational time for various models. The computations were performed on Deltares' h6 cluster using 1 core.

Model	cell size (nm)	# nodes	Maximum time step (s)	Average time step (s)	Comp. time (min/day)	Comp. time (hr/year)
5th generation						
DCSMv6	1 nm	859,217	120	120.0	16	97
Before calibration						
DCSM-FM (1nm)	4nm-1nm	373,522	200	198.9	3.9	24
DCSM-FM (0.5 nm)	4nm-0.5nm	629,187	120	114.0	11.2	68
After calibration						
DCSM-FM (0.5 nm)	4nm-0.5nm	629,187	120	118.7	10.9	66

Differences with 2019 release

- The above mentioned results were obtained with (variations of) the 2019 release of DCSM-FM. The computational time of the 2022 release is presented in Table 2.8. This shows an increase in computational time that is partially explained by a decrease in average time step. Note that there are also differences in hardware and software version used.

Table 2.8 Maximum and average numerical time step and computational time for the 2019 and 2022 release of DCSM-FM. The computations were performed on Deltares' h6 cluster using 5 nodes with 4 cores each.

DCSM-FM release	Maximum time step (s)	Average time step (s)	Computational time (min/day)	Computational time (hr/year)
2019	120	118.7	1.36	8.3
2022	120	112.3	1.55	9.4

3 Calibration

3.1 Approach

3.1.1 Introduction

Generally, a first simulation with an initial model definition will not lead to an optimal representation of the required parameter (in this case water levels) known from measurements. Models contain errors that originate in the forcing terms (e.g. boundary conditions and meteorological forcing terms), uncertainty in the bathymetry, the model parameters (e.g. bottom friction) and the poorly described or neglected physical processes in the system equations as well as mathematical approximations (e.g. unresolved sub-grid scale motions and exchange of momentum with the atmosphere). In order to reduce the uncertainty of the model parameters and parameterisations used, an automated calibration using the DUD (Doesn't Use Derivative) algorithm (Ralston and Jennrich, 1978) available in the open source data assimilation toolbox OpenDA (version 2.4.5) has been performed. This derivative-free algorithm for non-linear least squares transforms a non-linear least square problem onto a well-known least square problem. DUD evaluates and optimizes uncertain model parameters by minimizing a cost function. The parameter values corresponding to the minimum value of the cost function are considered as the optimal parameter values for the given problem. The general methodology followed is similar to the one used for the calibration of the previous generation models DCSMv6 and DCSMv6-ZUNOv4 (Zijl et al., 2013).

3.1.2 Calibration period

It is important to assess model results against sufficiently long measurement series, which include all relevant physical processes: e.g. spring and neap tide, various (seasonal) wind patterns, etc. Computing longer periods prevents optimization for specific, unrepresentative events, which would lead to a deterioration of the predictive value of the model.

For the final calibration, the entire year of 2017 has been used, preceded by a 10-day spin-up period. The use of an entire year is required since the annual modulation of the M2 tide cannot be properly represented in a 2D barotropic model. Optimization for a shorter period would result in an over- or underestimation of dissipation through bottom friction.

3.1.3 Observation data used

The same measurement stations were used for calibration of the model as in calibration of the 2019 release of DCSM-FM 0.5nm. Accounting for stations without measurements data in the calibration period, a total of 194 stations were used. The measurements (and model output) were provided with a 30-minute interval because of computer memory restrictions.

Differences with 2019 release

- Compared to the calibration of the 2019 release, one tide gauge station has been removed from the set of calibration stations: Vlielandhaven. This station has been removed since computed water levels there are affected by erroneous drying. The option of shifting the observation location to an adjacent cell has been considered, but was rejected because this would result in a significantly worsening phase of the M2 tidal constituent.
- Since internal memory restrictions have eased compared to the calibration of the 2019 release, the interval of the measurements used for calibration has decreased from the previously used interval of 60 min to 30 min. While in theory the smaller 30 min interval should be better, the impact is expected to be small.

3.1.3.1 Removal of data (thresholds)

In some tide gauge stations, the representation of especially the low waters is negatively affected by the poor resolution of the model in some areas. If these measurements are included in the calibration, this would adversely influence the results. An option could be to exclude these stations altogether from the calibration. While this is done for some stations, for others where the higher water levels are well represented in the model, it was decided to just remove the water level measurements below a certain threshold. This threshold is determined by making scatter plots of the modelled and measured total water levels, and visually determining from which level the model accuracy is sufficiently accurate. An example for station Nes is presented in Figure 3.1.

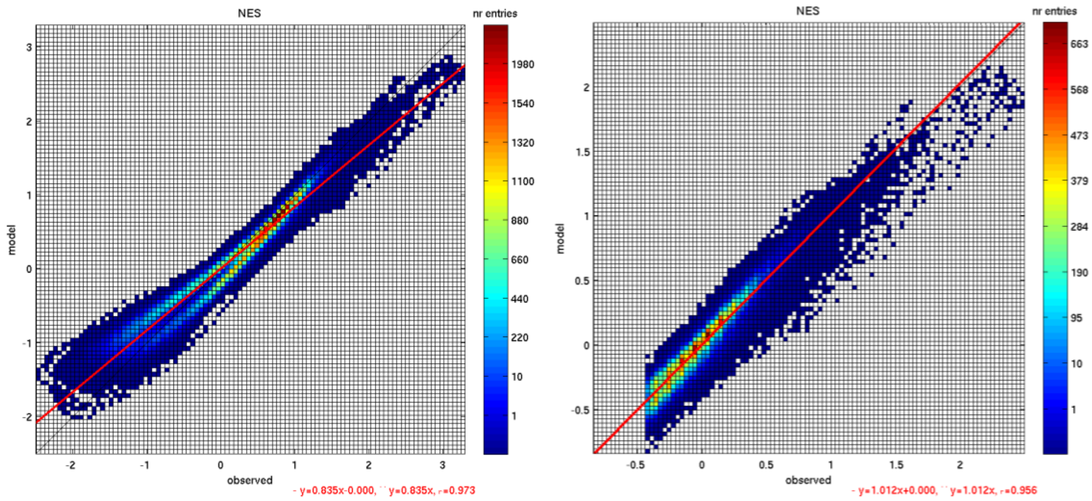

Figure 3.1 Scatter plots of the measured (horizontal) and modelled (vertical) water level at station Nes before (left) and after (right) water levels below the provided threshold are removed.

The resulting thresholds, which were taken into account in both the calibration and validation, are presented in Table 3.1 and visually shown in Figure 3.2. Note that the thresholds are prescribed relative to MSL, which is determined before the removal of the water levels below the threshold. This causes an apparent mismatch between the threshold in Table 3.1 (Nes: 0.5 m +MSL) and the lowest observed water level in the (right; around -0.4 m +MSL).

Table 3.1 Threshold values relative to MSL below which water level measurements are not taken into account during calibration or validation.

Station name	Threshold (m +MSL)	Station name	Threshold (m +MSL)
Ballum	0.5	LAUWOG	0.5
BARMH	-1.5	Mando	0.0
BayonneBoucau	-1.0	NES	0.5
BHV_ALTER_LT'	0.0	NEWPT	-1.0
Brons	0.5	PortBury	-1.0
Dagebull	-0.5	PORTSMH	-0.5
DELFZL	0.0	Ribe	1.0
DENOVBTN	0.0	ROBBENSUDSTEERT	-1.0
Dundalk	0.5	SaintNazaire	-2.0
Esbjerg	-0.5	SCHIERMNOG	0.5

HARLGN	-0.5	Vidaa	0.5
HOLWD	1.0	WITTDUN	0.0
KNOCK	0.0		

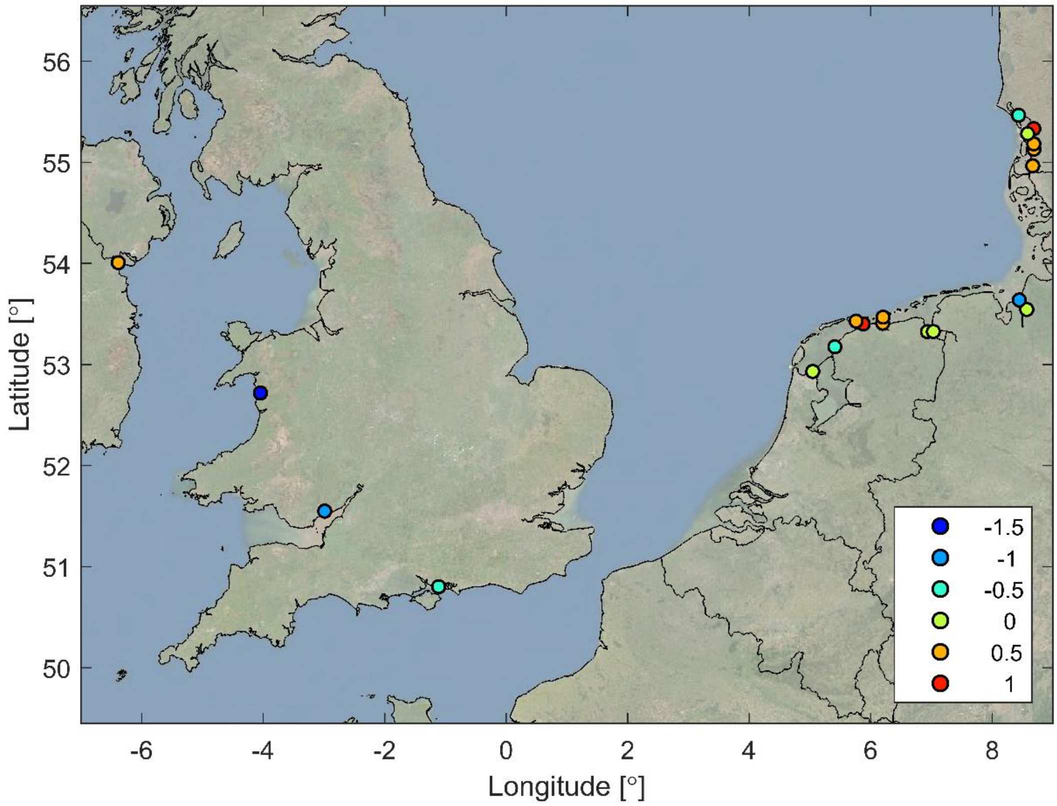

Figure 3.2 Threshold values relative to MSL below which water level measurements are not taken into account during calibration or validation (thresholds for station Bayonne Boucau and Saint Nazaire are not shown).

Differences with 2019 release

- The update of the model bathymetry in the present release has affected the level from which higher water levels are well represented in some of the stations adversely affected by the poor resolution. The thresholds below which measurements at some stations are not taken into account during the calibration have therefore also been updated. For stations DEVPT, Havneby and Kornewerderzand buiten, the thresholds have been removed altogether, while new thresholds have been added in stations BARMH, Ribe and WITTDUN.

3.1.4 Cost function and weights

DUD is a derivative-free algorithm for nonlinear least squares that minimises a quadratic cost function by adjusting model parameters. DUD should be initialised with one unperturbed run and n sensitivity runs, where n is the number of control parameters.

For the present calibration we have used a quadratic cost function over the complete total water level time series. It is essentially the total sum of squares of water level residuals, made dimensionless with the measurement uncertainty.

In the quadratic cost function minimised during the experiments, the bias between computed and measured water levels is ignored, since this bias is hardly related to the uncertainty in the control parameters, but mostly caused by physical (e.g. baroclinic) processes not considered in this model.

Since the primary focus of this model is the accurate representation of water levels in Dutch waters, additional weight in the cost function has been given to Dutch coastal stations (by a factor 16). This is done by decreasing the uncertainty of the measurements that is specified for each station in the OpenDA-DUD input files. In addition, the WMCN-kust main locations have their weight increased by a factor 4. Stations along the North Sea coast of the UK have their weight increased by a factor 2. This is because of the importance of this region for the correct propagation of the tide towards the Dutch coast. Stations in the Skagerrak and Kattegat on the other hand have been given a reduced weight (by a factor 0.5). In addition, stations which are poorly represented in the model compared to neighbouring stations (but nonetheless retained in the calibration) have also been given a reduced weight. This holds for example for the Dutch Wadden Sea and estuarine stations, as well as stations like Sheerness, where the generation of the complex higher harmonics is hampered by a poor representation of the relatively variable bathymetry. The resulting weights are visually presented in Figure 3.3 for the entire model area, and in Figure 3.4 focusing on Dutch waters.

Differences with 2019 release

- During the experiments leading up to the final calibration experiment of the 2022 release model calibration adjustments were made to the weights of some stations. Primarily, stations where the water level quality is affected by poor resolution were given reduced weights.

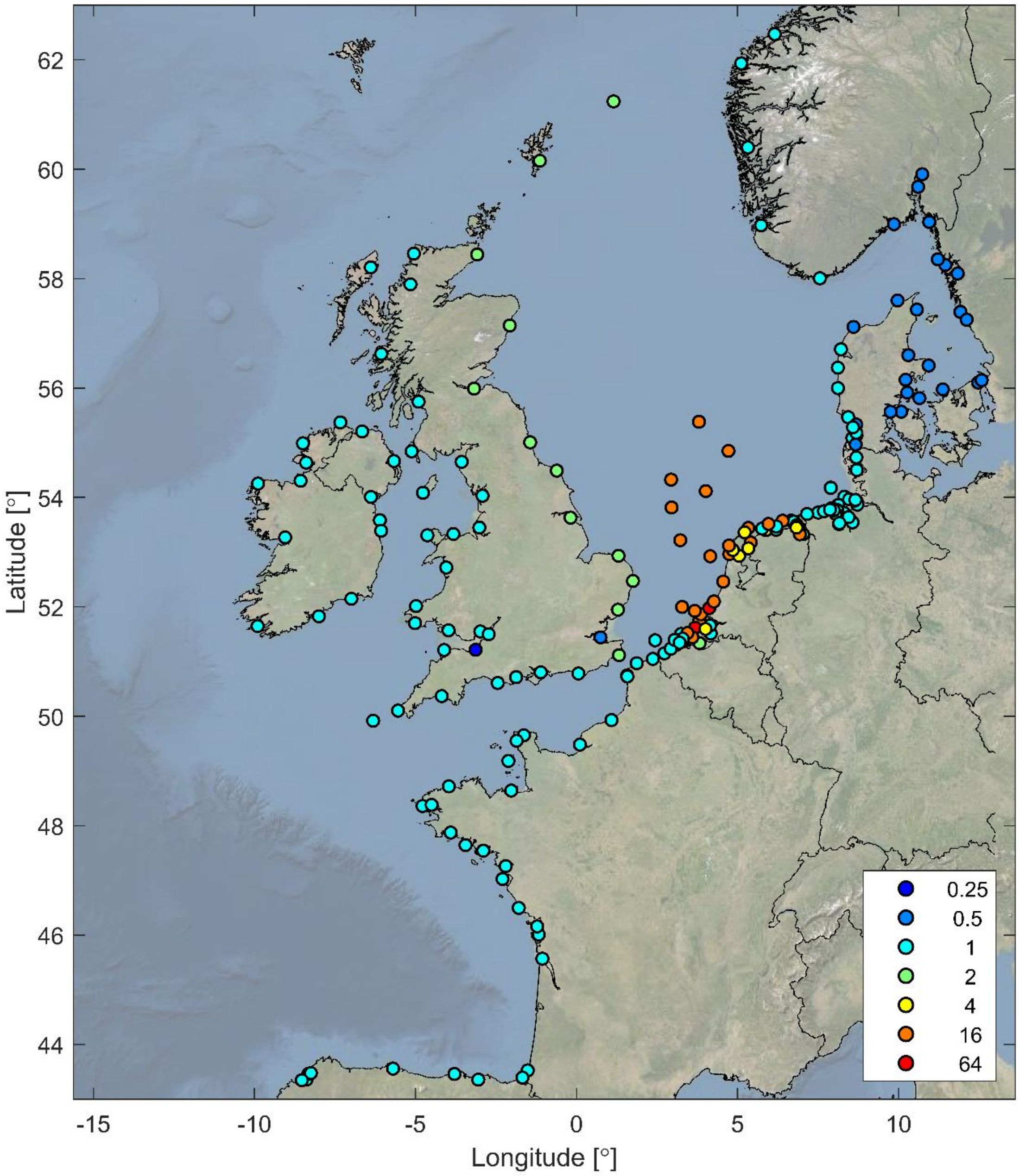

Figure 3.3 Relative weight given to a station in the OpenDA-DUD cost function for the complete model area.

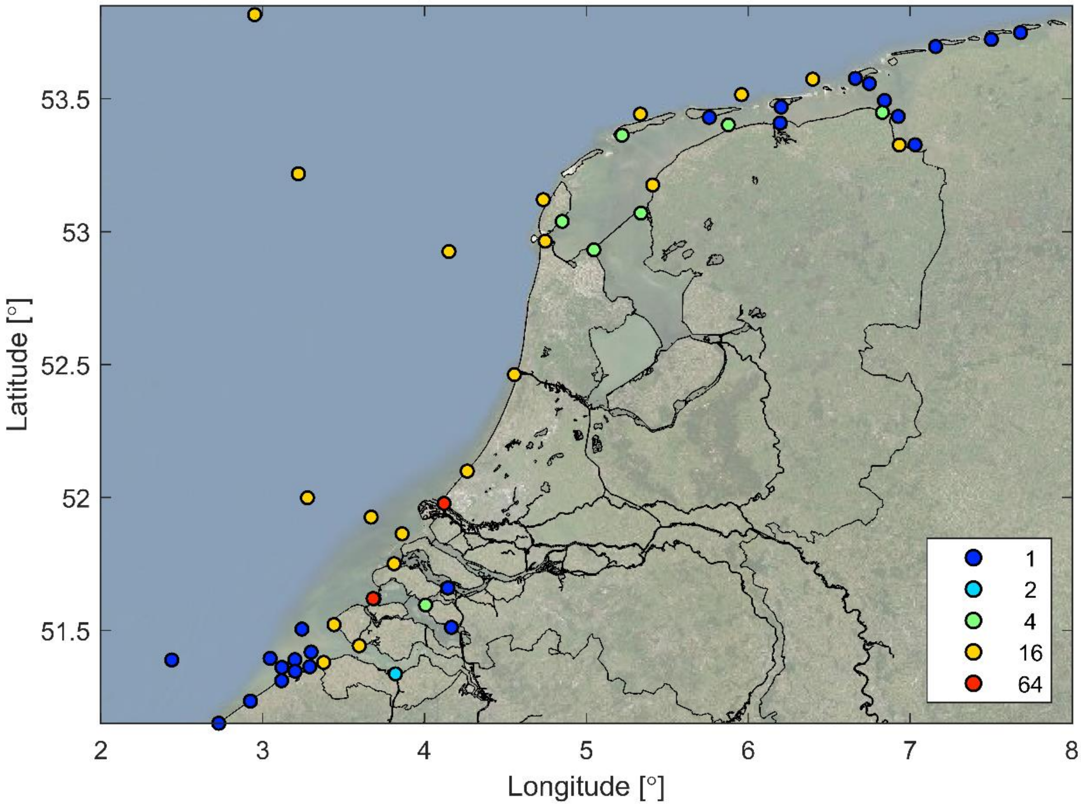

Figure 3.4 Relative weight given to a station in the OpenDA-DUD cost function for the Dutch part of the model area.

3.1.5 Calibration parameters

During the development of the previous generation models for the North Sea uncertainty in both bathymetry and bed roughness coefficients has been reduced during calibration to achieve optimal model representation of water levels (Zijl et al., 2013). At the time, the adjustment of bathymetry was necessary because an M2 phase lag of 15-20° occurred in the uncalibrated model. This phase lag could not be reduced sufficiently by adjusting the bottom roughness.

In the older models, NOOS bathymetry was used. By using an improved bathymetry, to a large extent derived from EMODnet (section 2.4), the need to adjust bathymetry during the calibration was reduced. Therefore, in DCSM-FM only the bottom roughness is calibrated. This approach is identical to the calibration procedure of the 2019 release of DCSM-FM 0.5nm. A justification of this approach can be found in Zijl & Groenenboom (2019).

3.1.6 Roughness area distribution

Practically it is impossible to adjust the bottom roughness in each network node since far too many parameters would then have to be estimated in proportion to the available amount of measurement data, which would lead to the problem of identifiability. Therefore, our approach is to specify larger sections as adaptation parameters. These sections are defined as samples with a section number. During the calibration OpenDA-DUD prescribes a uniform adjustment factor to each section, after which these values are interpolated on the network using triangular interpolation. By leaving a distance between the prescribed samples a smooth transition in the resulting bottom roughness is ensured.

A set of 61 roughness sections has been chosen. The initial roughness before calibration was chosen to be equal to the 2019 release of DCSM-FM 0.5nm. Deviations between 0.012 s/m$^{1/3}$

and 0.050 s/m$^{1/3}$ were allowed during calibration. An overview of the final roughness sections (samples) is presented in Figure 3.5. In Figure 3.6 and Figure 3.7 the sections in the German Bight and Dutch waters are shown in more detail.

During the recalibration of the 2022 release an experiment with a tighter upper limit for an area between the English and Zeeland coast was performed, since the resulting roughness is relatively high there (significantly higher than most surrounding areas). However, this experiment resulted in a deterioration of water level results. Therefore, this additional restriction was discarded in the final calibration.

Differences with 2019 release

- The locations of the roughness areas (each with uniform values) has mostly remain the same, except the addition of a separate roughness section in the deep (>800m), oceanic areas of the model domain.

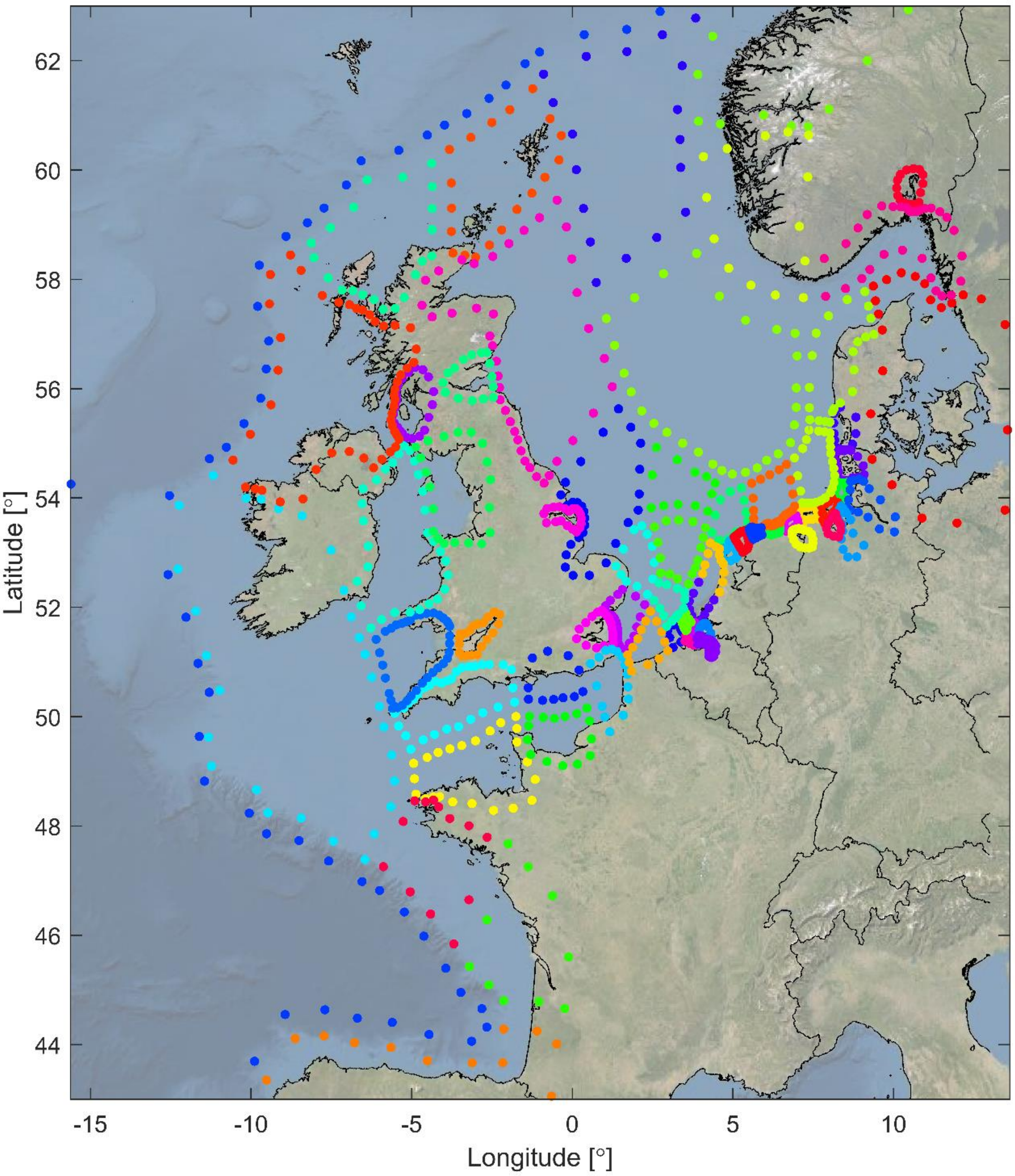

Figure 3.5 Overview of samples used to define roughness adjustments. Each colour represents a different calibration area.

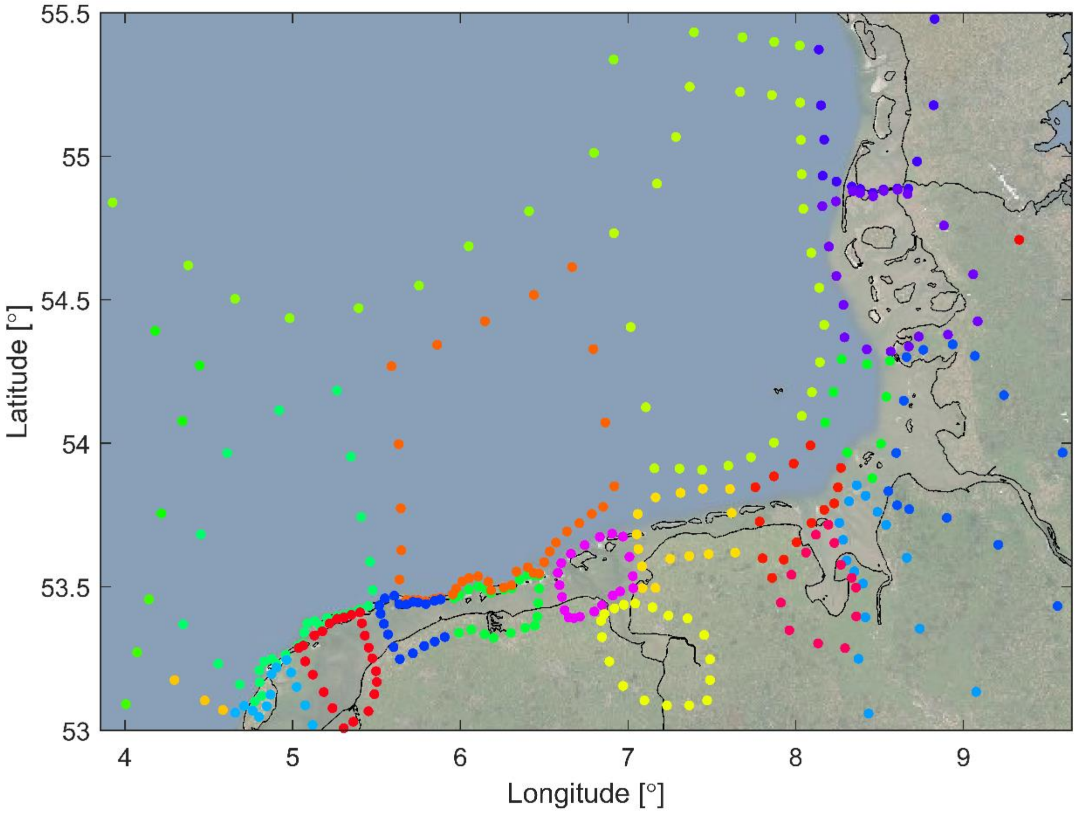

Figure 3.6 Samples used to define roughness adjustments in the German Bight. Each colour represents a different calibration area.

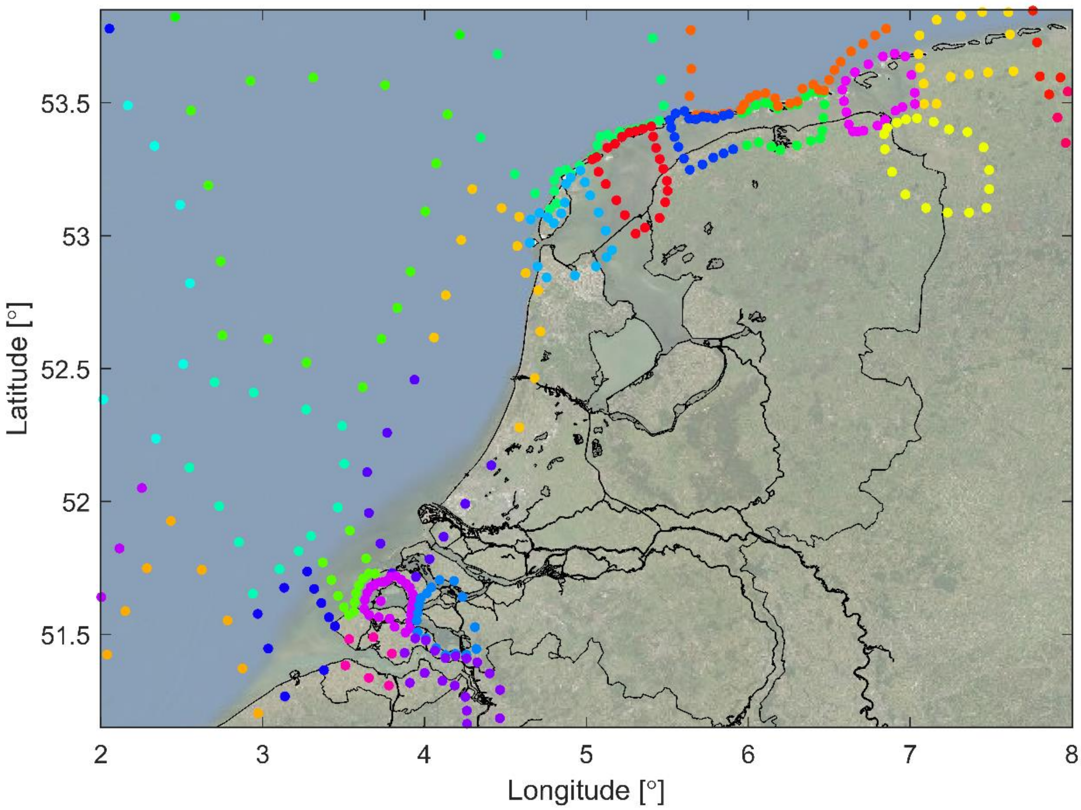

Figure 3.7 Samples used to define roughness adjustments in Dutch waters. Each colour represents a different calibration area.

3.2 Calibration results

The final calibration experiment, using 61 roughness areas and covering the entire year 2017 is described in this section. In Figure 3.8, the calibration process and improvement in cost function is visualised. The yellow dot indicates the model performance without calibration, using a uniform roughness of 0.028 s/m$^{1/3}$. The green dot indicates model performance using the starting roughness coefficients for the final calibration experiment. Five calibration experiments were performed during the recalibration of the 2022 release, with incremental changes in setup. Each time the starting roughness of an experiment was the final roughness of the previous calibration experiment. For each experiment the initial roughness perturbation for all roughness areas was set to 5% of the initial roughness.

The other small dots on the green line represent the cost function for single perturbations of each roughness area. Once this is known for all roughness areas, the problem is linearised, and combinations of adjusted roughness fields are assessed in the optimization (indicated by the blue line) to minimize the cost function.

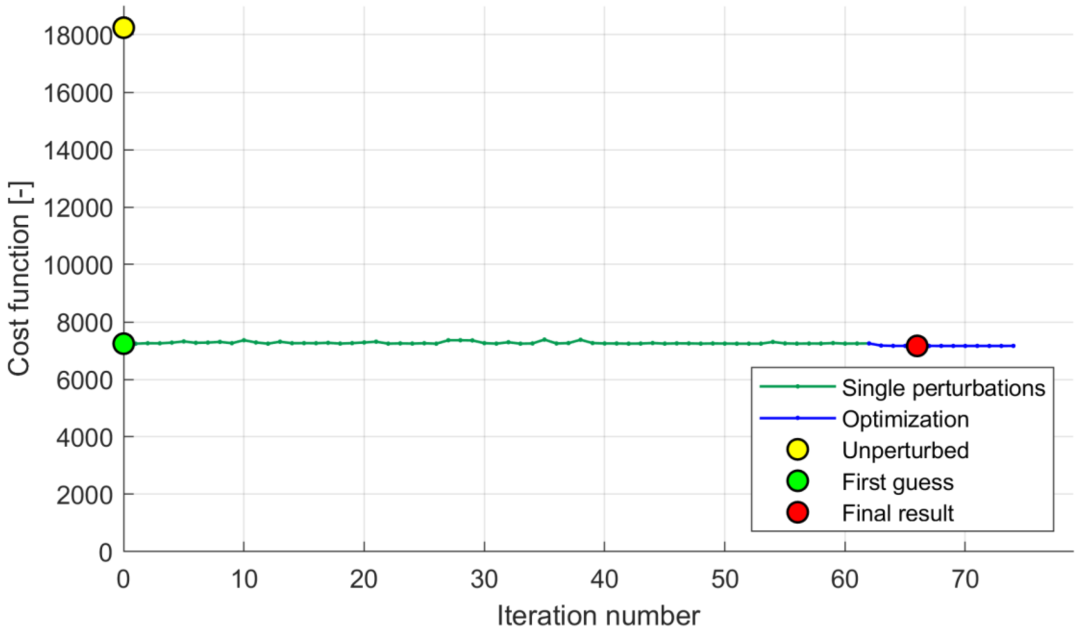

Figure 3.8 Cost function of the OpenDA-dud calibration during the final calibration experiment.

In Figure 3.9, the iteration part of the optimization is shown in more detail, by leaving out the single perturbations. The green dot represents the first guess of the OpenDA-DUD experiment. This figure illustrates how the cost function only reduces little during the first four iterations. The iteration with the minimum cost function is picked as the final roughness field, indicated here with a red dot.

During the calibration, the cost function starts at 7242 and reduces to 7165, which is a percentage decrease of about 1%. However, note that this final calibration starts with a roughness field that followed from earlier calibration experiments. The uncalibrated run with an initial, uniform roughness value of 0.028 s/m$^{1/3}$, yields a cost function is 18246. This implies that due to calibration of the bottom roughness a final improvement of 60% is achieved.

The resulting roughness field can be found in section 2.5.

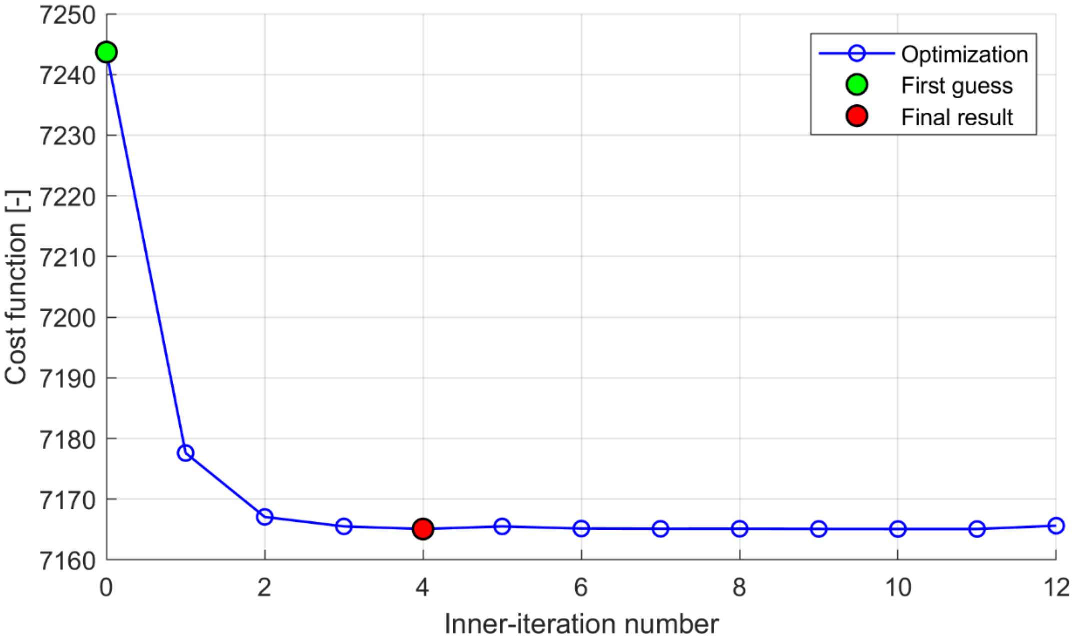

Figure 3.9 Cost function of the OpenDA-dud calibration for the optimization.

4 Validation

4.1 Introduction

After reducing uncertainty in the bottom roughness by means of an OpenDA-DUD optimization for the year 2017 (Chapter 3), the model is validated against shelf-wide measurements for the five-year period 2013-2017. This period includes the significant 5-6 December 2013 storm Xaver (the so-called 'Sinterklaasstorm' in Dutch). The validation results are presented in this chapter.

4.1.1 Model comparison to previous DCSM models

In this chapter, validation results are compared to other numerical models. The three models of interest for comparison are:

- DCSMv6 (fifth-generation model)
- DCSMv6-ZUNOv4 (fifth-generation model)
- DCSM-FM 0.5nm release 2019

All three models mentioned use Hirlam for meteorological forcing. The 2022 release of DCSM-FM 0.5nm uses ECMWF meteorological forcing. For a fair comparison of pure hydrodynamical model quality, using the same meteorological forcing is preferred. Therefore, we also make use of Hirlam forcing for the 2022 release when comparing to older models.

4.1.2 Quantitative evaluation measures (Goodness-of-Fit parameters)

Time series: total water level, tide and surge

To assess the quality of the computed water levels, the root-mean-square error (RMSE) is computed based on measured and computed total water levels for the entire 2013-2017 validation period. In addition, as it provides further insight in the origins of remaining errors, the tide and surge component are separated from the total water level (see section 4.1.3) and the quality of both tide and surge is assessed separately.

High waters

The validation results were also assessed on the capacity to accurately hindcast peaks in water level, including the most extreme high waters in the validation period. Minor differences in timing between computed and measured high waters are less critical than a correct representation of the peak water level. Therefore, the vertical difference between each computed and measured high water (approximately twice a day) is computed and based on this, the error statistics can be determined. Measured and modelled high waters are matched if the difference in timing is less than 4 hrs.

The same can be done for the tidal signal derived from measured and modelled water levels, which yields the quality of the tidal high waters. What remains after subtracting these tidal high waters from the total high waters is called the skew surge, i.e. the difference between the peak water level and the astronomical peak. Note that the skew surge is generally lower than the highest 'normal' surge in the hours surrounding the high water peak.

In addition, a subdivision is made between three categories of high water events, based on the height of the measured skew surge:

- events with the 99% lowest skew surge heights,
- events with skew surge heights between 99.0% and 99.8%
- the highest 0.2% skew surges

The latter category represents storm conditions yielding the most extreme skew surge conditions observed in the years 2013-2017. If measurements are complete, this category consists of 8 values, while the first two categories then contain 3492 and 28 values, respectively.

For the total high waters, tidal high waters and skew surge, the bias, standard deviation (std) and RMSE is determined for each of these categories.

Low waters
Since there is also an interest in the accuracy with which low waters are represented (e.g. relevant for water authorities draining into the sea by gravity flow), especially during storm surges, the error statistics for low waters are also computed. This is done in a similar manner as for the high waters. This also holds for the subdivision in categories. Note that the skew surge on which the event classification is based is then determined for the low waters.

Mean water level
The water levels computed with DCSM-FM (or any other hydrodynamic model) refer to an equipotential surface of the Earth's gravity field. Gradients in baroclinic pressure (i.e. due to density differences) affect the movement of water and can, consequently, affect the long-term mean water level (or Mean Dynamic Topography). However, the density in the model is assumed to be constant and uniform. Furthermore, while tide and surge caused by variations in atmospheric pressure are accounted for at the open boundaries, steric effects (i.e., changes in sea level due to thermal expansion and salinity variations) are not. This affects the representation of the mean water level. In an operational setting, a post-processing correction using a constant offset is therefore commonly added. In the present report, the bias between measured and computed water levels in each station, determined over the entire five-year validation period, will be disregarded in most Goodness-of-Fit criteria used here. This is achieved by correcting the measurements for this bias before these criteria are determined. Consequently, when considering the entire period, the Root-Mean-Square (RMS) of the error signal is equal to the standard deviation thereof. Another advantage of this approach is that it removes the need to convert all measurements to a uniform vertical reference plane that is valid for the entire model domain.

The addition of the MDT-correction to DCSM-FM in the 2022 release (see section 2.9.2) should to a large extent remove the bias in water level compared to NAP-referenced water level measurements. These mean water levels, including the effect of the added MDT-correction, are analysed in section 4.3.3 by computing the bias in Dutch, NAP-referenced coastal stations.

4.1.3 Harmonic analysis

The separation of the tide and surge contribution to the total water level is done by means of harmonic analysis using the MATLAB package t_tide (Pawlowicz et al., 2002). After obtaining the tide through harmonic analysis and prediction, the surge (or ‘non-tidal residual’) is obtained by subtracting the predicted tide from the total water level signal.
Since the 18.6-year nodal cycle is assumed to be constant in the harmonic analysis, we restricted the analysis period to one year. This implies that for each year in the 5-year validation period, the harmonic analysis is performed.
Harmonic analysis is only performed when the completeness index of the measurements is larger than 80% and the length of the available measurements within the analysis period is larger than 300 days.

Based on the possibility to separate constituents using a time series of one year, 118 constituents have been selected to be used in the harmonic analysis (Table 4.1). Note that the number of constituents used here is much larger than the number of constituents prescribed on the open boundaries of the model (Table 2.1). This is because many more shallow water constituents, such as compound tides and overtides, are generated inside the model domain, especially in shallow areas where non-linear processes become important. At the location of the open boundaries the amplitudes of these additional constituents are generally assumed to be negligible.

Table 4.1 List of harmonic constituents used for harmonic analysis

Component name	Angular frequency (°/h)	Component name	Angular frequency (°/h)
SA	0.0410667	3MS4	56.9523127
SSA	0.0821373	MN4	57.4238338
MSM	0.4715211	ST9	57.5059711
MM	0.5443746	ST40	57.8860712
MSF	1.0158958	M4	57.9682085
MF	1.0980330	ST10	58.0503457
ALP1	12.3827652	SN4	58.4397296
2Q1	12.8542863	KN4	58.5218669
SIG1	12.9271398	MS4	58.9841042
Q1	13.3986609	MK4	59.0662415
RHO1	13.4715145	SL4	59.5284789
O1	13.9430356	S4	60.0000000
TAU1	14.0251729	SK4	60.0821373
BET1	14.4145567	MNO5	71.3668694
NO1	14.4966940	2MO5	71.9112441
CHI1	14.5695475	MNK5	72.4649025
PI1	14.9178647	2MP5	72.9271398
P1	14.9589314	2MK5	73.0092771
S1	15.0000020	MSK5	74.0251729
K1	15.0410686	2SK5	75.0410686
PSI1	15.0821353	ST11	85.4013260
PHI1	15.1232059	2NM6	85.8635634
THE1	15.5125897	ST12	85.9457007
J1	15.5854433	2MN6	86.4079380
SO1	16.0569644	ST13	86.4900753
OO1	16.1391017	ST41	86.8701754
UPS1	16.6834763	M6	86.9523127
2NS2	26.8794591	MSN6	87.4238338
ST37	26.9523127	MKN6	87.5059711
OQ2	27.3509802	2MS6	87.9682085
EPS2	27.4238338	2MK6	88.0503458

Component name	Angular frequency (°/h)	Component name	Angular frequency (°/h)
ST2	27.5059711	NSK6	88.5218669
2N2	27.8953549	2SM6	88.9841042
MU2	27.9682085	MSK6	89.0662415
N2	28.4397296	ST16	101.9112441
NU2	28.5125831	3MK7	101.9933814
OP2	28.9019670	ST18	114.8476676
H1	28.9430376	3MN8	115.3920423
M2	28.9841043	ST19	115.4741796
H2	29.0251709	M8	115.9364170
MKS2	29.0662415	ST20	116.4079381
LDA2	29.4556253	ST21	116.4900753
L2	29.5284789	3MS8	116.9523127
T2	29.9589333	3MK8	117.0344500
S2	30.0000000	ST22	117.5059711
R2	30.0410667	ST23	117.9682085
K2	30.0821373	ST24	118.0503458
MSN2	30.5443747	ST26	130.4331109
ETA2	30.6265119	4MK9	130.9774856
2SM2	31.0158958	ST27	131.9933813
SKM2	31.0980330	ST28	144.3761465
NO3	42.3827652	M10	144.9205212
MO3	42.9271398	ST29	145.3920423
M3	43.4761564	ST30	145.9364170
SO3	43.9430356	ST31	146.4900753
MK3	44.0251729	ST32	146.9523127
SK3	45.0410687	M12	173.9046254
ST8	56.4079380	ST34	174.9205212
N4	56.8794591	ST35	175.4741796

4.2 Shelf-wide results

A spatial overview of the RMSE-values of the total water level, tide and surge of all shelf-wide tide gauge stations is given in Figure 4.1 and Figure 4.2 (left- and right-hand side panel), respectively.

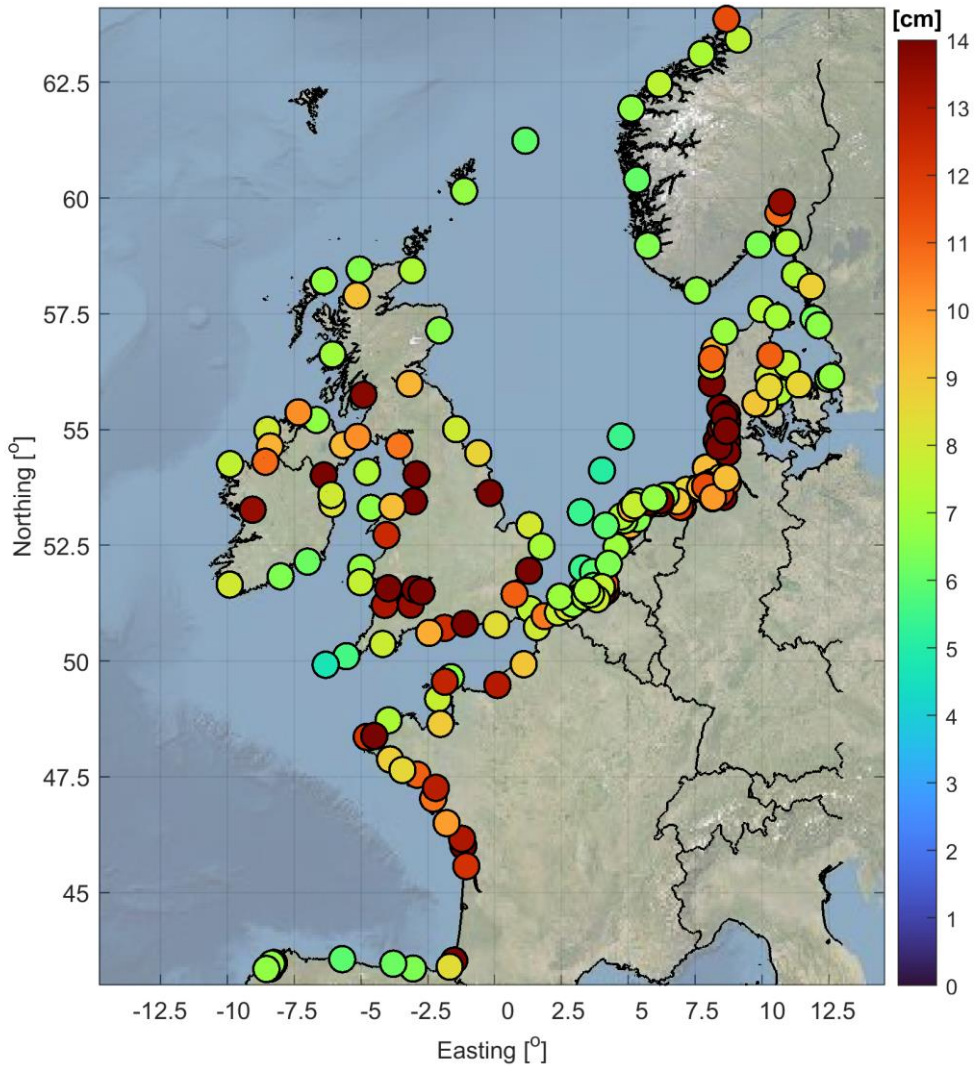

Figure 4.1 Spatial overview of the RMSE-values (cm) of the total water level for the period 2013-2017 of all shelf-wide tide gauge stations.

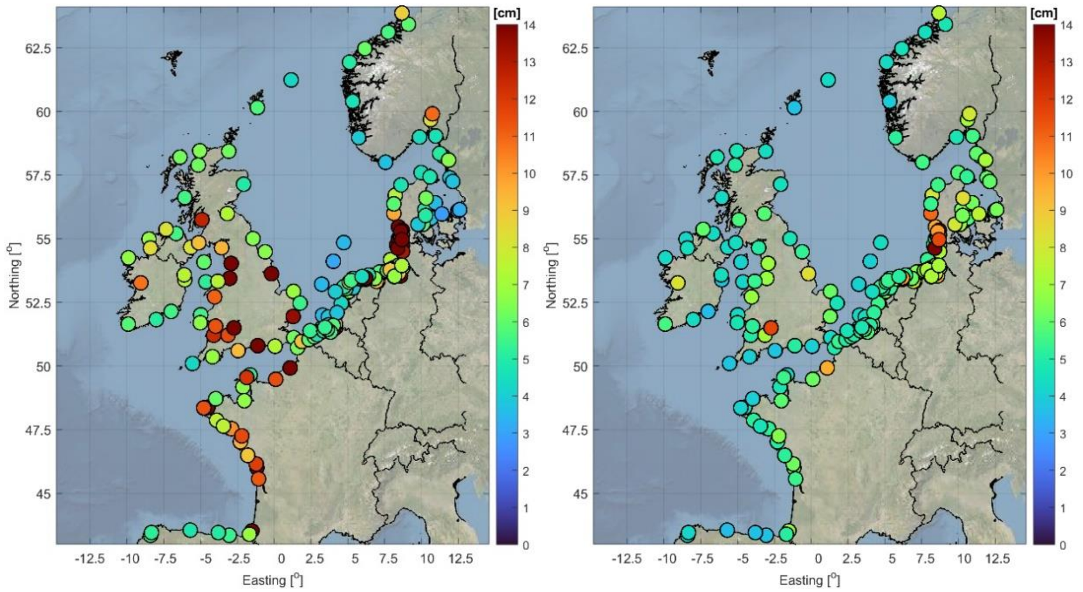

Figure 4.2 Spatial overview of the RMSE-values (cm) of the tide (left panel) and surge (right panel) for the period 2013-2017 of all shelf-wide tide gauge stations.

The mean model skill in terms of RMSE for the tide, surge and total water level for all shelf-wide tide gauge stations is summarized in Table 4.2. The table shows that the 2022 release of DCSM-FM 0.5nm has improved mean tidal representation by around 8%, from 8.9 cm to 8.2 cm, based on the same Hirlam meteorological forcing as used for the 2019 release. Changing the meteorological forcing of the 2022 release from Hirlam to ECWMF IFS improves the mean surge quality from 6.2 cm to 6.0 cm.

Table 4.2 Mean statistics (RMSE in cm) of the tide, surge and total water level for the period 2013-2017 of all shelf-wide tide gauge stations.

DCSM-FM 0.5nm release	Meteorological forcing	RMSE tide (cm)	RMSE surge (cm)	RMSE water level (cm)
2019	Hirlam	8.9	6.2	11.1
2022	Hirlam	8.2	6.2	10.8
2022	ECMWF IFS	8.2	6.0	10.7

4.3 Dutch coastal water results

4.3.1 Observation stations

For further analysis of the results, the emphasis will be on a set of 37 Dutch coastal stations with four nearby Belgian and four German stations added. A list of these 45 stations is presented in Table 4.3, in order of increasing M2 phase lag.

To further aid analysis of the model quality, a sub-division is also made in four different sets of stations: 17 stations along the North Sea coast, 5 offshore stations (more than 10-15 km from coast), 7 stations in the Eastern and Western Scheldt and 16 stations in the Wadden Sea and Ems-Dollard. In Zijl & Groenenboom (2019), station Hansweert was erroneously placed in area ‘coast’. This station has been moved to area ‘SWD’ in this report.

Table 4.3 Names of the tide gauge stations used for quantitative model evaluation in Dutch coastal waters. Some Belgian and German stations nearby have been added, indicated here with BE and DE, respectively. The stations are further subdivided in four groups: coast, offshore, south-western delta (SWD) and Wadden Sea (incl. Ems-Dollard).

ID	Station	Area	ID	Station	Area
1	Wandelaar (BE)	coast	24	Texel Noordzee	coast
2	Zeebrugge (BE)	coast	25	K13a Platform	offshore
3	Bol van Heist (BE)	coast	26	F16	offshore
4	Scheur Wielingen (BE)	coast	27	Oudeschild	Wadden Sea
5	Cadzand	coast	28	Den Oever Buiten	Wadden Sea
6	Westkapelle	coast	29	Terschelling Noordzee	coast
7	Europlatform	offshore	30	Vlieland Haven	Wadden Sea
8	Vlissingen	SWD	31	West-Terschelling	Wadden Sea
9	Roompot Buiten	coast	32	Kornwerderzand Buiten	Wadden Sea
10	Lichteiland Goeree	offshore	33	Wierumergronden	coast
11	Brouwershavense Gat 08	coast	34	Huibertgat	coast
12	Terneuzen	SWD	35	Harlingen	Wadden Sea
13	Haringvliet 10	coast	36	Nes	Wadden Sea
14	Hansweert	SWD	37	Lauwersoog	Wadden Sea
15	Roompot Binnen	SWD	38	Schiermonnikoog	Wadden Sea
16	Hoek van Holland	coast	39	Borkum Sudstrand (DE)	Wadden Sea
17	Stavenisse	SWD	40	Borkum Fischerbalje (DE)	Wadden Sea
18	Berge Diepsluis West	SWD	41	Emshorn (DE)	Wadden Sea
19	Krammerssluizen West	SWD	42	Eemshaven	Wadden Sea
20	Scheveningen	coast	43	Dukegat	Wadden Sea
21	IJmuiden Buitenhaven	coast	44	Delfzijl	Wadden Sea
22	Platform Q1	offshore	45	Knock (DE)	Wadden Sea
23	Den Helder	coast			

4.3.2 Total water levels, tide and surge

4.3.2.1 DCSM-FM 0.5nm

A spatial overview of the RMSE-values of the total water level, tide and surge of the Dutch coastal stations is presented in Figure 4.3 and Figure 4.4 (left- and right-hand side panel), respectively. Generally, the total water level RMSE is 6-8 cm in North Sea waters. In these stations, the tide and surge RMSE is generally 4-5 cm. The quality deteriorates inside the Dutch estuaries and Wadden Sea, where the model resolution is low compared to the variability in geometry and bathymetry. This is especially noticeable in the eastern Wadden Sea (including the Ems-Dollard estuary) and the eastern part of the Eastern Scheldt where tidal channels are too narrow to properly represent on the model network. The result is a poor representation of the tide, while some impact is also noticeable in the surge quality, presumably due to a poor representation of the non-linear tide-surge interaction.

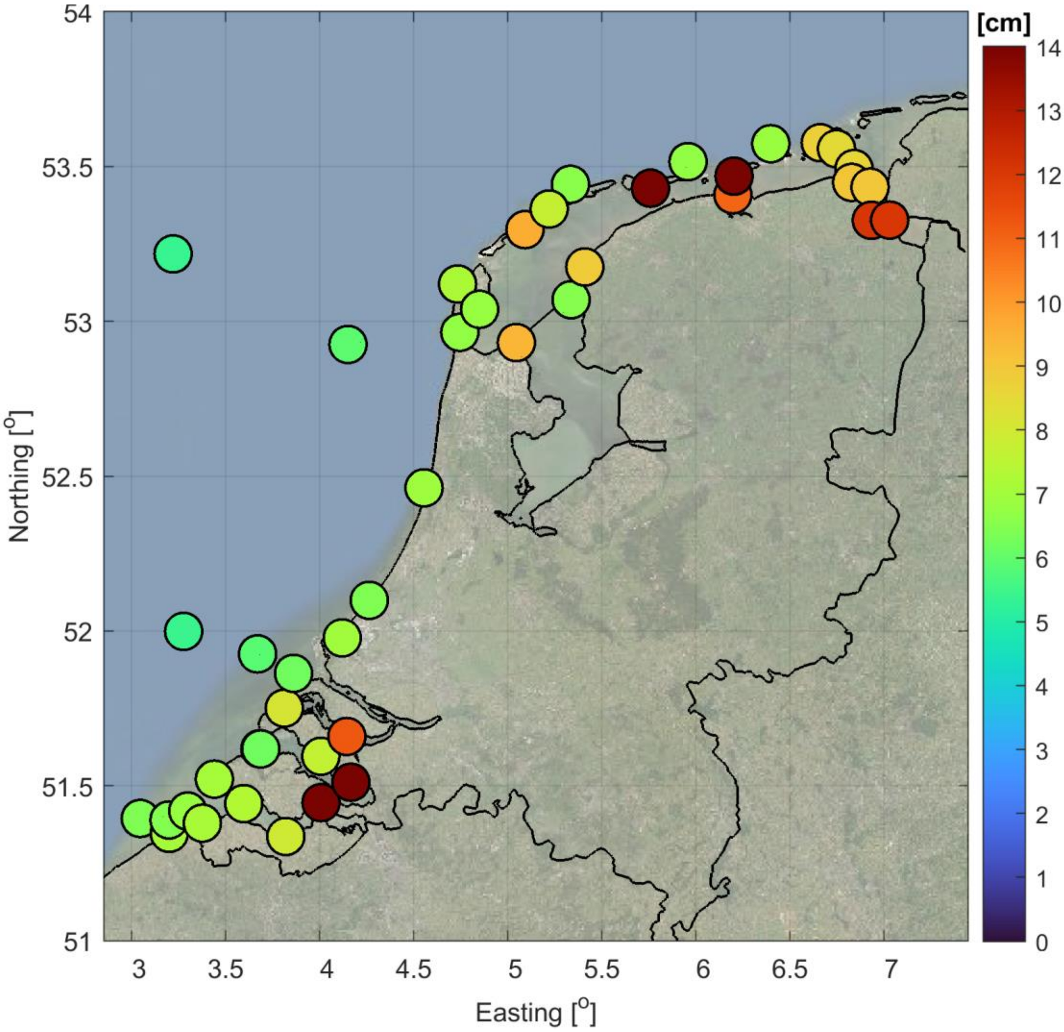

Figure 4.3 Spatial overview of the RMSE-values (cm) of the total water level for the period 2013-2017 of the Dutch coastal stations.

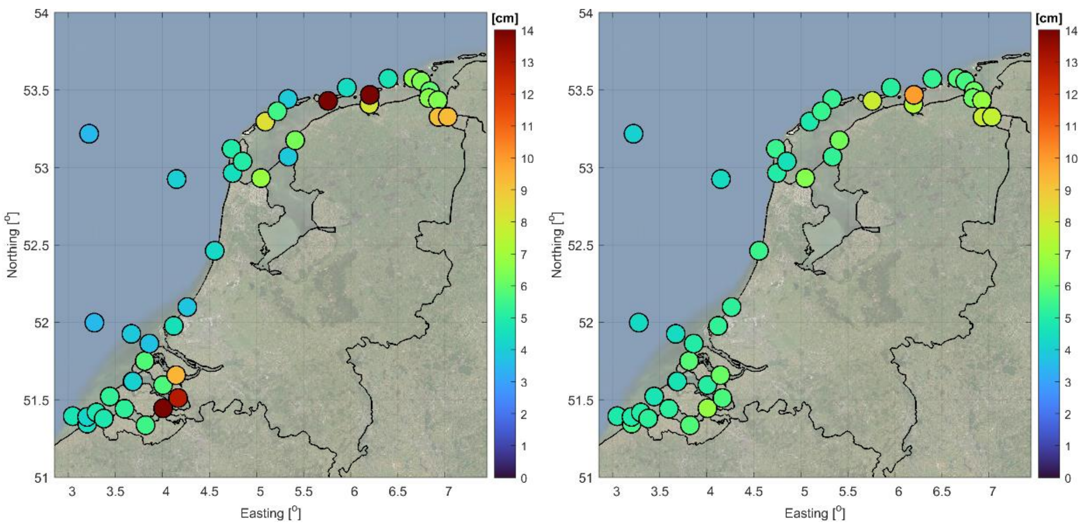

Figure 4.4 Spatial overview of the RMSE-values (cm) of the tide (left panel) and surge (right panel) for the period 2013-2017 of the Dutch coastal stations

4.3.2.2 Comparison of DCSM-FM 0.5nm with previous release

Table 4.4 shows the RMSE of tide, surge and total water level in Dutch coastal stations for the 2019 and 2022 release of DCSM-FM 0.5nm. For the 2022 release, results using both Hirlam and ECWMF meteorological forcing are presented. While the 2022 release was calibrated using ECMWF forcing, results with Hirlam were added to aid comparison with the 2019 release, which was validated in Zijl & Groenenboom (2019) using Hirlam only. A spatial overview of absolute and relative difference between the 2019 and 2022 released, for total water level, tide and surge, both forced by Hirlam, is illustrated in Figure 4.5 to Figure 4.7.

Table 4.4 shows that on the average total water level RMSE decreases from 9.2 to 8.6 cm, based on Hirlam forcing. This is due to a 10% improvement in tide representation, with the average tide RMSE decreasing from 7.0 cm to 6.3 cm. Applying ECMWF forcing yields a further total water level RMSE improvement from 8.6 to 8.5 cm. This improvement is caused by better surge representation, with the average surge RMSE decreasing from 5.8 cm to 5.6 cm.

Model performance increases in most individual stations and all four areas of interest, although the biggest increase is seen in the Wadden Sea. In the Wadden Sea, tidal error in the station Vlielandhaven (VLIELHVN) deteriorates from 3.8 to 8.2 cm RMSE, as can be seen in the dark red dot in Figure 4.5. This is caused by erroneous drying due to the coarseness of the grid and the removal of the station from the set of calibration stations. Stations Bergse Diepsluis west and Krammerssluizen west in the eastern part of the Eastern Scheldt are also affected by a poor representation of local bathymetry.

Table 4.4 Statistics (RMSE in cm) of tide, surge and total water level of the 2019 and 2022 release of DCSM-FM 0.5nm for different meteorological forcings. The first release of DCSM-FM 0.5nm used Hirlam forcing. The second release uses ECMWF. For comparability, the second release is also validated with Hirlam forcing.

Station	RMSE tide (cm)			RMSE surge (cm)			RMSE water level (cm)		
	2019 release	2022 release	2022 release	2019 release	2022 release	2022 release	2019 release	2022 release	2022 release
	Hirlam	Hirlam	ECMWF	Hirlam	Hirlam	ECMWF	Hirlam	Hirlam	ECMWF
Wandelaar	5.3	4.7	4.7	5.2	5.2	4.9	7.1	6.6	6.4
Zeebrugge_Leopold	5.8	4.4	4.4	5.8	5.8	5.5	8.2	7.3	7.1
Bol_Van_Heist	5.5	4.2	4.2	5.2	5.1	4.9	7.5	6.6	6.5
Scheur_Wielingen	5.7	4.8	4.8	5.4	5.3	5.0	7.7	7.1	6.8
CADZD	5.8	4.9	4.8	5.7	5.6	5.2	8.1	7.4	7.1
WESTKPLE	6.3	5.3	5.3	5.1	5.0	4.7	8.1	7.3	7.1
EURPFM	3.7	3.4	3.5	4.7	4.7	4.4	5.8	5.7	5.4
VLISSGN	**6.3**	**5.2**	**5.2**	**5.6**	**5.4**	**5.1**	**8.4**	**7.6**	**7.3**
ROOMPBTN	**3.8**	**3.6**	**3.7**	**5.0**	**5.0**	**4.7**	**6.3**	**6.2**	**6.0**
LICHTELGRE	4.7	3.8	3.9	4.7	4.7	4.4	6.7	6.1	5.9
BROUWHVSGT08	6.1	5.8	5.8	6.1	6.1	5.8	8.5	8.3	8.1
TERNZN	6.7	5.3	5.5	6.2	5.9	5.8	9.1	8.0	7.9
HARVT10	4.3	3.6	3.7	5.4	5.3	5.0	6.9	6.4	6.2
HANSWT	18.9	16.9	17.1	7.1	6.9	6.8	20.2	18.3	18.4
ROOMPBNN	4.4	4.1	4.1	4.9	4.9	4.7	6.6	6.4	6.2
HOEKVHLD	**4.4**	**4.4**	**4.5**	**5.8**	**5.6**	**5.3**	**7.3**	**7.1**	**7.0**

Station	RMSE tide (cm)			RMSE surge (cm)			RMSE water level (cm)		
	2019 release	2022 release	2022 release	2019 release	2022 release	2022 release	2019 release	2022 release	2022 release
	Hirlam	Hirlam	ECMWF	Hirlam	Hirlam	ECMWF	Hirlam	Hirlam	ECMWF
STAVNSE	5.5	5.7	5.7	5.4	5.3	5.1	7.7	7.8	7.7
BERGSDSWT	11.0	12.8	12.9	6.2	6.1	5.7	12.6	14.2	14.1
KRAMMSZWT	8.1	9.3	9.4	6.3	6.3	6.1	10.2	11.2	11.2
SCHEVNGN	4.5	3.8	3.8	5.6	5.5	5.2	7.1	6.7	6.5
IJMDBTHVN	5.4	4.2	4.3	5.8	5.7	5.4	7.9	7.1	6.9
Q1	4.2	3.9	4.0	4.6	4.5	4.4	6.3	6.0	5.9
DENHDR	**4.2**	**4.4**	**4.5**	**5.1**	**5.2**	**5.0**	**6.6**	**6.8**	**6.7**
TEXNZE	5.0	5.0	5.0	5.6	5.6	5.4	7.4	7.4	7.2
K13APFM	4.3	3.4	3.5	4.4	4.3	4.1	6.1	5.5	5.4
F16	3.0	2.9	3.1	4.1	4.1	4.0	5.0	5.0	5.1
OUDSD	4.6	4.9	5.0	4.7	4.8	4.6	6.6	6.8	6.8
DENOVBTN	7.4	6.6	6.8	6.9	6.9	6.5	10.1	9.5	9.4
TERSLNZE	4.4	4.0	3.9	5.6	5.6	5.4	7.1	6.8	6.6
VLIELHVN	3.8	8.2	8.3	5.0	4.9	4.8	6.3	9.6	9.6
WESTTSLG	4.8	5.4	5.6	5.0	5.3	5.4	7.0	7.5	7.7
KORNWDZBTN	4.6	3.6	3.8	5.7	5.6	5.3	7.3	6.7	6.5
WIERMGDN	4.8	4.5	4.4	5.5	5.4	5.1	7.2	6.9	6.7
HUIBGT	5.2	4.9	4.7	5.7	5.7	5.3	7.5	7.2	6.9
HARLGN	**8.7**	**6.2**	**6.3**	**6.8**	**6.4**	**6.2**	**11.0**	**8.9**	**8.9**
NES	15.4	15.1	15.1	7.6	7.6	7.9	17.2	16.9	17.0
LAUWOG	14.2	8.2	8.1	7.5	7.1	7.4	16.0	10.8	11.0
SCHIERMNOG	24.2	18.8	18.9	9.9	9.7	9.9	26.1	21.1	21.4
BORKUM_Sudstr.	7.3	6.5	6.6	5.7	5.7	5.8	9.2	8.6	8.8
BorkumFischerbalje	6.7	6.4	6.4	5.7	5.8	5.6	8.8	8.5	8.5
EMSHORN	7.6	6.0	5.9	6.1	6.1	6.2	9.7	8.6	8.6
EEMSHVN	7.2	6.6	6.6	6.2	6.2	6.1	9.5	9.1	9.0
DUKEGAT	8.0	6.5	6.4	7.0	6.9	6.8	10.1	9.1	8.9
DELFZL	**10.8**	**9.4**	**9.2**	**7.9**	**7.8**	**7.8**	**13.4**	**12.2**	**12.1**
KNOCK	11.0	9.6	9.3	7.7	7.6	7.7	13.4	12.2	12.0
Average (total)	**7.0**	**6.3**	**6.3**	**5.8**	**5.8**	**5.6**	**9.2**	**8.6**	**8.5**
Average (offshore)	**4.0**	**3.5**	**3.6**	**4.5**	**4.5**	**4.3**	**6.0**	**5.6**	**5.5**
Average (coast)	**5.1**	**4.5**	**4.5**	**5.5**	**5.5**	**5.2**	**7.4**	**7.0**	**6.8**
Average (ZWD)	**8.7**	**8.5**	**8.6**	**5.9**	**5.8**	**5.6**	**10.7**	**10.5**	**10.4**
Average (WS)	**9.1**	**8.0**	**8.0**	**6.6**	**6.5**	**6.5**	**11.4**	**10.4**	**10.4**

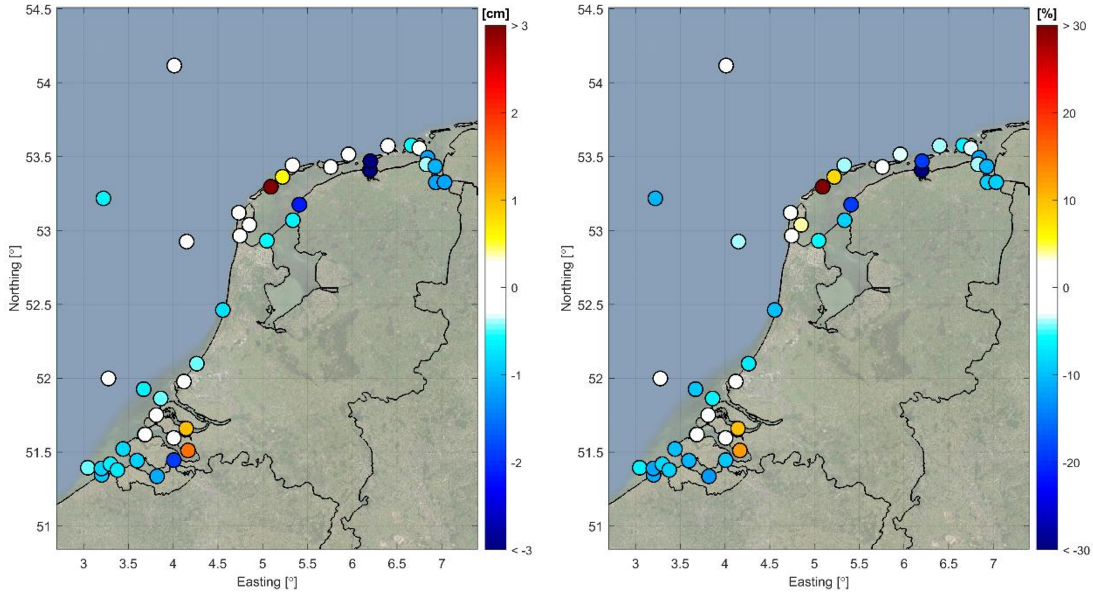

*Figure 4.5 Spatial overview of the difference (DCSM-FM 0.5nm release 2022 minus DCSM-FM 0.5nm release 2019) in RMSE of the **total water level** for the period 2013-2017 of the Dutch coastal stations. Left: difference (cm); right: relative difference (%).*

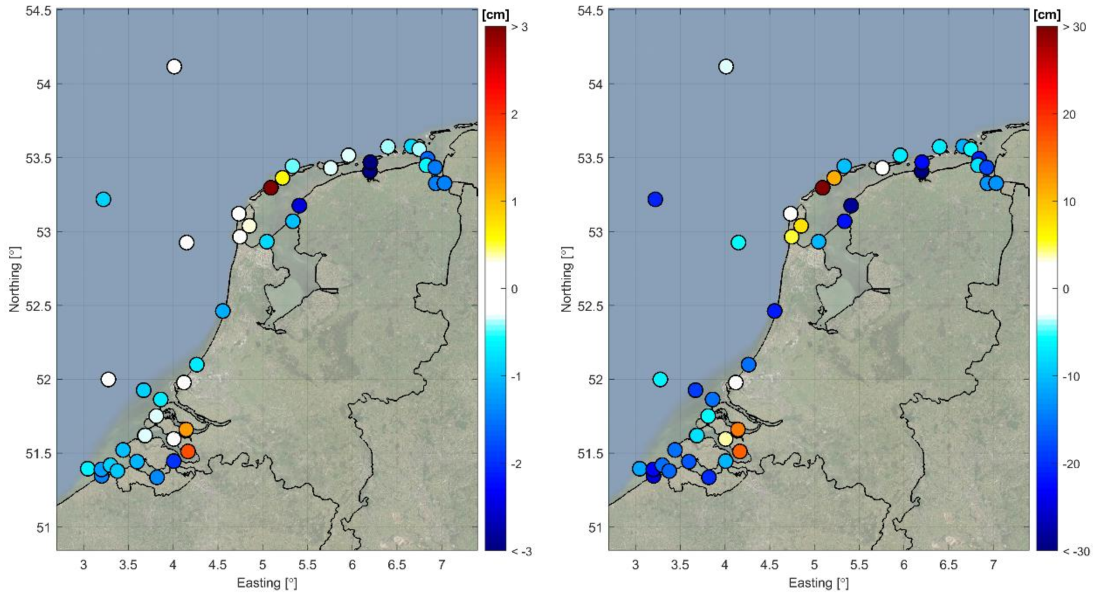

*Figure 4.6 Spatial overview of the difference (DCSM-FM 0.5nm release 2022 minus DCSM-FM 0.5nm release 2019) in RMSE of the **tide** for the period 2013-2017 of the Dutch coastal stations. Left: difference (cm); right: relative difference (%).*

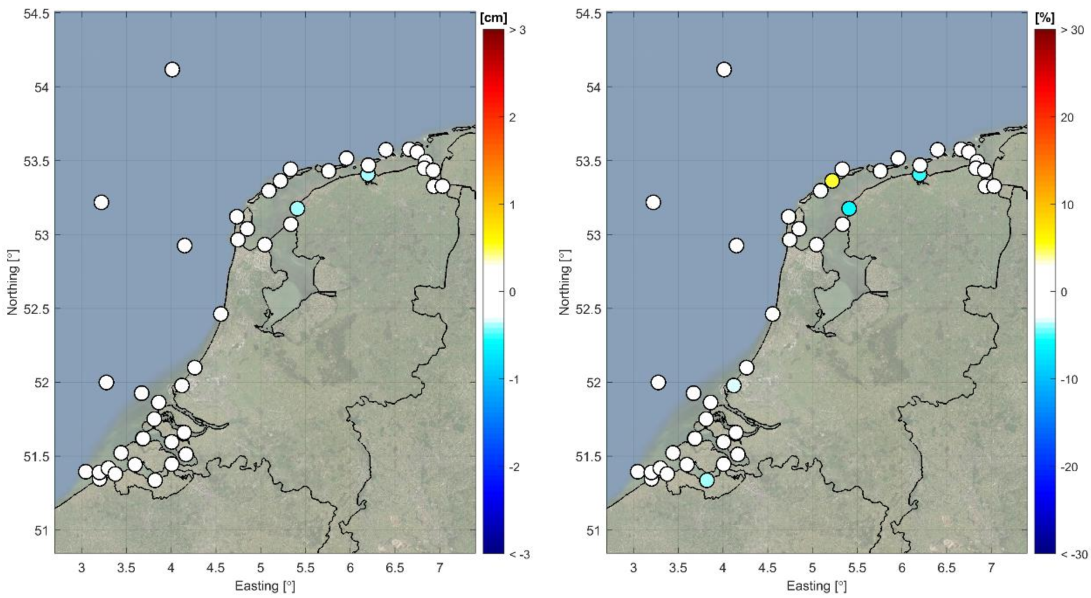

*Figure 4.7 Spatial overview of the difference (DCSM-FM 0.5nm release 2022 minus DCSM-FM 0.5nm release 2019) in RMSE of the **surge** for the period 2013-2017 of the Dutch coastal stations. Left: difference (cm); right: relative difference (%).*

4.3.2.3 Comparison of DCSM-FM 0.5nm against DCSMv6 and DCSMv6-ZUNOv4

Table 4.5 shows the RMSE of tide, surge and total water level in Dutch coastal stations, for the current release of the sixth-generation model DCSM-FM 0.5nm, in comparison to the fifth-generation models DCSMv6 and DCSMv6-ZUNOv4. A spatial overview of the absolute and percentage difference in RMSE (DCSMv6 minus DCSM-FM 0.5nm), for both total water level, tide and surge, is illustrated in Figure 4.8 to Figure 4.10. The results presented in this section are all based on Hirlam meteorological forcing.

These results show that on average the tide representation is slightly worse than both fifth-generation models. This is probably because of the exclusion of bathymetry as a calibration parameter in the development of DCSM-FM. Especially in coarsely represented areas, adjustments in bathymetry helped overcome the poor resolution and improve the tide representation locally. In the offshore and coastal stations, the tide representation of DCSM-FM has improved compared to both fifth-generation models. In addition, in all 6 main locations (Dutch: 'hoofdlocaties'), Roompot Buiten, Vlissingen, Hoek van Holland, Den Helder, Harlingen and Delfzijl, the tide representation of DCMS-FM is better or equal than that of DCSMv6. It should however be noted that the quality of the tide representation in DCSMv6 has deteriorated since the year for which it has been calibrated (2007).

The average quality of the surge (RMSE 5.7 cm) is in between the quality of DCSMv6 (RMSE 6.0 cm) and DCSMv6-ZUNOv4 (RMSE 5.6 cm). In the offshore and coastal stations, the surge representation of DCSM-FM has improved compared to both fifth-generation models. In the SWD and Wadden Sea area, as well as all main locations, the surge quality is better than DCSMv6.

Table 4.5 Statistics (RMSE in cm) of tide, surge and total water level of the fifth-generation models (DCSMv6 and DCSMv6-ZUNOv4) and the sixth generation model (DCSM-FM 0.5 nm) for the Dutch coastal stations. All models use Hirlam for meteorological forcing. The main locations (Dutch: 'hoofdlocaties') are shown in bold. Area averages are shown at the bottom of the table for stations that have available validation data in all models.

Station	RMSE tide (cm)			RMSE surge (cm)			RMSE water level (cm)		
	DCSMv6	DCSMv6-ZUNOv4	DCSM-FM 0.5nm	DCSMv6	DCSMv6-ZUNOv4	DCSM-FM 0.5nm	DCSMv6	DCSMv6-ZUNOv4	DCSM-FM 0.5nm
Wandelaar	4.9	4.4	4.7	5.4	5.3	5.2	7.0	6.6	6.6
Zeebrugge_Leop.	4.8	4.6	4.4	6.2	6.0	5.8	7.8	7.6	7.3
Bol_Van_Heist	4.3	4.7	4.2	5.5	5.3	5.1	7.0	7.1	6.6
Scheur_Wielingen.	4.4	5.3	4.8	5.6	5.5	5.3	7.1	7.6	7.1
CADZD	4.3	4.4	4.9	5.9	5.7	5.6	7.3	7.3	7.4
WESTKPLE	3.8	4.4	5.3	5.3	5.2	5.0	6.6	6.8	7.3
EURPFM	4.8	4.0	3.4	4.9	4.7	4.7	6.8	6.1	5.7
VLISSGN	**5.2**	**4.8**	**5.2**	**5.9**	**5.5**	**5.4**	**7.9**	**7.3**	**7.6**
ROOMPBTN	**3.9**	**4.4**	**3.6**	**5.4**	**5.2**	**5.0**	**6.6**	**6.8**	**6.2**
LICHTELGRE	4.1	4.9	3.8	4.9	4.8	4.7	6.4	6.8	6.1
BROUWHVSGT08	4.6	5.0	5.8	6.2	6.1	6.1	7.6	7.8	8.3
TERNZN	7.9	5.6	5.3	6.5	6.0	5.9	10.3	8.2	8.0
HARVT10	4.3	4.4	3.6	5.5	5.4	5.3	7.0	7.0	6.4
HANSWT	14.2	6.1	16.9	7.8	6.2	6.9	16.2	8.6	18.3
ROOMPBNN	7.2	4.3	4.1	5.1	4.9	4.9	8.8	6.4	6.4
HOEKVHLD	**4.8**	**5.0**	**4.4**	**5.8**	**5.3**	**5.6**	**7.5**	**7.3**	**7.1**
STAVNSE	5.8	3.9	5.7	5.5	5.2	5.3	7.9	6.4	7.8
BERGSDSWT	7.1	4.6	12.8	6.0	5.5	6.1	9.2	7.1	14.2
KRAMMSZWT		4.3	9.3		6.4	6.3		7.7	11.2
SCHEVNGN	5.0	5.2	3.8	5.7	5.6	5.5	7.6	7.6	6.7
IJMDBTHVN	5.9	6.3	4.2	6.0	5.9	5.7	8.4	8.7	7.1
Q1	4.7	4.2	3.9	4.6	4.6	4.5	6.6	6.2	6.0
DENHDR	5.1	4.6	4.4	5.3	5.2	5.2	7.4	6.9	6.8
TEXNZE	5.1	4.9	5.0	5.7	5.7	5.6	7.6	7.4	7.4
K13APFM	3.4	3.4	3.4	4.5	4.4	4.3	5.6	5.5	5.5
F16	2.8	2.9	2.9	4.1	4.4	4.1	5.0	5.2	5.0
OUDSD	4.3	4.8	4.9	4.9	4.7	4.8	6.5	6.7	6.8
DENOVBTN	6.0	6.5	6.6	6.8	6.8	6.9	9.1	9.4	9.5
TERSLNZE	4.3	4.1	4.0	5.8	5.8	5.6	7.2	7.0	6.8
VLIELHVN	5.8	4.7	8.2	5.1	5.0	4.9	7.7	6.9	9.6
WESTTSLG	4.5	3.6	5.4	5.5	5.0	5.3	7.1	6.1	7.5
KORNWDZBTN	4.3	3.7	3.6	6.3	5.7	5.6	7.6	6.8	6.7
WIERMGDN	4.8	4.1	4.5	5.7	5.7	5.4	7.4	6.9	6.9
HUIBGT	5.4	4.9	4.9	6.1	6.1	5.7	7.9	7.5	7.2

Station	RMSE tide (cm)			RMSE surge (cm)			RMSE water level (cm)		
	DCSMv6	DCSMv6 - ZUNOv4	DCSM-FM 0.5nm	DCSMv6	DCSMv6 - ZUNOv4	DCSM-FM 0.5nm	DCSMv6	DCSMv6 - ZUNOv4	DCSM-FM 0.5nm
HARLGN	**8.0**	**4.5**	**6.2**	**7.8**	**5.8**	**6.4**	**11.2**	**7.3**	**8.9**
NES	8.8	5.9	15.1	7.7	6.0	7.6	11.7	8.4	16.9
LAUWOG	9.4	6.5	8.2	7.5	6.8	7.1	12.0	9.4	10.8
SCHIERMNOG	10.3	7.2	18.8	7.9	6.9	9.7	13.0	10.0	21.1
BORKUM_Sudstr.		4.4	6.5		5.8	5.7		7.2	8.6
BorkumFischerbalje		4.7	6.4		5.8	5.8		7.4	8.5
EMSHORN		5.6	6.0		6.2	6.1		8.4	8.6
EEMSHVN	6.3	6.8	6.6	6.8	6.3	6.2	9.3	9.3	9.1
DUKEGAT		8.2	6.5		7.1	6.9		10.5	9.1
DELFZL	**15.4**	**6.8**	**9.4**	**11.1**	**7.5**	**7.8**	**19.0**	**10.1**	**12.2**
KNOCK		7.1	9.6		7.3	7.6		10.2	12.2
Average (total)	**5.9**	**4.9**	**6.1**	**6.0**	**5.6**	**5.7**	**8.5**	**7.4**	**8.4**
Average (offshore)	**4.0**	**3.9**	**3.5**	**4.6**	**4.6**	**4.5**	**6.1**	**6.0**	**5.6**
Average (coast)	**4.7**	**4.8**	**4.5**	**5.7**	**5.6**	**5.5**	**7.3**	**7.3**	**7.0**
Average (ZWD)	**7.9**	**4.9**	**8.3**	**6.2**	**5.6**	**5.8**	**10.1**	**7.4**	**10.4**
Average (WS)	**7.6**	**5.5**	**8.5**	**7.0**	**6.0**	**6.6**	**10.4**	**8.2**	**10.8**

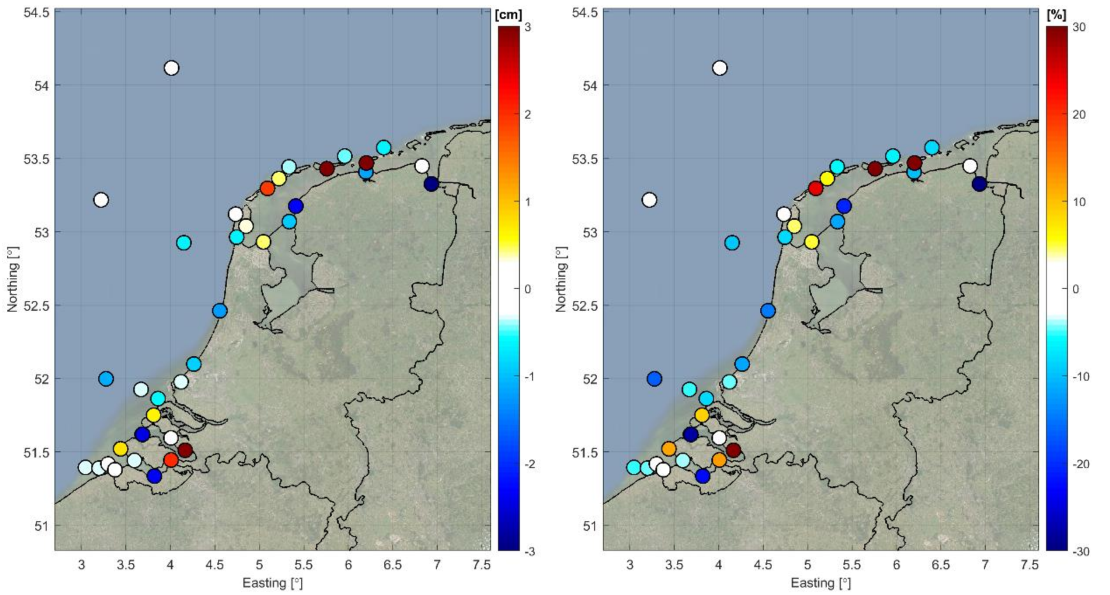

Figure 4.8 Spatial overview of the difference (DCSM-FM 0.5nm minus DCSMv6) in RMSE of the ***total water level*** *for the period 2013-2017 of the Dutch coastal stations. Left: difference (cm); right: relative difference (%).*

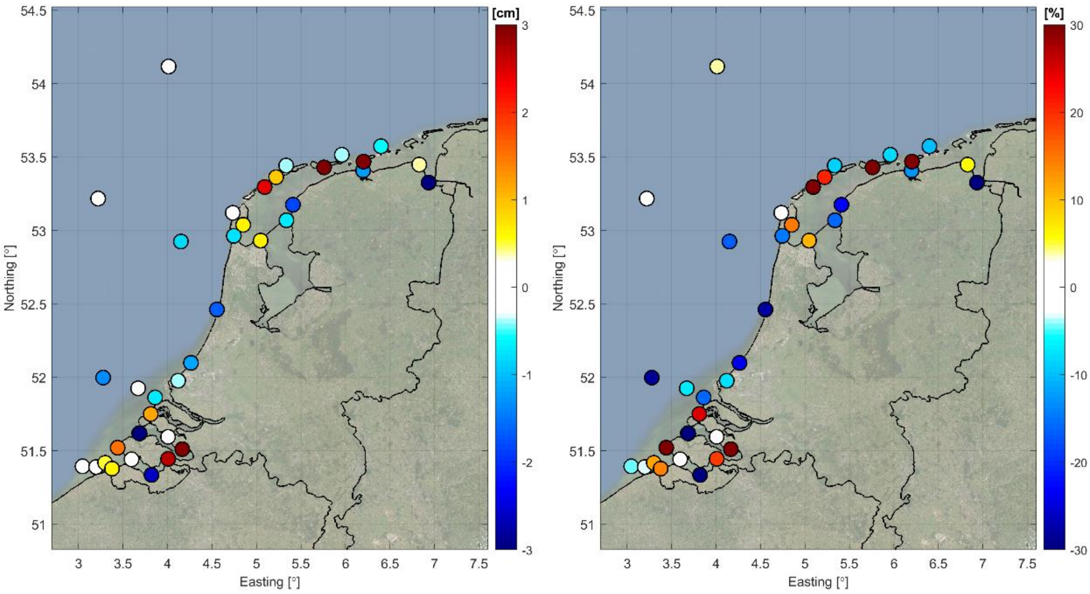

Figure 4.9 Spatial overview of the difference (DCSM-FM 0.5nm minus DCSMv6) in RMSE of the ***tide*** *for the period 2013-2017 of the Dutch coastal stations. Left: difference (cm); right: relative difference (%).*

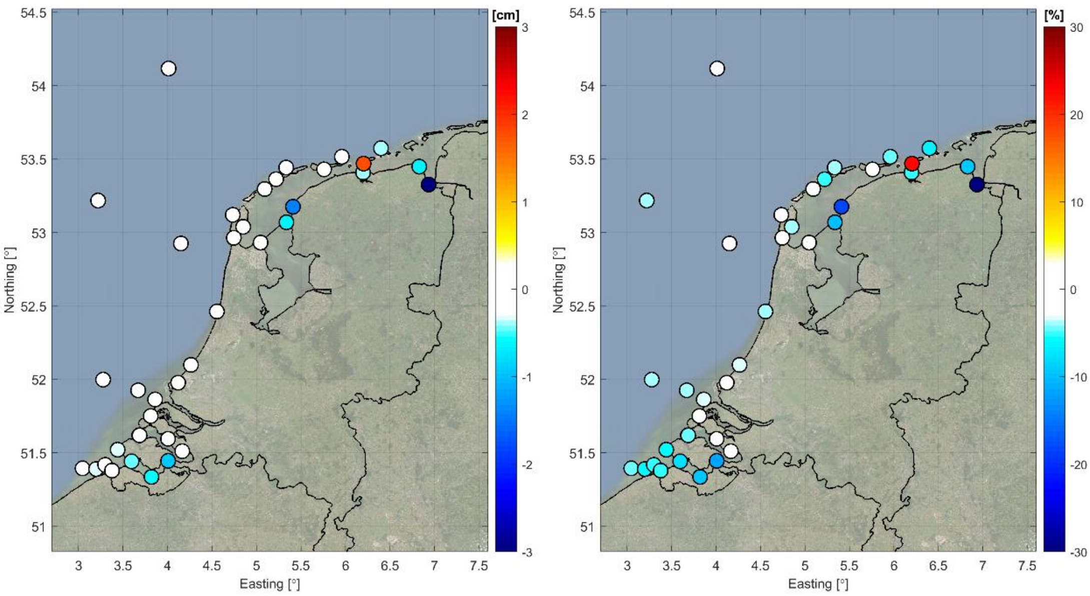

Figure 4.10 Spatial overview of the difference (DCSM-FM 0.5nm minus DCSMv6) in RMSE of the ***surge*** *for the period 2013-2017 of the Dutch coastal stations. Left: difference (cm); right: relative difference (%).*

4.3.3 Bias in Dutch NAP-referenced stations

With the addition of the MDT-correction (section 2.9.2), the constant bias in Dutch NAP-referenced stations is greatly reduced in the 2022 release of DSCM-FM 0.5nm, compared to the 2019 release. Table 4.6 shows the bias in Dutch NAP-referenced stations for the 2019 and 2022 release of DCSM-FM 0.5nm for different meteorological forcings. Figure 4.11 shows a spatial comparison of the bias in the 2019 and 2022 released, based on Hirlam forcing.

Table 4.6 shows that the average bias is reduced from 2.7 cm to 0.6 cm in the 2022 release based on Hirlam. Using ECMWF forcing, the average bias is 0.0 cm. The standard deviation of bias between stations is also reduced, from 3.6 cm to 2.4 cm in the 2022 release. This improvement can be seen in all area's (Wadden Sea, Southwestern delta, and coastal stations). Note that the bias in the Wadden Sea and the southwestern Delta shows a higher spread than in the coastal stations. This is probably partially due to a poor local resolution, also in the model on which the MDT-correction is based (3D DCSM-FM).

Table 4.6 Bias in Dutch NAP-referenced stations for different releases and meteo-forcings. For stations that are affected by drying up, water levels below the thresholds in Table 3.1 are not considered when calculating bias.

Station	**Water level bias**		
	2019 release	**2022 release**	**2022 release**
	Hirlam	**Hirlam**	**ECMWF**
CADZD	5.2	1.4	1.0
WESTKPLE	3.5	-1.3	-1.7
VLISSGN	1.9	-1.8	-2.3
ROOMPBTN	4.4	0.3	-0.2
BROUWHVSGT08	1.2	-2.5	-2.9
TERNZN	-3.3	-3.4	-3.9
HARVT10	5.6	2.2	1.9
HANSWT	-6.1	-5.3	-5.9
ROOMPBNN	5.3	1.5	1.1
HOEKVHLD	-3.4	-2.9	-3.3
STAVNSE	6.1	3.3	2.8
BERGSDSWT	6.4	4.8	4.3
KRAMMSZWT	5.0	2.3	1.7
SCHEVNGN	3.8	1.7	1.4
IJMDBTHVN	2.4	0.1	-0.1
DENHDR	2.5	0.0	-0.2
TEXNZE	4.6	0.7	0.6
OUDSD	3.9	2.4	2.1
DENOVBTN	1.7	2.0	1.3
TERSLNZE	6.3	1.7	1.0
VLIELHVN	6.3	0.6	0.0
WESTTSLG	5.9	3.1	3.0
KORNWDZBTN	2.3	2.7	2.3
WIERMGDN	4.9	0.6	-0.6
HUIBGT	3.5	-0.4	-1.8
HARLGN	-1.0	0.4	0.1
NES	-0.9	-1.5	-2.6
LAUWOG	1.0	1.6	-0.5
SCHIERMNOG	3.1	3.4	1.6
EEMSHVN	5.6	4.6	2.8
DELFZL	-2.7	-2.3	-4.4
Average (total)	**2.7**	**0.6**	**0.0**
Average (coast)	**3.4**	**0.1**	**-0.4**
Average (ZWD)	**2.2**	**0.2**	**-0.3**
Average (WS)	**2.3**	**1.5**	**0.5**
St. dev. (total)	**3.3**	**2.4**	**2.4**
St. dev. (coast)	**2.5**	**1.6**	**1.6**
St. dev. (ZWD)	**5.0**	**3.8**	**3.7**
St. dev. (WS)	**3.0**	**2.1**	**2.3**

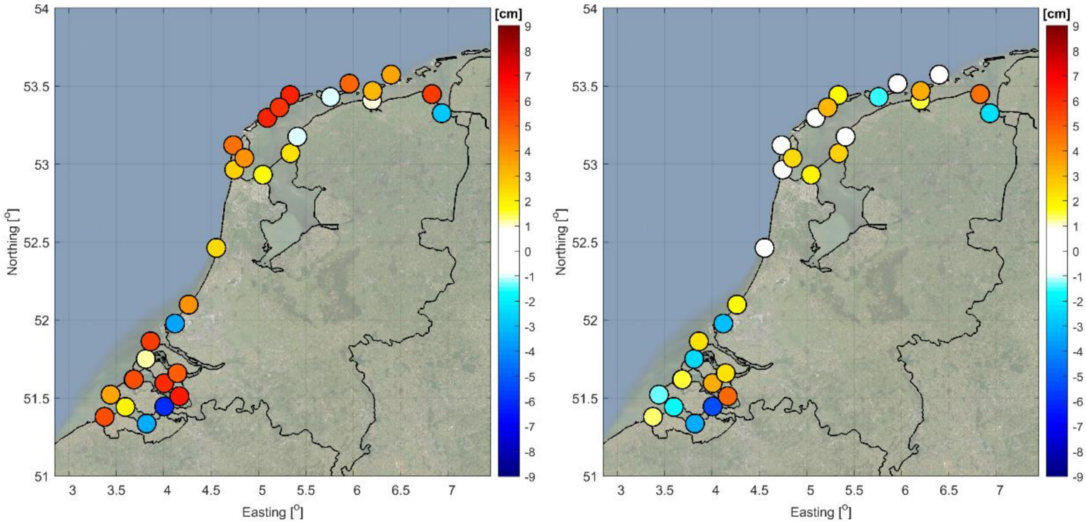

Figure 4.11 Spatial overview of the bias in the Dutch NAP-referenced stations over the period 2013-2017. ***Left:*** *DCSM-FM 0.5 nm release 2019, Hirlam meteo.* ***Right:*** *DCSM-FM 0.5 nm release 2022, Hirlam meteo.*

4.3.4 Tide (frequency domain)

4.3.4.1 Amplitude and phase error of the M2 component

Figure 4.12 illustrates the amplitude and phase error of the M2-component, respectively. These results show that generally, in stations not hampered by a poor model resolution, the amplitude error is less than 2 cm, while the phase error is less than 1°.

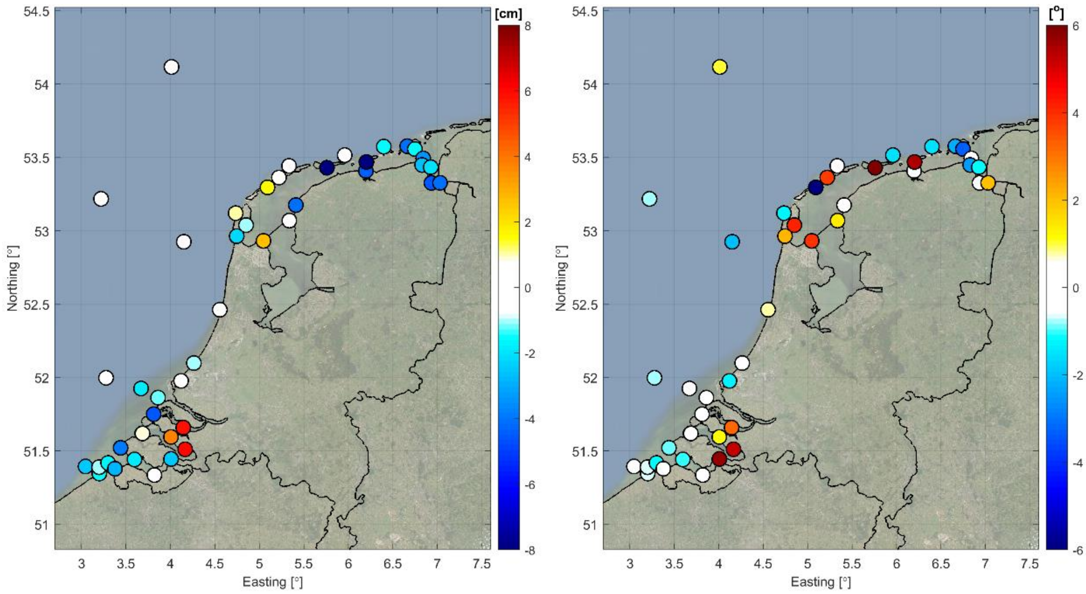

Figure 4.12 Spatial overview of the amplitude error (cm; left) and phase error (º) of the M2-component.

4.3.4.2 Contribution of harmonic components to tidal error

In Table 4.7 to Table 4.12 an overview is given of the errors in the 10 harmonic constituents with the largest contribution to the tidal error in each of the six main locations. M2 has the largest contribution to the tidal error in three of the six stations considered here. This is not surprising, since it is by far the largest constituent in Dutch coastal waters.

In the other three stations, M4 has the largest contribution to the tidal error. Since M4 is generated though non-linear processes, the correct representation of which requires sufficient spatial resolution, it is not surprising that the stations where M4 is the largest contributor (Hoek van Holland, Harlingen and Delfzijl) are all hampered by a poor resolution with which local geometry and bathymetry is represented. This also affects other compound and overtides, such as MS4, MN4, M6, 2MS6 and 3MS8, which can be found in these tables.

H1 has the largest error in one station (Delfzijl), the second largest error in four out of six stations (Vlissingen, Roompot buiten and Den Helder) and the third largest error in Harlingen. This is despite the relatively small observed H1 amplitude of 2-6 cm in Dutch coastal waters. The origin of H1, which together with H2 represents an annual modulation of the M2 tide that is non-gravitational in nature, is poorly understood. It is at least partially influenced by seasonal stratification in the southern North Sea, which is not included in this depth-averaged barotropic model, and can therefore not be expected to be well represented without dedicated parameterizations.

Errors in the annual and semi-annual constituents Sa and Ssa are also prominent in most stations presented here. Since Sa is much less gravitational than meteorological and baroclinic in nature, the Sa harmonic constituent at the boundary has been tuned to get a good average representation in Dutch coastal waters. While this is better than just using the gravitational contribution, this method is expected to misrepresent the spatial pattern of the phase and amplitude of Sa.

Table 4.7 Overview of the 10 tidal components that have the largest contribution (in terms of vector difference) to the tidal error for station Vlissingen.

Vlissingen									
Comp.	**Obs. ampl. (cm)**	**Ampl. error (cm)**	**Phase error (º)**	**VD (cm)**	**Comp.**	**Obs. ampl. (cm)**	**Ampl. error (cm)**	**Phase error (º)**	**VD (cm)**
M2	171.6	-1.8	-1.0	3.5	**M4**	12.7	-1.2	0.1	1.2
H1	3.6	-2.8	-44.3	3.0	**M6**	8.6	1.2	1.0	1.2
S2	46.4	-2.4	-1.5	2.7	**N2**	28.3	-0.8	-0.6	0.8
SSA	2.9	-0.8	26.0	1.4	**OP2**	1.2	-0.2	39.1	0.8
SA	7.8	-0.6	-8.3	1.3	**3MS8**	4.4	-0.7	2.8	0.7

Table 4.8 Overview of the 10 tidal components that have the largest contribution (in terms of vector difference) to the tidal error for station Roompot buiten.

Roompot buiten									
Comp.	**Obs. ampl. (cm)**	**Ampl. error (cm)**	**Phase error (º)**	**VD (cm)**	**Comp.**	**Obs. ampl. (cm)**	**Ampl. error (cm)**	**Phase error (º)**	**VD (cm)**
M4	12.3	1.5	5.5	2.0	**M2**	133.0	0.2	-0.4	0.9
H1	2.2	-1.5	-42.7	1.7	**MS4**	8.2	0.8	2.0	0.9
SSA	3.2	-0.9	26.4	1.5	**RHO1**	1.1	-0.6	-31.5	0.7
S2	34.7	-1.2	0.7	1.3	**MN4**	4.3	0.6	5.2	0.7
SA	8.3	-0.9	-4.8	1.1	**M6**	6.7	0.6	-2.5	0.7

Table 4.9 Overview of the 10 tidal components that have the largest contribution (in terms of vector difference) to the tidal error for station Hoek van Holland.

Hoek van Holland									
Comp.	**Obs. ampl. (cm)**	**Ampl. error (cm)**	**Phase error (º)**	**VD (cm)**	**Comp.**	**Obs. ampl. (cm)**	**Ampl. error (cm)**	**Phase error (º)**	**VD (cm)**
M4	17.9	1.0	-5.7	2.1	**SSA**	3.6	-1.0	18.0	1.4
SA	8.6	-0.8	-12.4	1.9	**MU2**	8.0	0.8	-5.9	1.2
M2	76.5	0.7	-1.2	1.8	**H2**	0.8	-0.0	81.1	1.0
MS4	11.1	0.2	-7.8	1.6	**S2**	18.1	-0.4	2.5	0.9
H1	1.6	-0.9	-79.0	1.6	**3MS8**	3.7	0.1	-12.5	0.8

Table 4.10 Overview of the 10 tidal components that have the largest contribution (in terms of vector difference) to the tidal error for station Den Helder.

Den Helder									
Comp.	**Obs. ampl. (cm)**	**Ampl. error (cm)**	**Phase error (º)**	**VD (cm)**	**Comp.**	**Obs. ampl. (cm)**	**Ampl. error (cm)**	**Phase error (º)**	**VD (cm)**
M2	62.6	-2.2	2.1	3.1	**M4**	10.3	0.0	6.1	1.1
H1	2.4	-1.8	-57.9	2.2	**H2**	0.8	-0.4	142.4	1.1
SA	10.8	-1.8	-6.4	2.2	**2MS6**	5.5	0.3	-7.8	0.8
SSA	4.7	-0.9	16.0	1.5	**MU2**	7.7	-0.7	-0.9	0.7
M6	5.8	0.3	-10.4	1.1	**RHO1**	1.0	-0.6	-30.2	0.7

Table 4.11 Overview of the 10 tidal components that have the largest contribution (in terms of vector difference) to the tidal error for station Harlingen.

Harlingen									
Comp.	**Obs. ampl. (cm)**	**Ampl. error (cm)**	**Phase error (º)**	**VD (cm)**	**Comp.**	**Obs. ampl. (cm)**	**Ampl. error (cm)**	**Phase error (º)**	**VD (cm)**
M2	80.8	-4.1	0.4	4.2	**M6**	4.2	-1.5	9.4	1.6
M4	10.7	-0.6	21.1	3.9	**SSA**	5.9	-0.8	13.1	1.5
H1	2.5	-2.2	82.0	2.4	**2MS6**	3.7	-1.4	10.1	1.4
MS4	5.9	-0.0	17.8	1.8	**MN4**	3.4	-0.1	24.1	1.4
SA	11.1	-1.5	-4.1	1.6	**MU2**	11.0	-1.1	3.1	1.3

Table 4.12 Overview of the 10 tidal components that have the largest contribution (in terms of vector difference) to the tidal error for station Delfzijl.

Delfzijl									
Comp.	**Obs. ampl. (cm)**	**Ampl. error (cm)**	**Phase error (º)**	**VD (cm)**	**Comp.**	**Obs. ampl. (cm)**	**Ampl. error (cm)**	**Phase error (º)**	**VD (cm)**
M4	18.1	-5.5	12.2	6.3	**2MS6**	6.5	-2.1	8.9	2.3

Delfzijl									
Comp.	**Obs. ampl. (cm)**	**Ampl. error (cm)**	**Phase error (º)**	**VD (cm)**	**Comp.**	**Obs. ampl. (cm)**	**Ampl. error (cm)**	**Phase error (º)**	**VD (cm)**
H1	6.1	-4.8	-34.5	5.1	**M6**	6.9	-1.6	12.7	2.1
M2	131.7	-4.6	0.4	4.7	**H2**	0.8	0.4	-117.4	1.7
MS4	10.7	-3.2	11.7	3.7	**S2**	32.4	-1.4	0.8	1.5
MN4	5.9	-2.0	14.8	2.3	**SSA**	6.2	-0.9	10.2	1.4

4.3.5 Skew surge (high water)

The error statistics for three skew surge categories, at the Dutch coastal stations, can be found in Table 4.13. A spatial overview of the RMSE of the high water skew surge (<99.0%, i.e., calm conditions) in the Dutch coastal stations is presented in Figure 4.13. These results are based on simulations with ECMWF meteorological forcing, and show a skew surge error of around 5 cm in North Sea waters. In the eastern Wadden Sea and Dutch estuaries, the error increases to about 6-7 cm. The high-water skew surge is less sensitive to the quality with which the tide is represented (compared to the surge), and therefore shows a more uniform model quality.

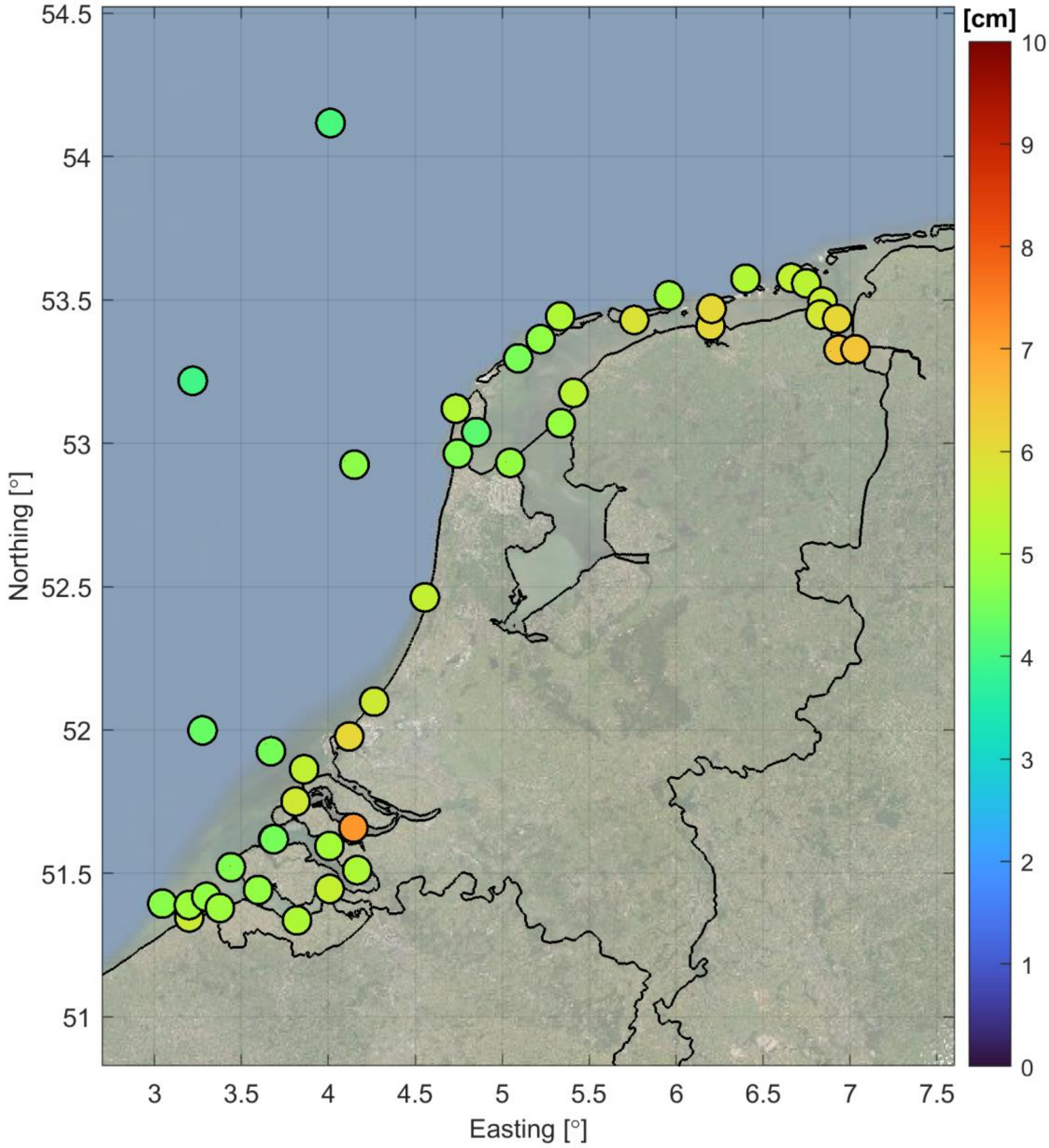

Figure 4.13 Spatial overview of the RMSE (cm) of the skew surge height for high waters (<99.0% skew surges)

In Figure 4.14, the bias and RMSE of the most extreme (>99.8%) skew surge events are presented. This shows an excellent quality in southern waters, with RMSE values less than 10-15 cm. One notable exception in that region is Brouwershavense Gat, which exhibits a bias of -14.1 cm and consequently has an RMSE of 20.7 cm. This is presumably caused by the presence of seiches during storms, which are not represented in the model.
Stations in the north, especially inside the Wadden Sea show larger skew surge errors. This is mostly due to a large systematic underestimation of the skew surge during storms. The bias is generally largest in the eastern part of the Wadden Sea and increases from north to south. In the Ems-Dollard the bias can reach 30-40 cm.

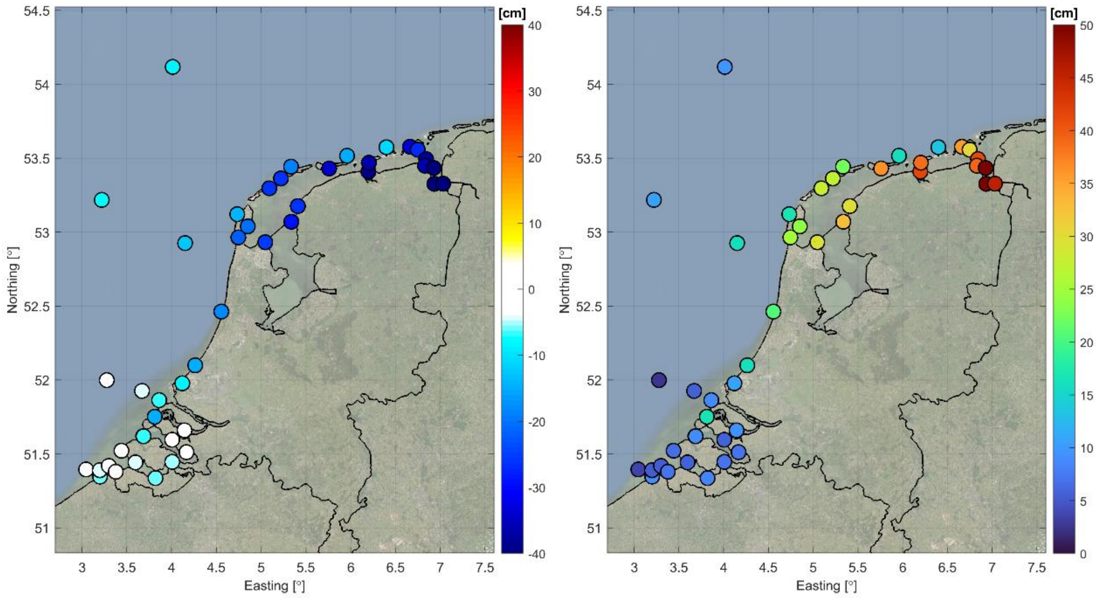

Figure 4.14 Spatial overview of the bias in cm (left panel) and RMSE in cm (right panel) of the skew surge height for high waters (>99.8% skew surges)

Table 4.13 Overview of the model skill to represent skew surge heights (high waters), for three different event classes, in terms of bias (cm) and the RMSE (cm) for Dutch coastal stations. Results are based on ECMWF meteorological forcing.

	Tidal high water		**Skew surge error (high water)**						
	all		**<99.0% skew surges**		**99.0% - 99.8% skew surges**		**>99.8% skew surges**		
Station	**bias (cm)**	**RMSE (cm)**	**bias (cm)**	**RMSE (cm)**	**bias (cm)**	**RMSE (cm)**	**Bias (cm)**	**Std (cm)**	**RMSE (cm)**
Wandelaar	-2.2	3.8	-0.5	5.1	1.7	8.0	-1.6	8.8	8.9
Zeebrugge_Leopold.	-0.2	3.0	-1.8	6.1	1.8	10.2	-4.6	11.3	12.2
Bol_Van_Heist	-0.1	2.7	-1.2	5.3	0.8	7.4	-1.9	9.5	9.7
Scheur_Wielingen_.	-1.0	3.1	-0.2	5.4	0.8	9.2	-2.8	11.0	11.4
CADZD	-3.0	4.4	0.1	5.5	2.6	8.0	1.1	8.4	8.5
WESTKPLE	-4.4	5.6	0.4	5.1	2.8	7.2	-1.0	8.9	9.0
EURPFM	-0.1	2.5	0.4	4.7	0.9	7.0	-1.6	9.0	9.2
VLISSGN	**-1.0**	**3.5**	**0.2**	**5.3**	**2.6**	**8.7**	**-0.3**	**10.6**	**10.6**
ROOMPBTN	**1.2**	**2.8**	**-0.6**	**4.9**	**-1.0**	**9.6**	**-8.9**	**9.5**	**13.0**
LICHTELGRE	-4.3	5.6	-0.2	4.9	-0.3	8.0	-2.9	9.0	9.5
BROUWHVSGT08	-8.2	9.3	-1.1	6.1	-5.2	13.7	-14.1	15.3	20.7
TERNZN	2.3	4.6	0.1	5.7	1.9	10.1	0.6	12.1	12.1
HARVT10	-3.0	4.3	-1.6	5.8	-0.9	11.3	-6.1	6.8	9.1
HANSWT	0.6	5.1	-0.2	6.1	2.0	10.0	0.3	10.1	10.1
ROOMPBNN	2.2	3.2	-0.9	5.0	2.7	10.0	0.5	6.2	6.2
HOEKVHLD	**0.6**	**3.6**	**-3.1**	**6.4**	**-2.2**	**12.8**	**-8.6**	**7.3**	**11.3**
STAVNSE	6.1	6.6	-0.3	5.7	8.2	13.1	5.2	7.7	9.3

	Tidal high water		Skew surge error (high water)						
	all		<99.0% skew surges		99.0% - 99.8% skew surges		>99.8% skew surges		
Station	**bias (cm)**	**RMSE (cm)**	**bias (cm)**	**RMSE (cm)**	**bias (cm)**	**RMSE (cm)**	**Bias (cm)**	**Std (cm)**	**RMSE (cm)**
BERGSDSWT	11.2	11.7	1.0	5.9	10.6	14.8	2.6	10.8	11.1
KRAMMSZWT	10.0	10.9	-1.3	7.8	7.7	13.5	4.6	11.5	12.4
SCHEVNGN	-1.3	3.7	-1.9	6.0	-3.6	10.7	-11.6	12.5	17.0
IJMDBTHVN	1.9	3.8	-1.2	5.9	-3.0	12.9	-16.4	8.2	18.4
Q1	1.3	3.6	-0.7	5.0	-1.2	10.0	-11.8	14.7	18.9
DENHDR	-1.5	3.3	-0.9	4.8	-5.9	9.3	-17.8	16.7	24.4
TEXNZE	2.0	4.3	-1.4	5.4	-4.7	13.3	-11.1	13.0	17.1
K13APFM	-1.9	3.4	-0.1	4.2	1.6	6.5	-6.7	10.1	12.1
F16	0.7	2.6	-0.3	4.2	0.6	5.7	-10.8	3.8	11.4
OUDSD	-0.3	2.7	-0.3	4.5	-2.6	7.3	-17.1	17.3	24.3
DENOVBTN	2.6	3.8	-0.8	5.2	-5.4	9.6	-20.2	22.5	30.2
TERSLNZE	0.9	2.7	-1.1	5.4	-3.9	11.3	-14.1	12.5	18.9
VLIELHVN	1.3	2.9	-0.5	4.7	-1.6	9.1	-22.7	8.4	24.2
WESTTSLG	-1.6	2.8	0.0	4.9	-2.0	10.2	-23.4	8.1	24.8
KORNWDZBTN	1.5	3.3	-0.6	5.2	-3.5	10.6	-21.4	20.5	29.7
WIERMGDN	-0.9	2.8	-0.5	5.2	4.6	10.5	-12.1	5.2	13.2
HUIBGT	-2.9	4.6	-0.7	5.7	8.7	12.3	-3.4	8.4	9.1
HARLGN	**-0.2**	**3.2**	**-0.3**	**5.6**	**-2.4**	**11.6**	**-17.0**	**17.9**	**24.6**
NES	-0.5	3.4	0.5	5.9	-6.2	13.6	-26.0	13.8	29.4
LAUWOG	-0.7	4.2	0.2	6.5	-5.5	13.2	-29.7	14.6	33.1
SCHIERMNOG	-3.2	4.7	0.4	6.5	-4.8	13.0	-28.4	12.9	31.2
BORKUM_Sudstran.	-2.9	4.6	-0.2	5.8	0.2	9.8	-24.2	12.3	27.1
BorkumFischerbalje	-0.2	3.2	0.0	5.9	4.3	10.2	-17.6	11.4	21.0
EMSHORN	0.5	3.6	0.2	5.9	-2.0	11.5	-27.5	13.7	30.7
EEMSHVN	0.4	3.8	-0.1	6.2	-1.7	11.3	-25.1	13.0	28.3
DUKEGAT	2.1	4.9	-0.2	6.6	-1.5	16.3	-41.5	14.5	43.9
DELFZL	**-1.2**	**4.4**	**-0.5**	**6.7**	**2.6**	**14.0**	**-32.0**	**17.2**	**36.4**
KNOCK	-1.0	4.3	0.2	6.7	5.8	14.9	-24.3	17.1	29.7
Average (total)	**-0.2**	**4.1**	**-0.5**	**5.5**	**-0.3**	**10.4**	**-10.8**	**11.4**	**17.1**
Average (offshore)	**-0.9**	**3.5**	**-0.2**	**4.6**	**0.3**	**7.4**	**-6.7**	**9.3**	**12.2**
Average (coast)	**-1.3**	**4.0**	**-1.0**	**5.5**	**-0.4**	**10.4**	**-7.9**	**10.2**	**13.6**
Average (SWD)	**3.6**	**5.8**	**0.0**	**5.6**	**4.7**	**11.1**	**1.5**	**9.6**	**9.9**
Average (WS)	**-0.2**	**3.6**	**-0.2**	**5.6**	**-3.0**	**11.2**	**-23.9**	**15.1**	**28.7**

Comparison against DCSMv6, DCSMv6-ZUNOv4 and DCSM-FM 0.5nm 2019 release
The error statistics at the Dutch coastal stations can be found in Appendix table A.2 to Appendix table A.4 for the fifth-generation models (at the Dutch coastal stations) and previous release of

DCSM-FM 0.5nm. These results are summarised in Table 4.14, where the station-averaged error statistics are compared. For a fair comparison, Hirlam meteorological forcing is used for all four models presented here.

These results show that on average the quality of the tidal high waters has improved since the 2019 release. The quality is on average better than DCSMv6 and the same as DCSMv6-ZUNOv4, although the spatial distribution is different. The skew surge error under calm conditions (<99.0%) has also improved in the 2022 release and is in all areas better than both fifth-generation models. The quality of the most extreme skew surges (>99.8%) has on average remained the same as in the 2019 release. Differences with the previous generation models are also relatively small; much smaller than the spatial variation in representation quality of the most extreme skew surges.

Table 4.14 Comparison of the station-averaged model skill to represent skew surge heights (high waters), for three different event classes, in terms of bias (cm) and the RMSE (cm) for Dutch coastal stations. The area averages are computed over areas that are available in all models. For all models, Hirlam was used for meteorological forcing.

	Tidal error high water		Skew surge (high water)						
	all		<99.0% skew surges		99.0% - 99.8% skew surges		>99.8% skew surges		
	bias (cm)	RMSE (cm)	bias (cm)	RMSE (cm)	bias (cm)	RMSE (cm)	bias (cm)	std (cm)	RMSE (cm)
Total									
DCSMv6	2.8	5.5	-0.2	5.7	1.5	11.5	-10.7	12.3	17.8
DCSMv6-ZUNOv4	2.5	4.4	-0.3	5.4	-0.9	10.8	-13.5	12.1	19.0
DCSM-FM 0.5nm (2019)	-0.8	4.8	-0.4	5.5	-0.5	10.5	-11.9	11.4	18.0
DCSM-FM 0.5nm (2022)	-0.7	4.4	-0.4	5.2	-1.7	10.5	-12.7	11.0	18.0
Offshore									
DCSMv6	0.9	3.4	-0.2	4.8	0.2	7.7	-8.2	9.6	13.5
DCSMv6-ZUNOv4	0.8	3.0	-0.2	4.6	0.1	7.5	-9.0	9.4	13.5
DCSM-FM 0.5nm (2019)	-1.9	4.3	-0.3	4.6	-0.4	7.4	-7.7	9.8	13.0
DCSM-FM 0.5nm (2022)	-1.7	4.1	-0.3	4.5	0.0	7.4	-7.4	9.3	12.5
Coast									
DCSMv6	1.6	3.9	-0.8	5.6	0.2	11.1	-8.8	11.1	14.8
DCSMv6-ZUNOv4	2.9	4.5	-0.6	5.5	-1.2	11.2	-10.6	11.2	15.9
DCSM-FM 0.5nm (2019)	-2.2	4.8	-1.0	5.6	-1.2	10.7	-9.3	10.1	14.3
DCSM-FM 0.5nm (2022)	-1.6	4.3	-0.7	5.4	-1.2	10.5	-8.7	9.8	13.6
South-western Delta									
DCSMv6	3.3	9.6	0.4	6.4	8.1	13.2	2.7	9.6	10.2
DCSMv6-ZUNOv4	2.0	4.4	0.0	5.4	2.7	10.1	-2.9	10.1	10.6
DCSM-FM 0.5nm (2019)	2.7	6.4	0.2	5.9	6.7	11.8	2.7	8.8	9.6
DCSM-FM 0.5nm (2022)	-2.8	5.3	0.2	5.3	3.9	10.3	-0.4	8.8	8.8
Wadden Sea									
DCSMv6	5.0	6.4	0.1	6.0	0.2	12.9	-21.5	16.7	27.8
DCSMv6-ZUNOv4	3.2	4.8	-0.1	5.6	-2.8	12.2	-25.3	15.8	30.2

	Tidal error high water		Skew surge (high water)						
	all		<99.0% skew surges		99.0% - 99.8% skew surges		>99.8% skew surges		
	bias (cm)	RMSE (cm)	bias (cm)	RMSE (cm)	bias (cm)	RMSE (cm)	bias (cm)	std (cm)	RMSE (cm)
DCSM-FM 0.5nm (2019)	-0.4	4.1	-0.1	5.6	-3.7	11.0	-25.2	15.3	30.0
DCSM-FM 0.5nm (2022)	2.2	4.2	-0.2	5.3	-6.0	11.9	-27.2	14.6	31.5

4.3.6 Skew surge (low water)

The error statistics for three low water skew surge categories, at the Dutch coastal stations, can be found in Table 4.15. A spatial overview of the RMSE of the low water skew surge (<99.0%, i.e., calm conditions) in the Dutch coastal stations is presented in Figure 4.15. These results are based on simulations with ECMWF meteorological forcing, and show a low water skew surge error of around 5 cm in North Sea waters. In the eastern Wadden Sea and Dutch estuaries, the error increases to about 7 cm and up to 10 cm in Schiermonnikoog. While the low water skew surge is less sensitive to the quality with which the tide is represented (compared to the surge, and similar to the high water skew surge), it is sensitive to the accuracy with which the bathymetry is represented. Particularly in areas where the resolution of the model is coarse relative to the variability in bathymetry, this hampers the quality of the low water skew surge representation.

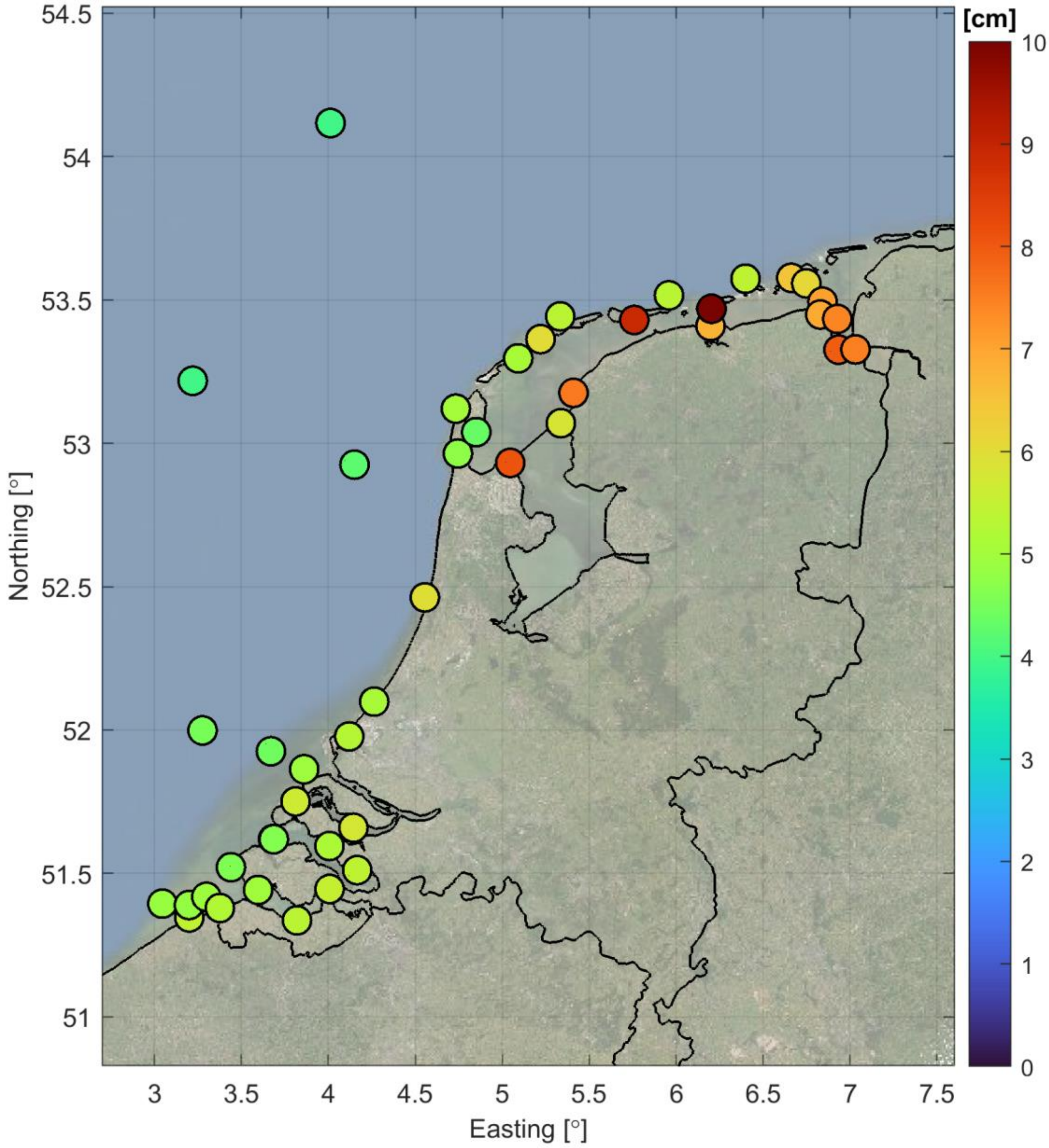

Figure 4.15 Spatial overview of the RMSE (cm) of the skew surge height for low waters (<99.0% skew surges).

In Figure 4.16, the bias and RMSE of the low water skew surge during the most extreme (>99.8%) skew surge events is presented. In southern waters this shows a larger systematic underestimation of low waters, than for high waters during the same category of events. The underestimation increases in upstream direction inside the Eastern and Western Scheldt. The most extreme biases are presumably caused by a poor representation of the local bathymetry due to the coarseness of the network.

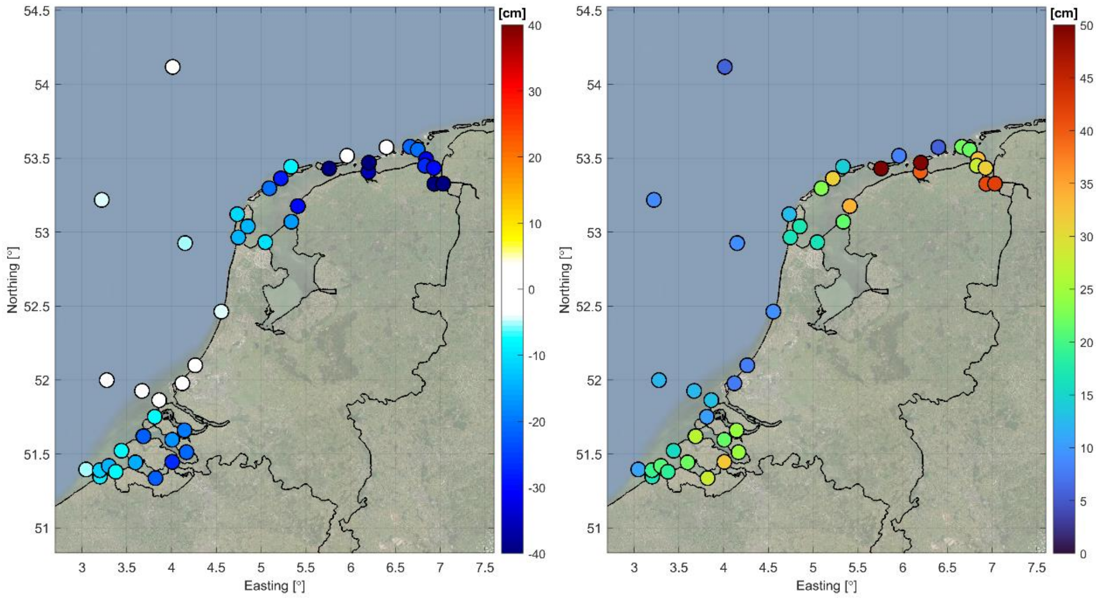

Figure 4.16 Spatial overview of the bias in cm (left panel) and RMSE in cm (right panel) of the skew surge height for low waters (>99.8% skew surges)

Table 4.15 Overview of the model skill to represent skew surge heights (high waters), for three different event classes, in terms of bias (cm) and the RMSE (cm) for Dutch coastal stations. Results are based on ECMWF meteo forcing.

	Tidal error low water		**Skew surge error (low water)**						
	all		**<99.0% skew surges**		**99.0% - 99.8% skew surges**		**>99.8% skew surges**		
Station	**bias (cm)**	**RMSE (cm)**	**bias (cm)**	**RMSE (cm)**	**bias (cm)**	**RMSE (cm)**	**Bias (cm)**	**Std (cm)**	**RMSE (cm)**
Wandelaar	0.6	4.7	0.3	5.2	-2.5	10.9	-4.7	7.2	8.6
Zeebrugge_Leopold.	0.1	4.4	0.5	5.8	0.5	11.6	-7.6	11.5	13.8
Bol_Van_Heist	-0.4	4.4	0.1	5.1	-0.6	10.5	-9.8	12.9	16.2
Scheur_Wielingen_.	0.1	4.3	-0.3	5.3	-0.5	11.4	-14.3	10.6	17.8
CADZD	0.1	4.3	-0.5	5.6	0.8	10.1	-8.1	14.7	16.8
WESTKPLE	2.9	5.0	0.0	5.0	1.2	9.0	-9.3	12.3	15.4
EURPFM	-1.4	4.3	0.7	4.9	3.7	8.5	-2.0	7.8	8.1
VLISSGN	**-1.3**	**4.3**	**-0.3**	**5.3**	**-1.1**	**9.0**	**-14.4**	**14.7**	**20.6**
ROOMPBTN	**0.2**	**3.3**	**0.2**	**4.9**	**-0.5**	**11.1**	**-9.0**	**11.7**	**14.8**
LICHTELGRE	1.2	4.1	0.2	4.8	1.9	8.3	0.8	11.1	11.2
BROUWHVSGT08	7.2	9.2	-0.6	6.0	-3.2	10.8	-9.7	7.2	12.1
TERNZN	-4.2	6.1	0.0	5.5	-2.7	9.8	-19.6	16.0	25.3
HARVT10	1.6	4.5	0.3	5.3	5.0	9.5	3.0	13.3	13.7
HANSWT	-2.0	5.3	-0.6	5.4	-7.6	14.9	-20.2	17.4	26.7
ROOMPBNN	1.8	3.8	-0.4	4.7	-2.9	10.3	-19.6	19.3	27.5
HOEKVHLD	**0.2**	**3.8**	**1.0**	**5.7**	**5.5**	**10.1**	**6.3**	**10.1**	**11.9**
STAVNSE	0.5	3.9	0.5	5.0	-5.2	11.7	-14.7	14.3	20.5

	Tidal error low water		Skew surge error (low water)						
	all		<99.0% skew surges		99.0% - 99.8% skew surges		>99.8% skew surges		
Station	**bias (cm)**	**RMSE (cm)**	**bias (cm)**	**RMSE (cm)**	**bias (cm)**	**RMSE (cm)**	**Bias (cm)**	**Std (cm)**	**RMSE (cm)**
BERGSDSWT	2.4	5.8	1.3	5.3	-6.9	15.6	-16.9	15.8	23.2
KRAMMSZWT	-2.1	4.7	1.1	5.4	-2.7	10.8	-16.0	15.0	22.0
SCHEVNGN	2.9	4.9	0.9	5.4	4.3	8.9	3.4	6.6	7.4
IJMDBTHVN	1.7	5.1	1.6	6.1	3.6	8.4	-4.2	11.0	11.8
Q1	-1.2	3.4	0.4	4.3	1.9	6.4	-3.9	9.6	10.3
DENHDR	**-1.1**	**3.6**	**0.5**	**4.9**	**-1.8**	**8.5**	**-11.1**	**11.3**	**15.9**
TEXNZE	-2.3	4.0	1.2	5.3	4.6	8.2	-8.4	9.0	12.2
K13APFM	0.7	2.7	0.4	4.1	1.4	5.6	-2.8	10.2	10.6
F16	-1.1	2.9	0.4	4.1	2.1	6.6	-1.5	4.8	5.0
OUDSD	-0.7	3.3	0.1	4.5	-3.5	8.3	-11.2	12.0	16.4
DENOVBTN	-5.0	7.1	-0.5	8.8	3.7	10.5	-5.2	14.5	15.4
TERSLNZE	-0.4	3.2	0.7	5.5	5.7	11.3	-5.2	10.0	11.3
VLIELHVN	-2.3	4.2	1.0	5.0	-3.7	11.2	-20.3	10.8	23.0
WESTTSLG	-0.5	4.0	-0.1	5.6	-9.7	15.3	-25.6	16.5	30.4
KORNWDZBTN	-0.7	3.1	0.1	6.3	2.1	10.6	-9.5	16.4	18.9
WIERMGDN	0.1	3.8	0.2	5.6	5.4	11.3	1.5	12.4	12.5
HUIBGT	2.9	5.3	0.3	5.8	4.2	9.6	1.2	10.4	10.5
HARLGN	**10.7**	**11.6**	**-0.1**	**7.5**	**-10.6**	**14.7**	**-25.5**	**19.5**	**32.1**
NES	17.6	19.7	-0.7	8.3	-26.0	28.4	-41.3	19.2	45.5
LAUWOG	7.3	9.5	0.3	6.4	-17.1	21.0	-25.4	20.8	32.9
SCHIERMNOG	20.7	22.9	-1.5	10.0	-32.3	35.3	-38.0	20.4	43.2
BORKUM_Sudstran.	7.1	9.0	0.4	6.1	-10.0	15.0	-14.0	11.7	18.2
BorkumFischerbalje	3.2	6.0	0.1	6.0	-7.5	12.5	-12.4	11.3	16.8
EMSHORN	7.3	9.0	0.7	6.8	-13.9	17.2	-22.0	11.4	24.8
EEMSHVN	4.9	7.4	1.1	6.7	-10.0	14.8	-17.3	10.3	20.1
DUKEGAT	7.2	9.2	1.4	7.4	-10.9	15.3	-16.0	10.1	18.9
DELFZL	**16.0**	**17.5**	**1.5**	**8.0**	**-16.6**	**20.7**	**-25.3**	**11.6**	**27.8**
KNOCK	12.3	13.9	0.5	7.5	-16.8	20.8	-25.8	12.4	28.6
Average (total)	**2.1**	**6.0**	**0.3**	**5.7**	**-2.8**	**12.0**	**-11.4**	**12.7**	**18.4**
Average (offshore)	**-0.4**	**3.5**	**0.4**	**4.4**	**2.2**	**7.1**	**-1.9**	**8.7**	**9.0**
Average (coast)	**1.0**	**4.6**	**0.4**	**5.4**	**1.9**	**10.1**	**-5.1**	**10.7**	**13.1**
Average (SWD)	**-0.5**	**4.9**	**0.1**	**5.2**	**-4.4**	**11.9**	**-17.6**	**16.3**	**24.0**
Average (WS)	**6.2**	**10.0**	**0.1**	**7.0**	**-11.2**	**17.3**	**-22.2**	**15.6**	**27.8**

Comparison against DCSMv6, DCSMv6-ZUNOv4 and DCSM-FM 0.5nm 2019 release
The error statistics for the fifth-generation models (at the Dutch coastal stations) and previous release of DCSM-FM 0.5nm can be found in Appendix table A.5 to Appendix table A.7. These

results are summarised in Table 4.16, where the station-averaged error statistics are compared. For a fair comparison, Hirlam meteorological forcing is used for all four models presented here.

These results show that on average the quality of the tidal low waters has improved since the 2019 release. The quality is on average the same as DCSMv6 and lower than DCSMv6-ZUNOv4, although the spatial distribution is different. In most areas DCSM-FM performs better, although in the Wadden Sea this is not the case. The fact that DCSMv6-ZUNOv4 performs better there is probably because of adjustments in bathymetry during the calibration.

The skew surge error under calm conditions (<99.0%) has remained the same or improved in the 2022 release and is in all areas better than DCSMv6 (and only worse than DCSv6-ZUNOv4 in the Wadden Sea). The quality of the most extreme low water skew surges (>99.8%) has on average slightly improved compared to the 2019 release. The quality of the highest low water skew surge events is slightly worse than in the fifth generation models, mainly due to worse results in the South-western Delta and Wadden Sea.

Table 4.16 Comparison of the station-averaged model skill to represent skew surge heights (low waters), for three different event classes, in terms of bias (cm) and the RMSE (cm) for Dutch coastal stations. The area averages are computed over areas that are available in all models. For all models, Hirlam meteo forcing was applied.

	Tidal error low water		Skew surge (low water)						
	all		<99.0% skew surges		99.0% - 99.8% skew surges		>99.8% skew surges		
	bias (cm)	RMSE (cm)	bias (cm)	RMSE (cm)	bias (cm)	RMSE (cm)	bias (cm)	std (cm)	RMSE (cm)
Total									
DCSMv6	0.3	6.0	0.2	5.9	-2.1	12.2	-10.1	12.7	17.5
DCSMv6-ZUNOv4	-3.2	5.3	0.3	5.7	0.3	11.0	-7.6	12.1	15.6
DCSM-FM 0.5nm 2019	2.7	6.9	0.2	5.8	-3.3	12.0	-12.2	13.1	19.1
DCSM-FM 0.5nm 2022	2.1	6.0	0.3	5.7	-2.8	12.0	-11.4	12.7	18.4
Offshore									
DCSMv6	-2.3	4.1	0.4	4.5	2.0	7.4	-3.5	8.9	9.7
DCSMv6-ZUNOv4	-1.4	3.8	0.4	4.5	1.8	7.2	-3.9	8.6	9.5
DCSM-FM 0.5nm 2019	0.4	3.7	0.4	4.4	1.2	6.7	-3.3	9.4	10.2
DCSM-FM 0.5nm 2022	-0.4	3.5	0.4	4.4	2.2	7.1	-1.9	8.7	9.0
Coast									
DCSMv6	-1.7	4.8	0.3	5.6	1.7	10.7	-5.1	11.2	14.0
DCSMv6-ZUNOv4	-2.9	5.1	0.5	5.6	1.9	10.8	-5.1	11.0	14.0
DCSM-FM 0.5nm 2019	0.6	4.8	0.3	5.5	1.4	9.8	-6.2	11.5	14.1
DCSM-FM 0.5nm 2022	1.0	4.6	0.4	5.4	1.9	10.1	-5.1	10.7	13.1
South-western Delta									
DCSMv6	1.5	6.0	0.1	5.5	-1.2	11.7	-13.4	12.4	18.8
DCSMv6-ZUNOv4	-3.8	5.6	-0.1	5.4	0.4	11.4	-9.6	13.0	16.9
DCSM-FM 0.5nm 2019	-0.8	5.9	0.0	5.2	-4.2	11.4	-15.2	14.3	21.0
DCSM-FM 0.5nm 2022	-0.5	4.9	0.1	5.2	-4.4	11.9	-17.6	16.3	24.0

	Tidal error low water		Skew surge (low water)						
	all		<99.0% skew surges		99.0% - 99.8% skew surges		>99.8% skew surges		
	bias (cm)	RMSE (cm)	bias (cm)	RMSE (cm)	bias (cm)	RMSE (cm)	bias (cm)	std (cm)	RMSE (cm)
Wadden Sea									
DCSMv6	3.8	8.6	0.1	7.2	-10.3	16.8	-19.2	16.8	25.9
DCSMv6-ZUNOv4	-4.0	6.1	0.2	6.5	-3.1	12.6	-12.0	15.0	20.0
DCSM-FM 0.5nm 2019	8.7	12.2	0.1	7.1	-12.3	18.2	-24.0	16.7	29.8
DCSM-FM 0.5nm 2022	6.2	10.0	0.1	7.0	-11.2	17.3	-22.2	15.6	27.8

5 Conclusions and recommendations

5.1 Background

Upon request of Rijkswaterstaat (RWS) Deltares has developed a sixth-generation hydrodynamic model of the Northwest European Shelf: the Dutch Continental Shelf Model – Flexible Mesh (DCSM-FM). This model is the latest in a line of DCSM models developed by RWS and Deltares and a successor to the fifth-generation WAQUA model DCSMv6. Specifically, this model covers the North Sea and adjacent shallow seas and estuaries in the Netherlands, such as the Wadden Sea, the Ems-Dollard estuary, the Western Scheldt and the Eastern Scheldt.

The development of the present model is part of a more comprehensive project in which sixth-generation models were developed for all waters managed and maintained by RWS. An important difference with the previous fifth-generation models is the use of the D-HYDRO Suite, the new software framework for modelling free surface flows, which was first released in 2015 and allows for the use of unstructured grids.

Since the proposed applications on the North Sea pose a wide range of sometimes mutually exclusive demands on a model, two horizontal schematizations were proposed: a relatively coarse two-dimensional model (DCSM-FM 0.5nm; described in the present report) and a relatively fine schematization (DCSM-FM 100m) with further refinement in most Dutch coastal waters. DCSM-FM 0.5nm is primarily aimed at ensemble forecasting, but also forms a sound basis for a subsequent 3D model development, including temperature and salinity as state parameters. DCSM-FM 100m is primarily aimed at deterministic water level forecasting at HMC and WMCN-kust.

5.2 Primary changes in the 2022 release

In 2019 a first version of DCSM-FM 0.5nm was released. In the current 2022 release several improvements were made, the most important and consequential of which are listed below.

- The model bathymetry off the Dutch coastal zone is now based on the EMODnet 2020 bathymetry instead of the 2016 version. The updated bathymetry shows the large changes in the central and Danish North Sea as well as an increase of the bed level of about 2 m in a large area off the Zeeland coast. A new addition is the application of a MSL-NAP conversion to the EMODnet bathymetry data. For Dutch coastal waters a more recent Baseline database was used.
- To account for baroclinic processes that influence the mean water level but cannot be properly represented explicitly in a 2D model, an additional water level difference field is forced on the model. With this so-called Mean Dynamic Topography correction, the modelled mean water level approaches NAP in the Dutch coastal zone and the European Vertical Reference Frame (EVRF) outside Dutch waters. The correction field is based on DCSM-FM and 3D DCSM-FM model results for the period 2013-2017.
- The previous model release made use of FES2012 tidal constituents, with only Sa added based on DCSMv6. Some FES2012 constituents have been replaced with FES2014, while the others are replaced with GTSM and EOT20 values. In additions, new constituents have been added. The total number of constituents prescribed has increased from 32 to 39.
- The numerical keywords relating to the numerical implementation of the Coriolis force (*Newcorio* and *Corioadamsbashfordfac*) were adjusted to be in line with the current standard sixth-generation settings as well as 3D DCSM-FM settings. This affects the

tidal propagation in DCSM-FM, with a reduction in M2 amplitude and phase along the Dutch coast of 0.6 cm and 0.4°, respectively.
- The standard meteorological forcing used for calibration and validation of DCSM-FM has been changed from Hirlam to ECMWF IFS.

5.3 Calibration and validation

Because of the adjustments in the DCSM-FM 2022 release, a recalibration of the bottom roughness was required. This was done with the open-source data assimilation toolbox OpenDA, using 194 shelf-wide tide-gauge measurements, covering the entire calendar year 2017. Compared to the uncalibrated version of the model, this has led to a 60% reduction in the cost function.

Similar to the 2019 release, DCSM-FM was validated against measurements for the period 2013-2017 and compared against the previous 2019 release of the same model as well as the fifth generation models DCSMv6 and DCSMv6-ZUNOv4. An analysis of total water levels as well as the contribution of tide and surge in Dutch waters showed that:

- Generally, the total water level RMSE is 6-8 cm in North Sea waters. In these stations, the tide and surge RMSE is generally 4-5 cm. The quality deteriorates inside the Dutch estuaries and Wadden Sea, where the model resolution is low compared to the variability in geometry and bathymetry.
- Compared to the previous 2019 release the total water level has generally improved, mainly due to a 10% improvement in tide quality. Applying ECMWF forcing instead of Hirlam yields a better surge representation, with the average surge RMSE decreasing from 5.8 cm to 5.6 cm.
- Even though the tide quality of DCSM-FM 0.5nm has increased in the 2022 release, on average the tide representation is still slightly worse than both fifth generation models. This is probably because of the exclusion of bathymetry as a calibration parameter in the development of DCSM-FM.
- Compared to DCSMv6, the surge error of DCSM-FM is lower in all sub-areas, even using the same Hirlam meteorological forcing. In none of the six main locations (Dutch: ‘hoofdlocaties’) is the surge quality worse than the fifth generation model DCSMv6.
- With the addition of the MDT-correction, the average bias in DCSM-FM has reduced from 2.7 cm in the 2019 release (using Hirlam) to 0.0 cm in the 2022 release (using ECMWF). The standard deviation of bias between stations is also reduced, from 3.6 cm to 2.4 cm.

The model was also assessed with respect of its capacity to represent the high water skew surge, i.e., the difference between a total high water and the associated astronomical high water, ignoring small differences in timing. This is done for three categories of events, subdivided based on the height of the measured skew surge. With respect to the skew surge the following can be concluded:

- The RMSE of the high water skew surge (<99.0%, i.e., calm conditions) in the Dutch coastal stations is around 5 cm in North Sea waters and increases to about 6-7 cm in the eastern Wadden Sea and Dutch estuaries.
- The most extreme (>99.8%) skew surge events shows an excellent quality in southern waters, with RMSE values less than 10-15 cm. Errors are much larger inside the (eastern) Wadden Sea, mostly due to a large systematic underestimation of the skew surge during storms. In the Ems-Dollard the bias can reach 30-40 cm during these events, using ECWMF meteorological forcing.
- Compared to the 2019 release the tidal high water error as well as the skew surge error under calm (<99.0%) conditions have improved on average. The average quality is now the same or better in all Dutch sub-areas considered. The quality of the most

extreme skew surges (>99.8%) has on average remained the same as in the 2019 release. Differences with the previous generation models are also relatively small; much smaller than the spatial variation in representation quality of the most extreme skew surges.

Since there is also an interest in the accuracy with which low waters are represented (e.g. relevant for water authorities draining into the sea by gravity flow), especially during storm surges, the error statistics for low waters were also computed. With respect to the low water skew surge, the following can be concluded:

- In North Sea waters a skew surge RMSE of around 5 cm is found. In the eastern Wadden Sea and Dutch estuaries, the error increases to about 7 cm.
- The low water skew surge (and low water representation in general) is sensitive to the accuracy with which the bathymetry is represented. Especially in areas where the resolution of the model is coarse relative to the variability in bathymetry, this hampers the quality of the low water skew surge representation.
- In southern Dutch waters, the low water skew surge during the most extreme (>99.8%) skew surge events shows a larger systematic underestimation of low waters, than for high waters during the same category of events. The underestimation increases in upstream direction inside the Eastern and Western Scheldt. On the other hand, in northern Dutch waters, the systematic error (bias) is less severe than for the high water skew surge, with a bias of 20-25 cm in the Ems-Dollard (compared to 30-40 cm for the high water skew surge).
- On average the quality of the tidal low waters has improved since the 2019 release. The quality of the tidal low waters is on average the same as DCSMv6 and lower than DCSMv6-ZUNOv4, although the spatial distribution is different. In most areas DCSM-FM performs better, although in the Wadden Sea this is not the case. The fact that DCSMv6-ZUNOv4 performs better there is probably because of adjustments in bathymetry during the calibration.
- The low water skew surge error under calm conditions (<99.0%) has remained the same or improved in the 2022 release and is in all areas better than DCSMv6 (and only worse than DCSv6-ZUNOv4 in the Wadden Sea).
- The quality of the most extreme low water skew surges (>99.8%) has on average slightly improved compared to the 2019 release, but is still slightly worse than the fifth generation models, mainly due to worse results in the South-western Delta and Wadden Sea.

5.4 Recommendations

5.4.1 Bathymetry

While the 2022 release has increased the quality of the tide representation of DCSM-FM 0.5nm, it has still deteriorated slightly compared to the fifth generation models DCSMv6 and DCSMv6-ZUNOv4. This is based on the validation for the years 2013-2017 and is even more striking given that the quality of the tide representation in the fifth generation models has deteriorated since the year for which these have been calibrated (2007). A possible reason for the slightly worse tide representation in the sixth generation model is the exclusion of bathymetry as a calibration parameter. It is therefore recommended to investigate whether adjusting the bathymetry within reasonable bounds would be beneficial to the quality of the tide.

5.4.2 Meteorological forcing

The present calibration and validation were performed using ECMWF IFS meteorological forcing, using neutral wind speed and the time- and space-varying Charnock parameter to compute the wind stress that acts on the water surface. The air density is assumed uniform and constant, which is not consistent with boundary layer parameterization used in the ECMWF IFS model. With a pseudo-wind approach, it has been shown that using a time- and space-varying air density consistent with or directly taken from the ECWMF model would improve the surge quality. It is therefore recommended to implement this as an option in the D-HYDRO software and apply this in a next release of DCSM-FM.

5.4.3 Annual M2 modulation

In tide gauge stations Roompot buiten and Den Helder, H1 is the harmonic constituent with the largest contribution to the tidal error, while in Hoek van Holland and Delfzijl this constituent has the second largest contribution. H1 (and H2) has an angular frequency that differs one cycle per year from the M2 frequency and represents an annual modulation of the M2 tide. Only a minor part of this modulation is gravitational in nature. While the origin is poorly understood, it is at least to some extent related to the seasonal nature of dissipation due to storms as well as seasonal temperature stratification in the central North Sea. The latter contribution cannot be represented with a 2D barotropic model such as DCSM-FM. It is therefore recommended to investigate whether a better tide quality can be achieved by using a 3D baroclinic version of DCSM-FM.

5.4.4 Forecast accuracy

The validation in the present report is based on hindcast computations. Since the model will be used for forecasting applications, it is recommended to also assess the forecast quality as a function of the lead time.

5.4.5 Radiational tides

The improvement of the model bias in NAP-referenced stations using a MDT-correction proved to be successful. This was made possible by the existence of a 3D model for the same area (3D DCSM-FM), in which some of the phenomena that are missing in the 2D version (DCSM-FM 0.5nm) are well represented. The same approach could be used to include or improve periodic phenomena that are partially baroclinic in origin, such as the annual and semi-annual Sa and Ssa constituent, the daily S1 constituent and possibly also the semi-diurnal H1 and H2 constituents. The Sa, Ssa and H1 radiational tides are prominent in the list of harmonic constituents with the largest contribution to the tidal error in the six main locations. It is therefore recommended to implement the possibility to prescribe period surface forcing as an option in the D-HYDRO software and investigate the potential DCSM-FM model improvements.

5.4.6 Update calibration period

Since the end of the calibration period (2017) and the validations period (2013-2017) the tide along the Dutch coast has changed. This probably implies a deterioration in model quality under current conditions. It is therefore recommended to use a more recent calibration and validation period in future work. Since the changes in tide are probably most prominent in Dutch and German waters, recalibration could be restricted to the roughness sections in these areas. This could decrease the time that needs to be spent on collecting quality-checking shelf-wide tide gauge measurements.

5.4.7 Severe and systematic underestimation of skew surge during storm surges

During storm surge events, DCSM-FM systematically underestimates skew surge levels in some locations. This includes two of the five primary warning locations (Harlingen and Delfzijl), both located in the eastern Dutch Wadden Sea, where the underestimation can reach several decimetres. It is recommended to further investigate the source of this severe underestimation, testing a range of hypotheses.

One hypothesis is related to wave-current interaction, which is currently not taken into account in DCSM-FM. From literature it is known that wave-current interaction processes can contribute more than 30% to the surge during extreme storm events. Preliminary tests with DCSM-FM, online coupled to a wave model, have shown an impact on water levels of up to decimetres and an improvement compared to measurements (Zijl & Laan, 2021b). However, this was a first attempt, without validation of the wave model and using default values for the parametrization of the various wave-driven interaction processes. It is therefore recommended to continue this effort and possibly expand with fine sediment interactions.

Literature

Carrère L., F. Lyard, M. Cancet, A. Guillot, L. Roblou (2012). FES2012: A new global tidal model taking advantage of nearly 20 years of altimetry. Proceedings of 20 Years of Progress in Radar Altimetry, 710, 13.

Charnock, H. (1955). Wind stress on a water surface. Quarterly Journal of the Royal Meteorological Society, 81(350), 639-640.

Groenenboom, J., Zijl, F. (2021). Hindcastvalidatie DCSM-FM 100m. Deltares, memo 11206814-004, Delft.

Hart-Davis, M. G., Piccioni, G., Dettmering, D., Schwatke, C., Passaro, M., & Seitz, F. (2021). EOT20: a global ocean tide model from multi-mission satellite altimetry. Earth System Science Data, 13(8), 3869-3884.

Laan, S., Zijl, F. (2021). Update naar FES2014 astronomische randvoorwaarden. Deltares, memo 11206814-004-ZKS-0001, Delft

Lellouche, J. M., Greiner, E., Le Galloudec, O., Garric, G., Regnier, C., Drevillon, M., ... & Le Traon, P. Y. (2018). Recent updates to the Copernicus Marine Service global ocean monitoring and forecasting real-time 1⁄12 high-resolution system. *Ocean Science*, *14*(5), 1093-1126.

Lyard, F., D. Allain, M. Cancet, L. Carrere, N. Picot (2021). FES2014 global ocean tides atlas: design and performances. Ocean Science 17, 3, 615–649.

Minns, T., A. Spruyt & D. Kerkhoven (2022): Specificaties zesde-generatie modellen met D-HYDRO - Generieke technische en functionele specificaties. Deltares report 11208053-012-ZWS-0002.

Muis, S., M. Verlaan, H.C. Winsemius, J.C.J.H. Aerts, P.J. Ward (2016). A global reanalysis of storm surges and extreme sea levels. Nature Communications 7, 11969.

Pawlowicz, R., Beardsley, B., Lentz, S. (2002). Classical tidal harmonic analysis including error estimates in MATLAB using T_TIDE. Computers and Geosciences 28 (2002), 929-937.

Zijl, F., Verlaan, M., Gerritsen, H., (2013). Improved water-level forecasting for the Northwest European Shelf and North Sea through direct modelling of tide, surge and non-linear interaction. Ocean Dyn. 63 (7).

Zijl, F., Irazoqui Apecechea, M., Groenenboom, J. (2016). Kustmodellen in D-HYDRO - Pilot-applicatie Noordzee; Advies voor algemeen functioneel ontwerp voor de zesde-generatie modellen van RWS. Deltares, report 1230071-011-ZWS-0018.

Zijl, F. (2016a). On the impact of hydrodynamic model resolution on water levels. Deltares, memo 1220073-003-ZKS-0009.

Zijl, F. (2016b). Representation of the 18.6-year nodal cycle in DCSMv6. Deltares, memo 1230072-003-ZKS-0007.

Zijl, F. (2016c). The impact of relative wind effect on water levels. Deltares, memo 1230072-003-ZKS-0008.

Zijl, F., Groenenboom, J. (2019). Development of a sixth-generation model for the NW European Shelf (DCSM-FM 0.5nm). Deltares, report 11203715-004-ZKS-0003, Delft.

Zijl, F. (2021). Gevolgen van uitzetten RWE in DCSM-FM 100m. Deltares, memo 11206814-004, Delft.

Zijl, F., Laan, S. (2021). Forcing the Mean Dynamic Topography in 2D DCSM-FM. Deltares, memo 11206814-004-ZKS-0005, Delft.

Zijl, F., Laan, S. (2021b). Impact golfkoppeling DCSM-FM. Deltares, memo 11206814-004-ZKS-0008, Delft.

Zijl, F., Groenenboom, J. (2021). 3D DCSM-FM Consolidatie z-sigma versie en uitlijnen met standaard settings. Deltares, memo 11206814-004-ZKS-0007, Delft.

A Validation

A.1 Shelf-wide results

Appendix table A.1 Statistics (RMSE in cm) of tide, surge and total water level of the first and second release of DCSM-FM 0.5nm for different meteorological forcings. The first release of DCSM-FM 0.5nm used Hirlam forcing. The second release uses ECMWF. For comparability, the second release is also validated with Hirlam forcing.

	RMSE tide (cm)			RMSE surge (cm)			RMSE water level (cm)		
	2019 release	2022 release	2022 release	2019 release	2022 release	2022 release	2019 release	2022 release	2022 release
Station	Hirlam	Hirlam	ECMWF	Hirlam	Hirlam	ECMWF	Hirlam	Hirlam	ECMWF
BAKE_A	9.2	8.5	8.2	7.9	8.0	7.6	10.2	9.6	9.3
BAKE_Z	8.0	7.3	6.9	7.2	7.3	6.2	10.5	10.0	9.3
BHV_ALTER_LT	30.5	15.9	15.7	9.9	9.6	9.3	32.0	18.6	18.3
BORKUM_Sudstrand	7.3	6.5	6.6	5.7	5.7	5.8	9.2	8.6	8.8
BorkumFischerbalje	6.7	6.4	6.4	5.7	5.8	5.6	8.8	8.5	8.5
CUXHAVEN_STEUBH	8.6	8.2	8.2	7.7	7.6	7.2	11.5	11.2	11.0
DAGEBULL	14.6	14.8	14.7	8.5	8.6	8.7	16.9	17.1	17.1
DUKEGAT	8.0	6.5	6.4	7.0	6.9	6.8	10.1	9.1	8.9
DWARSGAT	12.4	9.0	8.7	7.6	7.7	7.2	14.5	11.9	11.3
EMSHORN	7.6	6.0	5.9	6.1	6.1	6.2	9.7	8.6	8.6
HELGOLAND_BINNENH	7.7	7.0	6.9	5.5	5.5	5.3	9.4	8.9	8.7
HELGOLAND_SUDH	8.2	7.4	7.3	5.8	5.8	5.3	10.1	9.5	9.2
HOOKSIELPLATE	7.6	7.1	7.0	6.9	7.0	6.6	10.3	10.0	9.6
HORNUM	16.8	17.9	18.1	5.6	5.7	5.4	17.7	18.8	18.8
KNOCK	11.0	9.6	9.3	7.7	7.6	7.7	13.4	12.2	12.0
LANGEOOG	7.7	7.1	7.1	7.0	7.0	7.3	9.6	9.0	9.3
LEUCHTTURM_ALTE_WESER	7.2	6.6	6.4	6.2	6.3	5.8	9.5	9.1	8.6
LIST	11.3	14.9	15.0	5.9	5.6	5.5	12.7	15.9	16.0
MELLUMPLATE	7.4	6.7	6.5	6.8	6.9	6.4	10.1	9.6	9.2
MITTELGRUND	9.8	9.1	9.0	8.0	7.9	7.6	11.3	10.5	10.4
NORDERNEX_RIFFG	7.3	5.6	5.5	6.0	6.1	6.4	9.4	8.3	8.5
PELLWORM_Anleger	12.4	13.1	13.0	7.4	7.7	7.3	14.4	15.1	14.9
ROBBENSUDSTEERT	14.9	9.1	8.9	8.1	8.2	7.6	16.9	12.3	11.7
SCHARHORN	7.3	6.5	6.4	7.0	7.1	6.7	9.9	9.4	9.0
SCHILLIG	6.7	6.0	5.8	6.5	6.6	6.2	9.3	8.9	8.5
SPIEKEROOG	7.4	6.3	6.3	6.5	6.7	6.8	9.8	9.2	9.3
WANGEROOGE_NORD	7.8	7.3	7.3	6.5	6.5	6.3	10.4	10.1	9.8

Station	RMSE tide (cm)			RMSE surge (cm)			RMSE water level (cm)		
	2019 release	2022 release	2022 release	2019 release	2022 release	2022 release	2019 release	2022 release	2022 release
	Hirlam	Hirlam	ECMWF	Hirlam	Hirlam	ECMWF	Hirlam	Hirlam	ECMWF
WANGEROOGE_OST	6.0	6.0	6.0	6.5	6.6	6.6	8.7	8.8	8.8
WANGEROOGE_WEST	9.6	9.0	9.0	7.0	7.0	7.2	11.8	11.3	11.5
WHV_ALTER_VORHAFEN	9.4	7.3	7.0	7.8	7.9	7.4	12.2	10.8	10.2
WHV_NEUER_VORHAFEN	8.5	7.0	6.8	7.6	7.8	7.3	11.5	10.4	10.0
WITTDUN	15.2	39.8	40.1	6.3	18.4	18.7	16.3	43.7	44.2
ZEHNERLOCH	8.1	7.0	7.3	7.5	7.5	7.1	10.3	9.5	9.2
ABDN	4.8	4.8	4.9	4.6	4.5	4.5	6.6	6.6	6.6
BANGR	12.2	8.1	8.2	4.6	4.4	4.3	13.1	9.2	9.3
BARMH	13.5	10.8	11.0	6.6	6.4	6.8	14.8	12.0	12.4
BOURNMH							6.3	12.3	12.3
CROMR	8.0	6.7	6.8	6.7	6.6	6.1	9.4	8.3	8.0
DEVPT	13.4	6.8	6.8	4.5	4.1	4.0	14.2	7.8	7.8
DOVR	8.9	6.2	6.2	4.4	4.6	4.3	9.7	7.7	7.5
FISHGD	6.8	5.6	5.5	4.4	4.3	4.3	7.7	6.7	6.7
HARWH	13.6	13.4	13.4	6.9	6.7	6.2	14.9	14.6	14.4
HEYSHM	28.7	25.9	26.0	7.8	7.3	6.9	29.6	26.6	26.6
HINKLPT	13.0	11.1	11.5	7.2	7.1	7.1	14.7	13.2	13.5
HOLHD	6.8	5.0	5.2	4.3	4.2	4.2	8.1	6.6	6.7
ILFCBE	10.0	12.3	12.4	4.9	4.9	4.9	11.0	13.1	13.2
IMMHM	16.2	14.5	14.6	8.7	8.6	8.3	18.5	17.0	16.9
KINLBVE	7.3	6.1	6.5	5.0	5.1	4.7	7.7	6.6	6.5
LEITH	10.3	7.2	7.3	6.4	6.3	5.8	12.1	9.5	9.4
LERWK	4.3	5.6	5.7	3.7	3.7	3.7	5.6	6.7	6.7
LIVPL	17.4	17.8	17.9	7.1	7.1	6.8	18.3	18.8	18.7
LLANDNO	7.6	7.4	7.5	5.5	5.4	5.4	9.4	9.2	9.2
LOWST	5.1	5.4	5.4	5.3	5.2	4.6	7.2	7.5	7.1
MILFHVN	7.1	6.7	6.6	4.9	4.8	4.7	8.1	7.6	7.7
MILLPT	18.5	12.5	12.6	6.2	6.0	5.7	19.4	13.8	13.7
MUMBS	9.3	11.1	11.3	5.2	5.2	5.2	12.7	14.5	14.7
NEWHVN	11.2	7.4	7.4	4.2	4.2	4.0	12.0	8.5	8.4
NEWLN	4.4	4.2	4.4	3.8	3.8	3.8	5.7	5.6	5.6
NEWPT							29.0	92.6	93.1
NORTHSS	8.6	6.2	6.5	5.0	4.9	4.7	9.9	7.8	7.9
PORTERIN	5.9	5.8	6.0	4.1	4.1	4.1	7.2	7.1	7.2
Portbury	59.2	29.3	29.5	17.0	11.5	11.6	62.1	31.6	31.9
PORTPTK	10.6	9.0	9.2	4.4	4.3	4.4	11.5	10.0	10.2

	RMSE tide (cm)			RMSE surge (cm)			RMSE water level (cm)		
	2019 release	2022 release	2022 release	2019 release	2022 release	2022 release	2019 release	2022 release	2022 release
Station	**Hirlam**	**Hirlam**	**ECMWF**	**Hirlam**	**Hirlam**	**ECMWF**	**Hirlam**	**Hirlam**	**ECMWF**
PORTRH	7.2	5.3	5.6	4.6	4.5	4.3	8.3	6.7	6.7
PORTSMH	18.6	17.3	17.4	5.1	5.2	5.1	19.1	17.9	18.0
SHEERNS							18.2	11.6	11.1
StHelierJersey	8.6	6.7	6.6	4.8	4.8	4.7	9.5	7.9	7.8
STMARYS							5.0	4.7	4.7
STORNWY	8.3	6.1	6.3	5.0	5.1	4.8	8.8	6.9	6.7
TOBMRY	7.0	5.5	5.5	4.5	4.5	4.3	8.3	7.1	7.0
ULLPL	7.7	6.0	6.2	5.4	5.5	5.0	10.4	9.2	9.1
WEYMH	4.7	9.2	9.2	4.0	3.9	3.8	5.8	9.6	9.6
WHITBY	8.9	6.3	6.5	5.5	5.3	5.3	10.6	8.6	8.7
WICK	5.3	6.1	6.2	4.5	4.4	4.4	6.5	7.1	7.2
WORKTN	9.8	9.4	9.4	5.4	5.2	5.0	11.2	10.7	10.6
Aalesund	5.4	5.8	6.1	4.5	4.5	4.5	7.0	7.3	7.5
Aranmore	5.3	6.6	6.7	4.4	4.4	4.2	6.8	7.9	7.9
Ballum	14.8	18.8	19.5	14.2	13.3	13.2	19.8	22.7	23.2
Ballycotton	5.2	4.9	5.1	4.4	4.4	4.4	6.6	6.2	6.4
Ballyglass	5.0	6.7	6.7	4.4	4.4	4.3	6.3	7.7	7.7
Bergen	5.1	4.5	4.6	4.1	4.2	4.0	6.5	6.0	6.0
BoulogneSurMer	11.0	6.4	6.3	4.9	5.0	4.9	12.0	8.1	7.9
Brest	20.4	16.3	16.4	6.7	4.3	4.2	21.2	16.8	16.9
Calais	9.9	9.2	9.1	5.3	5.6	5.4	11.2	10.7	10.6
Castletownbere	5.7	5.7	5.8	5.7	5.6	5.6	8.0	8.0	8.0
Cherbourg	7.2	5.2	5.3	4.4	4.3	4.3	8.4	6.6	6.7
Dielette	17.8	12.2	12.1	5.3	5.4	5.4	18.0	12.7	12.6
Dieppe	11.5	14.3	14.3	6.3	9.7	9.6	12.8	9.1	9.0
Dundalk							36.9	35.1	35.4
Dunkerque	7.8	5.8	5.9	5.2	5.3	5.0	9.4	7.9	7.8
Dunmore	6.0	5.6	5.6	3.8	3.8	3.6	6.6	6.2	6.1
Esbjerg	12.2	20.7	20.8	10.1	9.8	9.7	15.7	22.8	22.9
GalwayPort	11.6	10.6	10.7	9.2	9.0	8.2	14.8	13.9	13.5
Havneby	23.2	7.3	7.3	10.2	7.3	6.9	24.9	8.7	8.5
Heimsjoe	6.8	5.6	5.9	4.6	4.6	4.7	8.2	7.2	7.5
Helgeroa	4.2	4.4	4.4	4.6	4.7	4.7	6.2	6.4	6.4
Hirtshals	4.2	4.5	4.6	5.1	5.8	5.8	6.6	7.3	7.3
Howth	7.4	7.3	7.4	4.0	3.9	3.8	8.4	8.2	8.3
HvideSandeKyst	9.2	9.1	9.7	10.4	10.5	10.9	13.5	13.5	14.2
Killybegs	5.8	8.3	8.4	5.1	5.0	4.5	7.7	9.7	9.5

	RMSE tide (cm)			RMSE surge (cm)			RMSE water level (cm)		
	2019 release	2022 release	2022 release	2019 release	2022 release	2022 release	2019 release	2022 release	2022 release
Station	Hirlam	Hirlam	ECMWF	Hirlam	Hirlam	ECMWF	Hirlam	Hirlam	ECMWF
Kristiansund	5.0	5.4	5.6	4.5	4.6	4.5	6.7	7.1	7.2
LeConquet	6.2	11.3	11.4	4.1	4.1	4.1	7.4	12.0	12.1
LeHavre	10.1	11.4	11.4	6.3	6.2	6.2	11.9	12.9	12.9
MalinHead	9.5	8.1	8.2	6.2	6.2	6.0	11.3	10.2	10.2
Maloy	5.3	4.8	5.0	4.4	4.4	4.4	6.9	6.5	6.6
Mausund	8.5	8.7	8.8	7.2	7.4	7.5	11.1	11.4	11.5
Oscarsborg	8.2	8.2	8.3	6.8	7.0	7.0	10.7	10.8	10.8
Oslo	10.2	10.8	10.9	7.7	8.0	8.0	12.8	13.4	13.5
Ribe	8.4	42.5	43.2	11.5	21.3	22.2	13.7	47.5	48.5
Roscoff	8.5	6.1	6.1	4.0	4.0	4.0	9.4	7.2	7.2
SaintMalo	10.5	6.7	6.7	6.0	5.9	5.9	12.1	8.9	8.9
SkerriesHarbour	10.3	7.4	7.5	4.7	4.7	4.5	10.5	8.0	8.0
Sligo							9.0	11.0	10.9
Stavanger	4.0	3.8	3.9	5.3	5.2	5.1	6.6	6.5	6.5
ThyboronKyst	7.6	7.9	7.5	7.9	8.0	7.9	9.5	9.7	9.5
TorsmindeKyst	5.6	5.9	5.9	6.1	6.1	5.4	7.8	8.0	7.6
Tregde	3.5	3.7	3.7	5.7	5.7	5.6	6.7	6.7	6.7
Viker	4.6	4.6	4.6	5.3	5.5	5.5	7.0	7.2	7.2
VLAKTVDRN	5.6	5.0	4.9	5.9	5.9	5.5	7.9	7.3	6.9
Aarhus	6.3	4.9	4.9	6.2	6.3	6.4	8.7	7.9	7.9
Ballen	4.8	3.7	3.8	5.9	5.8	5.7	8.0	7.2	7.3
BayonneBoucau	16.4	17.1	17.2	6.9	6.7	6.9	17.7	18.4	18.5
Bilbao	5.2	5.4	5.4	3.7	3.6	3.7	6.3	6.4	6.4
Bogense	7.6	5.7	5.8	7.3	7.1	6.9	10.1	8.5	8.5
BrestNus30							23.8	18.6	18.6
Brons	31.1	11.7	11.3	21.3	12.0	11.2	37.0	16.0	15.1
Concarneau	8.6	7.5	7.6	5.2	5.1	5.1	9.7	8.7	8.8
Coruna	4.7	5.2	5.3	4.1	4.1	4.1	6.3	6.6	6.6
Ferring							10.6	10.9	11.0
Ferrol2							6.8	7.6	7.4
Ferrol	4.7	5.2	5.2	4.2	4.2	4.3	6.3	6.6	6.7
Fredericia	4.8	3.7	3.8	9.3	8.1	8.0	10.7	9.2	9.0
Frederikshavn	4.2	4.7	4.8	4.8	5.2	5.3	6.3	7.0	7.1
Gijon	4.7	4.8	4.8	3.7	3.7	3.6	5.9	6.0	5.9
Grena	4.0	3.7	3.6	5.5	6.3	6.3	6.9	7.3	7.5
Hanstholm	4.5	4.8	4.7	5.9	5.9	5.5	7.1	7.3	6.9
Herbaudiere	14.4	9.4	9.4	5.5	5.4	5.1	15.4	10.8	10.7

Station	RMSE tide (cm)			RMSE surge (cm)			RMSE water level (cm)		
	2019 release	2022 release	2022 release	2019 release	2022 release	2022 release	2019 release	2022 release	2022 release
	Hirlam	Hirlam	ECMWF	Hirlam	Hirlam	ECMWF	Hirlam	Hirlam	ECMWF
Hornbaek	3.0	3.4	3.2	5.3	5.5	5.2	6.3	6.5	6.4
Hov	6.1	4.9	5.0	6.1	6.4	6.3	9.1	8.4	8.6
Langosteira							6.4	6.8	6.7
IleDAix	19.2	14.2	14.1	7.3	7.3	6.3	20.3	15.9	15.3
Kristineberg1	4.9	4.8	5.0	5.2	5.4	5.4	7.0	7.1	7.2
LaRochelle	16.0	12.1	11.8	7.0	6.9	6.2	17.2	13.6	13.1
LeCrouesty	13.9	10.1	10.2	5.4	5.4	5.2	14.7	11.1	11.1
LesSablesDOlonne	12.4	8.9	8.9	5.5	5.4	5.2	13.2	10.0	9.9
Mando	8.5	23.2	23.7	12.3	10.3	9.9	13.6	24.8	25.1
Onsala	4.1	4.0	3.9	6.2	6.1	6.1	6.4	6.3	6.3
PortBloc	12.6	11.1	11.2	5.6	5.4	5.4	13.5	12.0	12.2
PortTudy	8.9	7.5	7.6	4.8	4.7	4.6	9.8	8.5	8.5
Ringhals	3.5	3.7	3.7	6.1	6.0	6.0	6.6	6.6	6.6
SaintNazaire	16.3	11.4	11.5	6.9	6.8	6.5	17.4	12.8	12.8
Santander	5.2	5.1	5.0	3.7	3.7	3.7	6.3	6.2	6.2
SjaellandsOdde	2.7	2.9	2.9	7.8	7.7	7.6	8.9	8.8	8.6
Smogen	4.8	5.0	5.1	6.0	6.1	6.0	6.9	7.2	7.2
Socoa	7.1	6.9	6.9	5.1	5.1	5.1	8.6	8.4	8.4
Stenungsund	5.1	6.6	6.6	6.6	6.8	7.1	7.2	8.6	8.8
Udbyhoej	8.2	6.3	6.3	8.0	8.6	8.4	11.9	11.1	11.0
Vidaa	8.5	13.6	14.2	11.5	11.4	11.6	14.2	17.6	18.1
Viken	3.0	3.2	3.3	7.0	6.4	6.3	7.2	6.9	6.7
A2	5.2	4.6	4.6	5.1	5.2	4.9	7.3	6.9	6.7
Appelzak	5.6	5.0	5.0	5.3	5.2	5.0	8.0	7.5	7.3
Blankenberge	6.7	5.1	5.2	5.6	5.6	5.3	8.5	7.4	7.3
Bol_Van_Heist	5.5	4.2	4.2	5.2	5.1	4.9	7.5	6.6	6.5
Nieuwpoort	8.5	6.1	6.2	5.5	5.6	5.3	10.1	8.2	8.1
Oostende	6.8	4.5	4.6	5.2	5.3	4.9	8.6	6.9	6.8
Scheur_Wielingen_Bol_van_Knokke	5.7	4.8	4.8	5.4	5.3	5.0	7.7	7.1	6.8
Westhinder	6.6	5.3	5.3	4.9	4.9	4.6	8.1	7.1	6.9
BERGSDSWT	11.0	12.8	12.9	6.2	6.1	5.7	12.6	14.2	14.1
BROUWHVSGT08	6.1	5.8	5.8	6.1	6.1	5.8	8.5	8.3	8.1
CADZD	5.8	4.9	4.8	5.7	5.6	5.2	8.1	7.4	7.1
DELFZL	**10.8**	**9.4**	**9.2**	**7.9**	**7.8**	**7.8**	**13.4**	**12.2**	**12.1**
DENHDR	4.2	4.4	4.5	5.1	5.2	5.0	6.6	6.8	6.7
DENOVBTN	7.4	6.6	6.8	6.9	6.9	6.5	10.1	9.5	9.4
EEMSHVN	7.2	6.6	6.6	6.2	6.2	6.1	9.5	9.1	9.0

Station	RMSE tide (cm)			RMSE surge (cm)			RMSE water level (cm)		
	2019 release	2022 release	2022 release	2019 release	2022 release	2022 release	2019 release	2022 release	2022 release
	Hirlam	Hirlam	ECMWF	Hirlam	Hirlam	ECMWF	Hirlam	Hirlam	ECMWF
EURPFM	3.7	3.4	3.5	4.7	4.7	4.4	5.8	5.7	5.4
HANSWT	18.9	16.9	17.1	7.1	6.9	6.8	20.2	18.3	18.4
HARLGN	**8.7**	**6.2**	**6.3**	**6.8**	**6.4**	**6.2**	**11.0**	**8.9**	**8.9**
HARVT10	4.3	3.6	3.7	5.4	5.3	5.0	6.9	6.4	6.2
HOEKVHLD	4.4	4.4	4.5	5.8	5.6	5.3	7.3	7.1	7.0
HOLWD	31.0	30.4	30.6	14.6	14.9	15.1	34.3	33.8	34.1
HUIBGT	5.2	4.9	4.7	5.7	5.7	5.3	7.5	7.2	6.9
IJMDBTHVN	5.4	4.2	4.3	5.8	5.7	5.4	7.9	7.1	6.9
KORNWDZBTN	4.6	3.6	3.8	5.7	5.6	5.3	7.3	6.7	6.5
KRAMMSZWT	8.1	9.3	9.4	6.3	6.3	6.1	10.2	11.2	11.2
LAUWOG	14.2	8.2	8.1	7.5	7.1	7.4	16.0	10.8	11.0
LICHTELGRE	4.7	3.8	3.9	4.7	4.7	4.4	6.7	6.1	5.9
NES	15.4	15.1	15.1	7.6	7.6	7.9	17.2	16.9	17.0
OUDSD	4.6	4.9	5.0	4.7	4.8	4.6	6.6	6.8	6.8
ROOMPBNN	4.4	4.1	4.1	4.9	4.9	4.7	6.6	6.4	6.2
ROOMPBTN	3.8	3.6	3.7	5.0	5.0	4.7	6.3	6.2	6.0
SCHEVNGN	4.5	3.8	3.8	5.6	5.5	5.2	7.1	6.7	6.5
SCHIERMNOG	24.2	18.8	18.9	9.9	9.7	9.9	26.1	21.1	21.4
STAVNSE	5.5	5.7	5.7	5.4	5.3	5.1	7.7	7.8	7.7
TERNZN	6.7	5.3	5.5	6.2	5.9	5.8	9.1	8.0	7.9
TERSLNZE	4.4	4.0	3.9	5.6	5.6	5.4	7.1	6.8	6.6
TEXNZE	5.0	5.0	5.0	5.6	5.6	5.4	7.4	7.4	7.2
VLIELHVN	3.8	8.2	8.3	5.0	4.9	4.8	6.3	9.6	9.6
VLISSGN	**6.3**	**5.2**	**5.2**	**5.6**	**5.4**	**5.1**	**8.4**	**7.6**	**7.3**
WESTKPLE	6.3	5.3	5.3	5.1	5.0	4.7	8.1	7.3	7.1
WESTTSLG	4.8	5.4	5.6	5.0	5.3	5.4	7.0	7.5	7.7
WIERMGDN	4.8	4.5	4.4	5.5	5.4	5.1	7.2	6.9	6.7
F16	3.0	2.9	3.1	4.1	4.1	4.0	5.0	5.0	5.1
F3PFM	3.6	3.6	3.5	4.5	4.7	4.4	5.5	5.6	5.4
K13APFM	4.3	3.4	3.5	4.4	4.3	4.1	6.1	5.5	5.4
NORTHCMRT	5.0	4.1	4.3	4.4	4.5	4.3	6.5	6.0	6.0
Q1	4.2	3.9	4.0	4.6	4.5	4.4	6.3	6.0	5.9
Average (total)	**8.9**	**8.2**	**8.2**	**6.2**	**6.2**	**6.0**	**11.2**	**10.8**	**10.7**

A.2 Dutch coastal waters

A.2.1 High waters

A.2.1.1. DCSMv6

Appendix table A.2 Overview of the DCSMv6 model skill to represent skew surge heights (high waters), for three different event classes, in terms of bias (cm) and the RMSE (cm) for Dutch coastal stations.

	Tidal high water		Skew surge error (high water)						
	all		<99.0% skew surges		99.0% - 99.8% skew surges		>99.8% skew surges		
Total	**bias (cm)**	**RMSE (cm)**	**bias (cm)**	**RMSE (cm)**	**bias (cm)**	**RMSE (cm)**	**Bias (cm)**	**Std (cm)**	**RMSE (cm)**
Wandelaar	2.5	3.8	-0.9	5.4	0.8	8.0	-2.8	8.5	8.9
Zeebrugge_Leopold.	3.8	4.8	-2.2	6.4	1.6	10.7	-3.8	11.6	12.2
Bol_Van_Heist	2.7	3.7	-1.6	5.6	0.4	7.9	-2.3	9.8	10.0
Scheur_Wielingen_.	1.9	3.5	-0.5	5.5	1.0	9.8	-3.9	10.8	11.5
CADZD	1.2	3.1	0.0	5.6	2.6	8.4	1.5	9.3	9.4
WESTKPLE	-2.2	4.0	0.4	5.3	3.6	7.8	-1.4	8.5	8.6
EURPFM	3.2	3.9	0.3	4.9	0.9	6.7	-2.7	11.5	11.8
VLISSGN	**-0.1**	**3.7**	**-0.1**	**5.6**	**5.0**	**10.0**	**1.6**	**9.9**	**10.1**
ROOMPBTN	**1.3**	**2.8**	**-0.4**	**5.1**	**-1.7**	**9.3**	**-10.0**	**12.4**	**15.9**
LICHTELGRE	-0.7	3.1	-0.1	5.1	-0.3	7.1	-4.3	10.9	11.7
BROUWHVSGT08	-1.4	3.9	-0.1	6.2	-5.3	13.3	-15.0	17.0	22.6
TERNZN	-2.8	7.4	0.0	6.3	9.1	14.4	6.1	8.9	10.8
HARVT10	0.6	2.8	-0.8	5.7	-0.1	10.3	-6.9	8.1	10.6
HANSWT	18.4	19.3	1.5	8.0	15.2	18.5	6.2	10.8	12.5
ROOMPBNN	1.9	3.4	-1.6	5.5	1.0	10.4	-0.3	7.2	7.2
HOEKVHLD	1.2	3.9	-2.4	6.1	-1.4	12.7	-9.6	8.3	12.6
STAVNSE	-10.1	10.6	-0.3	6.0	8.5	12.4	0.7	8.1	8.1
BERGSDSWT	12.3	13.0	3.1	6.7	10.1	13.4	1.8	12.7	12.9
KRAMMSZWT									
SCHEVNGN	2.4	4.1	-1.2	5.9	-3.2	11.1	-12.6	13.9	18.8
IJMDBTHVN	5.9	6.6	-1.5	6.1	-3.2	14.2	-17.7	10.1	20.4
Q1	2.6	4.6	-0.9	5.3	-0.9	11.3	-12.3	13.2	18.1
DENHDR	2.1	3.4	-0.3	4.7	-2.2	8.8	-14.1	16.4	21.6
TEXNZE	1.8	4.2	-1.2	5.5	-4.2	13.7	-12.3	13.3	18.1
K13APFM	-0.4	3.1	-0.1	4.4	1.7	7.2	-9.3	8.7	12.8
F16	-0.2	2.4	-0.4	4.2	-0.4	6.1	-12.4	3.5	12.9
OUDSD	2.4	3.5	-0.1	4.8	1.3	8.0	-12.0	15.7	19.8
DENOVBTN	3.3	4.4	-0.4	5.3	-4.1	10.6	-17.8	20.8	27.4
TERSLNZE	2.3	3.9	-0.8	5.5	-0.9	12.4	-11.7	11.8	16.6

Total	Tidal high water		Skew surge error (high water)						
	all		<99.0% skew surges		99.0% - 99.8% skew surges		>99.8% skew surges		
	bias (cm)	RMSE (cm)	bias (cm)	RMSE (cm)	bias (cm)	RMSE (cm)	Bias (cm)	Std (cm)	RMSE (cm)
VLIELHVN	3.1	4.3	0.1	5.0	1.2	10.1	-17.7	10.1	20.4
WESTTSLG	5.1	5.9	0.6	5.3	-2.0	11.4	-22.4	10.0	24.6
KORNWDZBTN	3.9	5.3	-0.3	5.5	-0.2	11.1	-17.9	20.8	27.5
WIERMGDN	1.9	3.7	-0.6	5.5	7.4	12.4	-11.6	7.0	13.6
HUIBGT	2.2	4.5	-0.6	5.9	10.4	14.3	-4.8	10.8	11.9
HARLGN	**4.0**	**5.6**	**0.0**	**5.8**	**-1.2**	**12.4**	**-15.0**	**20.8**	**25.7**
NES	5.2	6.6	0.2	5.9	-4.9	13.9	-25.2	13.9	28.8
LAUWOG	2.5	5.4	0.3	6.3	-6.8	14.4	-39.4	18.2	43.4
SCHIERMNOG	4.0	5.5	0.5	6.2	-3.1	13.5	-34.0	16.5	37.8
BORKUM_Sudstran.									
BorkumFischerbalje									
EMSHORN									
EEMSHVN	4.9	6.5	-0.4	7.2	10.9	17.0	-12.4	14.6	19.2
DUKEGAT									
DELFZL	**16.6**	**17.5**	**1.0**	**8.3**	**11.5**	**20.1**	**-22.9**	**22.0**	**31.7**
KNOCK									
Average (total)	**2.8**	**5.4**	**-0.3**	**5.7**	**1.5**	**11.4**	**-10.3**	**12.2**	**17.4**
Average (offshore)	**0.9**	**3.4**	**-0.2**	**4.8**	**0.2**	**7.7**	**-8.2**	**9.6**	**13.5**
Average (coast)	**1.8**	**3.9**	**-0.9**	**5.6**	**0.3**	**10.9**	**-8.2**	**11.0**	**14.3**
Average (SWD)	**3.3**	**9.6**	**0.4**	**6.4**	**8.1**	**13.2**	**2.7**	**9.6**	**10.2**
Average (WS)	**5.0**	**6.4**	**0.1**	**6.0**	**0.2**	**12.9**	**-21.5**	**16.7**	**27.8**

A.2.1.2. DCSMv6-ZUNOv4

Appendix table A.3 Overview of the DCSMv6-ZUNOv4 model skill to represent skew surge heights (high waters), for three different event classes, in terms of bias (cm) and the RMSE (cm) for Dutch coastal stations.

Total	Tidal high water		Skew surge error (high water)						
	all		<99.0% skew surges		99.0% - 99.8% skew surges		>99.8% skew surges		
	bias (cm)	RMSE (cm)	bias (cm)	RMSE (cm)	bias (cm)	RMSE (cm)	Bias (cm)	Std (cm)	RMSE (cm)
Wandelaar	1.6	3.3	-0.9	5.2	0.0	7.9	-5.3	9.0	10.4
Zeebrugge_Leopold.	1.8	3.6	-2.0	6.1	0.3	10.1	-6.8	11.9	13.7
Bol_Van_Heist	3.5	4.4	-1.6	5.5	-0.7	8.2	-4.3	10.2	11.1
Scheur_Wielingen_.	3.2	4.5	-0.6	5.4	0.0	9.5	-5.9	10.9	12.5
CADZD	0.6	3.7	-0.3	5.5	0.8	8.3	-1.0	9.1	9.2
WESTKPLE	1.0	3.5	-0.2	5.1	1.4	7.6	-3.8	9.2	10.0
EURPFM	1.7	2.8	0.3	4.7	0.7	6.1	-4.9	11.5	12.5

Total	Tidal high water		Skew surge error (high water)						
	all		<99.0% skew surges		99.0% - 99.8% skew surges		>99.8% skew surges		
	bias (cm)	RMSE (cm)	bias (cm)	RMSE (cm)	bias (cm)	RMSE (cm)	Bias (cm)	Std (cm)	RMSE (cm)
VLISSGN	**1.6**	**4.0**	**-0.3**	**5.3**	**1.5**	**8.7**	**-3.4**	**10.9**	**11.4**
ROOMPBTN	**3.3**	**4.0**	**0.3**	**5.1**	**-2.5**	**9.4**	**-10.8**	**13.7**	**17.4**
LICHTELGRE	1.9	3.3	0.0	4.9	-1.2	7.3	-7.6	11.0	13.4
BROUWHVSGT08	2.1	3.8	0.1	6.1	-6.9	14.3	-17.3	17.2	24.4
TERNZN	3.5	5.5	-0.2	5.6	0.2	10.0	-2.8	11.7	12.1
HARVT10	2.6	3.7	-0.1	5.6	-1.7	10.3	-9.6	8.0	12.5
HANSWT	6.2	7.8	0.8	5.7	1.5	10.3	-5.8	11.9	13.2
ROOMPBNN	-1.5	2.7	-0.4	4.8	0.8	9.4	-3.4	5.1	6.1
HOEKVHLD	**1.3**	**4.2**	**-1.2**	**5.6**	**-3.7**	**11.9**	**-10.7**	**9.0**	**13.9**
STAVNSE	1.1	2.8	0.1	5.3	5.5	10.6	-1.5	9.5	9.6
BERGSDSWT	0.9	3.3	0.2	5.5	6.6	11.4	-0.5	11.4	11.4
KRAMMSZWT	3.4	4.6	2.0	8.1	3.1	11.3	-3.5	7.9	8.7
SCHEVNGN	4.3	5.3	-1.0	5.8	-4.3	11.8	-14.5	14.1	20.2
IJMDBTHVN	8.3	8.9	-0.8	5.9	-4.6	15.0	-19.3	10.2	21.8
Q1	1.3	3.3	-0.8	4.8	-1.3	10.6	-11.8	12.6	17.3
DENHDR	**2.6**	**3.6**	**-0.5**	**4.6**	**-4.9**	**9.5**	**-17.0**	**15.4**	**22.9**
TEXNZE	2.7	5.0	-1.4	5.5	-4.6	14.3	-13.0	12.8	18.2
K13APFM	-1.3	3.3	-0.2	4.2	1.7	7.2	-9.6	8.5	12.8
F16	0.6	2.5	-0.3	4.4	0.7	6.5	-11.0	3.5	11.6
OUDSD	0.7	2.7	-0.2	4.5	-2.5	8.9	-17.8	15.8	23.8
DENOVBTN	2.6	3.8	-0.4	5.2	-4.6	10.1	-18.5	20.7	27.8
TERSLNZE	2.4	4.2	-0.8	5.5	-1.8	12.4	-13.1	11.5	17.5
VLIELHVN	2.6	3.9	-0.1	4.8	-2.5	11.2	-25.9	9.7	27.6
WESTTSLG	0.3	2.5	-0.1	4.7	-3.1	11.2	-27.0	8.2	28.2
KORNWDZBTN	2.4	3.8	-0.4	5.2	-3.9	11.7	-22.5	19.7	29.9
WIERMGDN	2.4	4.1	-0.5	5.3	5.2	11.4	-13.9	6.4	15.3
HUIBGT	2.8	4.7	-0.7	5.8	9.6	13.7	-4.2	10.1	10.9
HARLGN	**2.4**	**3.7**	**-0.3**	**5.4**	**-4.5**	**13.0**	**-19.2**	**18.9**	**26.9**
NES	5.6	6.7	-0.3	5.5	-10.5	16.8	-31.3	14.0	34.3
LAUWOG	3.5	5.8	-0.4	6.4	-2.6	12.9	-29.0	16.9	33.6
SCHIERMNOG	4.1	5.5	-0.5	6.5	-0.9	13.5	-28.0	14.8	31.7
BORKUM_Sudstran.	2.5	4.5	-0.2	5.8	1.7	10.4	-22.6	13.2	26.2
BorkumFischerbalje	4.6	5.7	0.1	5.8	4.6	11.1	-18.8	12.7	22.7
EMSHORN	5.9	7.0	-0.1	6.2	1.9	11.7	-26.2	14.2	29.8
EEMSHVN	5.9	7.1	-0.2	6.4	2.0	11.5	-23.8	14.2	27.7
DUKEGAT	7.9	9.2	-0.5	7.1	2.6	15.7	-40.3	17.5	44.0

Total	Tidal high water		Skew surge error (high water)						
	all		<99.0% skew surges		99.0% - 99.8% skew surges		>99.8% skew surges		
	bias (cm)	RMSE (cm)	bias (cm)	RMSE (cm)	bias (cm)	RMSE (cm)	Bias (cm)	Std (cm)	RMSE (cm)
DELFZL	**5.4**	**7.0**	**1.3**	**7.1**	**2.9**	**13.4**	**-35.4**	**20.8**	**41.1**
KNOCK	6.3	7.7	0.6	7.0	5.3	14.6	-27.3	20.2	34.0
Average (total)	**2.5**	**4.3**	**-0.4**	**5.4**	**-0.8**	**10.7**	**-13.1**	**12.1**	**18.6**
Average (offshore)	**0.8**	**3.0**	**-0.2**	**4.6**	**0.1**	**7.5**	**-9.0**	**9.4**	**13.5**
Average (coast)	**2.7**	**4.4**	**-0.7**	**5.5**	**-1.1**	**10.9**	**-10.0**	**11.1**	**15.4**
Average (SWD)	**2.0**	**4.4**	**0.0**	**5.4**	**2.7**	**10.1**	**-2.9**	**10.1**	**10.6**
Average (WS)	**3.2**	**4.8**	**-0.1**	**5.6**	**-2.8**	**12.2**	**-25.3**	**15.8**	**30.2**

A.2.1.3. DSCM-FM 0.5nm release 2019

Appendix table A.4 Overview of the DSCM-FM 0.5nm release 2019 model skill to represent skew surge heights (high waters), for three different event classes, in terms of bias (cm) and the RMSE (cm) for Dutch coastal stations.

Total	Tidal high water		Skew surge error (high water)						
	all		<99.0% skew surges		99.0% - 99.8% skew surges		>99.8% skew surges		
	bias (cm)	RMSE (cm)	bias (cm)	RMSE (cm)	bias (cm)	RMSE (cm)	Bias (cm)	Std (cm)	RMSE (cm)
Wandelaar	-1.8	3.3	-0.2	5.2	0.7	8.1	-2.9	8.9	9.4
Zeebrugge_Leopold.	-0.7	3.0	-1.5	6.0	0.9	10.2	-5.1	11.5	12.6
Bol_Van_Heist	-0.5	2.7	-1.0	5.3	0.3	7.5	-2.6	9.2	9.6
Scheur_Wielingen_.	-2.6	3.8	-0.2	5.3	0.1	9.3	-3.7	10.4	11.1
CADZD	-5.6	6.5	0.0	5.5	1.5	8.2	0.4	7.9	7.9
WESTKPLE	-7.0	7.9	0.5	5.1	3.0	7.2	-2.0	7.7	8.0
EURPFM	-2.9	4.0	0.1	4.7	0.4	7.1	-2.4	8.8	9.2
VLISSGN	**-4.6**	**6.0**	**0.1**	**5.6**	**2.7**	**8.5**	**-0.4**	**10.1**	**10.1**
ROOMPBTN	**-1.7**	**3.3**	**-0.5**	**5.0**	**-0.6**	**9.7**	**-8.2**	**8.9**	**12.1**
LICHTELGRE	-6.8	7.7	-0.5	4.9	0.0	7.8	-3.7	8.8	9.6
BROUWHVSGT08	-9.6	10.6	-1.4	6.2	-5.3	13.8	-15.4	14.6	21.2
TERNZN	0.4	4.7	1.0	6.0	1.9	10.1	3.6	10.4	11.0
HARVT10	-4.8	5.8	-0.9	5.6	-0.7	10.7	-6.3	6.5	9.0
HANSWT	1.8	5.9	0.0	6.7	9.8	14.4	8.7	8.3	12.1
ROOMPBNN	0.9	2.6	-0.8	5.2	5.2	10.0	1.2	5.9	6.0
HOEKVHLD	**-0.2**	**3.9**	**-3.9**	**7.1**	**-2.6**	**13.2**	**-9.7**	**7.4**	**12.2**
STAVNSE	6.3	6.9	0.1	5.8	8.1	12.3	0.6	8.4	8.4
BERGSDSWT	11.6	12.3	0.9	6.0	12.6	15.6	2.6	9.5	9.9
KRAMMSZWT	9.8	10.8	-0.9	7.5	2.8	11.8	1.4	11.7	11.8
SCHEVNGN	-1.5	3.9	-1.6	6.2	-3.8	10.5	-12.1	12.8	17.6

Total	Tidal high water		Skew surge error (high water)						
	all		<99.0% skew surges		99.0% - 99.8% skew surges		>99.8% skew surges		
	bias (cm)	RMSE (cm)	bias (cm)	RMSE (cm)	bias (cm)	RMSE (cm)	Bias (cm)	Std (cm)	RMSE (cm)
IJMDBTHVN	1.4	4.1	-1.5	6.1	-4.6	12.9	-16.7	8.5	18.8
Q1	0.9	3.7	-0.6	5.1	-1.8	10.1	-12.7	15.5	20.1
DENHDR	**0.6**	**3.3**	**-0.7**	**4.8**	**-5.7**	**9.0**	**-18.4**	**17.8**	**25.6**
TEXNZE	2.6	4.7	-1.2	5.4	-5.9	13.9	-12.7	13.5	18.5
K13APFM	-1.1	3.6	-0.1	4.3	0.3	6.6	-7.9	10.6	13.2
F16	0.5	2.7	-0.4	4.2	-0.6	5.3	-11.8	5.2	12.9
OUDSD	0.8	3.0	-0.3	4.5	-2.6	7.2	-17.7	17.7	25.0
DENOVBTN	3.4	4.5	-0.8	5.2	-5.3	9.6	-20.8	22.5	30.6
TERSLNZE	0.2	3.0	-1.0	5.5	-5.1	11.9	-15.9	12.5	20.2
VLIELHVN	0.8	2.9	-0.2	4.6	-3.4	9.0	-24.0	9.0	25.6
WESTTSLG	-1.4	3.1	-0.3	4.7	-2.2	9.0	-24.1	7.6	25.3
KORNWDZBTN	2.1	3.9	-0.5	5.3	-4.0	10.3	-22.9	21.1	31.2
WIERMGDN	-1.5	3.5	-0.4	5.3	4.2	10.2	-12.7	5.5	13.8
HUIBGT	-2.3	4.4	-0.7	5.7	8.0	11.9	-4.1	7.7	8.7
HARLGN	**0.3**	**3.6**	**0.1**	**5.7**	**-3.2**	**11.4**	**-18.1**	**18.4**	**25.8**
NES	-2.9	4.6	0.5	5.7	-7.1	13.6	-26.8	13.9	30.2
LAUWOG	-2.6	5.1	0.6	6.5	-5.5	13.0	-30.8	14.8	34.1
SCHIERMNOG	-4.4	5.9	0.8	6.5	-4.5	12.7	-28.8	13.1	31.6
BORKUM_Sudstran.	-2.9	4.8	-0.2	5.6	-0.3	9.5	-24.6	11.7	27.2
BorkumFischerbalje	-0.4	3.4	-0.1	5.6	3.3	9.8	-18.8	11.1	21.8
EMSHORN	0.2	3.8	0.0	5.7	-3.2	11.7	-29.0	13.8	32.1
EEMSHVN	0.3	4.0	-0.3	5.9	-3.2	11.7	-27.1	13.1	30.1
DUKEGAT	1.5	4.9	-0.3	6.4	-2.6	16.4	-42.7	15.8	45.6
DELFZL	**-0.9**	**4.6**	**-0.6**	**6.7**	**0.6**	**13.5**	**-36.5**	**17.5**	**40.4**
KNOCK	-0.7	4.4	0.3	6.7	3.1	13.6	-29.3	17.2	34.0
Average (total)	**-0.8**	**4.7**	**-0.4**	**5.5**	**-0.5**	**10.4**	**-11.5**	**11.3**	**17.7**
Average (offshore)	**-1.9**	**4.3**	**-0.3**	**4.6**	**-0.4**	**7.4**	**-7.7**	**9.8**	**13.0**
Average (coast)	**-2.1**	**4.6**	**-1.0**	**5.6**	**-0.9**	**10.5**	**-8.7**	**10.1**	**13.9**
Average (SWD)	**2.7**	**6.4**	**0.2**	**5.9**	**6.7**	**11.8**	**2.7**	**8.8**	**9.6**
Average (WS)	**-0.4**	**4.1**	**-0.1**	**5.6**	**-3.7**	**11.0**	**-25.2**	**15.3**	**30.0**

A.2.2 Low waters

A.2.2.1. DCSMv6

Appendix table A.5 Overview of the DCSMv6 model skill to represent skew surge heights (low waters), for three different event classes, in terms of bias (cm) and the RMSE (cm) for Dutch coastal stations.

	Tidal low		Skew surge error (high water)						
	all		<99.0% skew surges		99.0% - 99.8% skew surges		>99.8% skew surges		
Total	**bias (cm)**	**RMSE (cm)**	**bias (cm)**	**RMSE (cm)**	**bias (cm)**	**RMSE (cm)**	**Bias (cm)**	**Std (cm)**	**RMSE (cm)**
Wandelaar	-4.6	6.4	0.3	5.4	-2.4	11.4	-6.6	7.1	9.7
Zeebrugge_Leopold.	-2.4	4.9	0.4	6.2	0.3	11.9	-8.7	12.4	15.1
Bol_Van_Heist	-2.4	4.9	0.1	5.4	-0.7	11.4	-11.7	13.5	17.9
Scheur_Wielingen_.	-1.7	4.5	-0.3	5.6	0.7	12.3	-16.0	11.3	19.6
CADZD	-2.4	4.8	-0.3	6.0	2.1	11.6	-9.1	13.7	16.5
WESTKPLE	1.9	4.6	0.0	5.2	0.8	9.7	-12.3	11.0	16.5
EURPFM	-3.7	5.5	0.8	5.0	4.4	8.9	-3.3	8.3	9.0
VLISSGN	**0.8**	**4.6**	**0.2**	**5.5**	**0.1**	**10.3**	**-16.1**	**14.0**	**21.3**
ROOMPBTN	**-0.7**	**3.9**	**0.3**	**5.2**	**-2.3**	**12.2**	**-12.0**	**11.3**	**16.4**
LICHTELGRE	-2.1	4.4	0.3	4.9	0.3	8.2	-1.4	9.5	9.5
BROUWHVSGT08	-1.2	4.9	-0.7	6.2	-2.2	12.4	-7.7	8.1	11.2
TERNZN	4.7	6.7	0.3	5.8	-1.1	10.7	-22.1	16.0	27.2
HARVT10	-2.1	4.5	0.3	5.4	2.8	9.1	3.0	13.2	13.5
HANSWT	8.0	9.6	-0.8	5.7	-4.7	14.6	-24.8	16.1	29.6
ROOMPBNN	-4.9	6.0	0.4	5.0	1.3	10.1	-7.6	5.8	9.6
HOEKVHLD	**-2.5**	**4.8**	**0.5**	**5.8**	**3.7**	**10.0**	**3.7**	**11.4**	**12.0**
STAVNSE	2.6	4.4	0.1	5.4	-3.1	10.9	-7.2	10.8	12.9
BERGSDSWT	-2.3	4.5	0.2	5.4	0.2	13.5	-2.9	11.8	12.1
KRAMMSZWT									
SCHEVNGN	-1.8	4.5	0.8	5.5	3.6	9.6	4.8	7.9	9.3
IJMDBTHVN	-1.6	4.7	1.5	5.9	2.2	9.6	-1.9	11.1	11.3
Q1	-3.5	4.6	0.4	4.4	2.9	7.4	-4.2	10.3	11.1
DENHDR	**-4.2**	**5.5**	**0.5**	**5.0**	**-2.4**	**8.4**	**-11.8**	**12.1**	**16.9**
TEXNZE	-3.0	4.6	1.3	5.4	4.8	8.6	-8.6	9.7	12.9
K13APFM	-1.2	3.0	0.2	4.2	0.9	5.9	-6.0	10.7	12.3
F16	-1.0	2.9	0.4	4.2	1.4	6.6	-2.8	5.9	6.5
OUDSD	-2.7	4.4	0.3	4.8	-3.7	8.2	-13.5	11.2	17.5
DENOVBTN	-1.5	4.9	-0.7	8.6	0.6	9.7	-9.7	17.2	19.7
TERSLNZE	-1.7	4.1	0.6	5.8	7.6	11.9	-2.4	10.8	11.0
VLIELHVN	-7.4	8.3	0.4	5.2	-5.6	11.5	-19.6	12.2	23.1
WESTTSLG	-0.4	4.2	0.2	6.0	-10.9	16.3	-26.0	16.0	30.5
KORNWDZBTN	1.2	3.4	-0.3	6.8	1.5	11.4	-10.9	17.3	20.4
WIERMGDN	0.2	4.5	0.4	5.8	5.5	11.4	5.4	14.2	15.2

Total	Tidal low		Skew surge error (high water)						
	all		<99.0% skew surges		99.0% - 99.8% skew surges		>99.8% skew surges		
	bias (cm)	RMSE (cm)	bias (cm)	RMSE (cm)	bias (cm)	RMSE (cm)	Bias (cm)	Std (cm)	RMSE (cm)
HUIBGT	0.8	5.0	0.0	6.1	5.7	11.0	5.7	10.9	12.3
HARLGN	**13.4**	**14.3**	**-0.2**	**9.0**	**-11.4**	**17.0**	**-27.3**	**20.0**	**33.8**
NES	6.9	10.7	-1.1	8.5	-20.7	25.0	-30.5	21.9	37.6
LAUWOG	10.0	11.9	0.1	6.8	-18.8	23.1	-27.3	21.7	34.9
SCHIERMNOG	9.1	10.7	-0.6	6.8	-17.3	21.7	-21.9	18.3	28.5
BORKUM_Sudstran.									
BorkumFischerbalje									
EMSHORN									
EEMSHVN	0.2	6.1	0.8	7.4	-7.8	14.8	-6.9	13.8	15.5
DUKEGAT									
DELFZL	**13.3**	**16.0**	**1.7**	**9.5**	**-19.0**	**25.6**	**-17.9**	**15.6**	**23.7**
KNOCK									
Average (total)	**0.3**	**6.0**	**0.2**	**5.9**	**-2.1**	**12.2**	**-10.1**	**12.7**	**17.5**
Average (offshore)	**-2.3**	**4.1**	**0.4**	**4.5**	**2.0**	**7.4**	**-3.5**	**8.9**	**9.7**
Average (coast)	**-1.7**	**4.8**	**0.3**	**5.6**	**1.7**	**10.7**	**-5.1**	**11.2**	**14.0**
Average (SWD)	**1.5**	**6.0**	**0.1**	**5.5**	**-1.2**	**11.7**	**-13.4**	**12.4**	**18.8**
Average (WS)	**3.8**	**8.6**	**0.1**	**7.2**	**-10.3**	**16.8**	**-19.2**	**16.8**	**25.9**

A.2.2.2. DCSMv6-ZUNOv4

Appendix table A.6 Overview of the DCSMv6-ZUNOv4 model skill to represent skew surge heights (low waters), for three different event classes, in terms of bias (cm) and the RMSE (cm) for Dutch coastal stations.

Total	Tidal low water		Skew surge error (low water)						
	all		<99.0% skew surges		99.0% - 99.8% skew surges		>99.8% skew surges		
	bias (cm)	RMSE (cm)	bias (cm)	RMSE (cm)	bias (cm)	RMSE (cm)	Bias (cm)	Std (cm)	RMSE (cm)
Wandelaar	-2.7	5.3	0.2	5.3	-3.5	11.8	-7.0	6.5	9.6
Zeebrugge_Leopold.	-2.0	4.8	0.3	5.9	-1.2	11.9	-10.1	12.0	15.7
Bol_Van_Heist	-2.7	5.1	0.0	5.3	-1.7	11.9	-12.2	13.0	17.8
Scheur_Wielingen_.	-3.5	5.4	-0.2	5.5	-0.1	12.6	-15.6	10.8	19.0
CADZD	-3.6	5.4	-0.2	5.9	0.8	11.3	-9.7	13.9	16.9
WESTKPLE	-1.7	4.5	0.1	5.2	1.4	9.9	-11.9	10.9	16.1
EURPFM	-0.9	4.4	0.7	4.9	4.0	8.7	-4.6	7.6	8.9
VLISSGN	**-3.8**	**5.8**	**-0.2**	**5.5**	**-0.1**	**10.3**	**-15.4**	**14.5**	**21.1**
ROOMPBTN	**-3.5**	**5.2**	**0.2**	**5.2**	**-1.1**	**11.7**	**-10.3**	**10.9**	**15.0**
LICHTELGRE	-1.2	4.5	0.3	4.8	-0.7	7.6	-3.7	9.6	10.2
BROUWHVSGT08	-1.5	5.3	-0.3	6.0	-2.2	12.0	-8.4	8.4	11.8
TERNZN	-4.9	6.6	-0.2	5.8	-0.2	10.7	-17.9	16.5	24.4

Total	Tidal low water		Skew surge error (low water)						
	all		<99.0% skew surges		99.0% - 99.8% skew surges		>99.8% skew surges		
	bias (cm)	RMSE (cm)	bias (cm)	RMSE (cm)	bias (cm)	RMSE (cm)	Bias (cm)	Std (cm)	RMSE (cm)
HARVT10	-1.7	4.7	0.4	5.4	2.3	8.7	0.8	12.9	12.9
HANSWT	-4.6	6.4	-0.2	5.5	-2.0	13.2	-15.1	17.6	23.2
ROOMPBNN	-2.8	4.4	0.1	4.9	1.4	9.9	-6.7	5.8	8.9
HOEKVHLD	**-4.4**	**6.2**	**1.4**	**6.0**	**4.4**	**9.4**	**3.3**	**11.8**	**12.2**
STAVNSE	-2.2	4.3	0.2	5.2	0.7	10.6	-2.5	11.7	12.0
BERGSDSWT	-4.8	6.1	-0.1	5.3	2.4	13.8	-0.2	12.1	12.1
KRAMMSZWT	-2.3	4.6	0.6	5.6	2.2	11.4	-11.5	13.3	17.5
SCHEVNGN	-4.2	5.8	1.0	5.6	5.0	10.0	6.0	8.1	10.1
IJMDBTHVN	-3.7	5.6	1.4	5.8	3.0	9.7	-1.9	10.7	10.8
Q1	-2.3	3.9	0.4	4.4	2.2	7.2	-4.8	10.4	11.4
DENHDR	**-4.4**	**5.5**	**0.7**	**4.9**	**-1.4**	**8.9**	**-10.8**	**12.7**	**16.7**
TEXNZE	-2.4	4.2	1.6	5.5	4.4	8.3	-8.9	9.9	13.4
K13APFM	-0.6	2.8	0.2	4.1	1.4	5.6	-5.2	10.0	11.3
F16	-1.8	3.2	0.4	4.3	2.4	6.7	-1.2	5.3	5.4
OUDSD	-4.4	5.5	0.4	4.7	-1.5	7.7	-10.6	11.9	15.9
DENOVBTN	-7.5	9.0	-0.4	9.2	5.6	11.4	-1.6	15.5	15.5
TERSLNZE	-3.0	5.0	0.6	5.7	7.5	12.1	-3.4	10.0	10.6
VLIELHVN	-5.8	6.9	0.3	5.0	-4.2	12.1	-21.5	12.9	25.0
WESTTSLG	-1.6	4.0	0.3	5.3	-6.7	13.8	-21.5	15.6	26.6
KORNWDZBTN	-3.0	4.3	-0.6	6.5	4.4	11.6	-7.5	15.9	17.5
WIERMGDN	-2.3	4.7	0.3	5.9	7.4	11.9	5.4	14.2	15.2
HUIBGT	-1.7	4.8	0.4	6.2	7.8	12.3	8.3	10.9	13.7
HARLGN	**0.9**	**2.8**	**-0.5**	**6.0**	**-1.6**	**11.1**	**-18.0**	**16.4**	**24.4**
NES	-2.8	5.3	0.1	6.1	-11.0	15.3	-23.2	16.7	28.5
LAUWOG	-5.8	7.9	0.0	6.5	-5.1	13.9	-7.4	22.2	23.4
SCHIERMNOG	-2.1	5.4	0.1	6.3	-7.3	14.7	-9.3	20.1	22.1
BORKUM_Sudstran.	0.5	5.2	0.4	6.2	-6.3	13.4	-7.5	12.5	14.6
BorkumFischerbalje	-3.7	5.9	-0.2	6.2	-3.0	11.7	-8.3	11.4	14.1
EMSHORN	-2.1	5.2	0.5	6.7	-7.0	13.2	-13.0	12.1	17.7
EEMSHVN	-6.2	8.0	1.0	6.9	-2.7	12.4	-6.9	10.1	12.2
DUKEGAT	-7.3	8.8	1.1	7.7	-0.7	11.9	-2.2	10.3	10.6
DELFZL	**-5.7**	**7.8**	**1.3**	**8.5**	**-3.4**	**14.5**	**-4.6**	**8.0**	**9.2**
KNOCK	-6.2	8.2	0.2	8.1	-4.5	14.7	-5.4	10.4	11.7
Average (total)	**-3.2**	**5.3**	**0.3**	**5.7**	**0.3**	**11.0**	**-7.6**	**12.1**	**15.6**
Average (offshore)	**-1.4**	**3.8**	**0.4**	**4.5**	**1.8**	**7.2**	**-3.9**	**8.6**	**9.5**
Average (coast)	**-2.9**	**5.1**	**0.5**	**5.6**	**1.9**	**10.8**	**-5.1**	**11.0**	**14.0**

	Tidal low water		Skew surge error (low water)						
	all		<99.0% skew surges		99.0% - 99.8% skew surges		>99.8% skew surges		
Total	**bias (cm)**	**RMSE (cm)**	**bias (cm)**	**RMSE (cm)**	**bias (cm)**	**RMSE (cm)**	**Bias (cm)**	**Std (cm)**	**RMSE (cm)**
Average (SWD)	**-3.8**	**5.6**	**-0.1**	**5.4**	**0.4**	**11.4**	**-9.6**	**13.0**	**16.9**
Average (WS)	**-4.0**	**6.1**	**0.2**	**6.5**	**-3.1**	**12.6**	**-12.0**	**15.0**	**20.0**

A.2.2.3. DSCM-FM 0.5nm release 2019

Appendix table A.7 Overview of the DCSMv6-ZUNOv4 model skill to represent skew surge heights (low waters), for three different event classes, in terms of bias (cm) and the RMSE (cm) for Dutch coastal stations.

	Tidal low water		Skew surge error (low water)						
	all		<99.0% skew surges		99.0% - 99.8% skew surges		>99.8% skew surges		
Total	**bias (cm)**	**RMSE (cm)**	**bias (cm)**	**RMSE (cm)**	**bias (cm)**	**RMSE (cm)**	**Bias (cm)**	**Std (cm)**	**RMSE (cm)**
Wandelaar	0.6	4.7	0.3	5.2	-2.5	10.9	-4.7	7.2	8.6
Zeebrugge_Leopold.	0.1	4.4	0.5	5.8	0.5	11.6	-7.6	11.5	13.8
Bol_Van_Heist	-0.4	4.4	0.1	5.1	-0.6	10.5	-9.8	12.9	16.2
Scheur_Wielingen_.	0.1	4.3	-0.3	5.3	-0.5	11.4	-14.3	10.6	17.8
CADZD	0.1	4.3	-0.5	5.6	0.8	10.1	-8.1	14.7	16.8
WESTKPLE	2.9	5.0	0.0	5.0	1.2	9.0	-9.3	12.3	15.4
EURPFM	-1.4	4.3	0.7	4.9	3.7	8.5	-2.0	7.8	8.1
VLISSGN	**-1.3**	**4.3**	**-0.3**	**5.3**	**-1.1**	**9.0**	**-14.4**	**14.7**	**20.6**
ROOMPBTN	**0.2**	**3.3**	**0.2**	**4.9**	**-0.5**	**11.1**	**-9.0**	**11.7**	**14.8**
LICHTELGRE	1.2	4.1	0.2	4.8	1.9	8.3	0.8	11.1	11.2
BROUWHVSGT08	7.2	9.2	-0.6	6.0	-3.2	10.8	-9.7	7.2	12.1
TERNZN	-4.2	6.1	0.0	5.5	-2.7	9.8	-19.6	16.0	25.3
HARVT10	1.6	4.5	0.3	5.3	5.0	9.5	3.0	13.3	13.7
HANSWT	-2.0	5.3	-0.6	5.4	-7.6	14.9	-20.2	17.4	26.7
ROOMPBNN	1.8	3.8	-0.4	4.7	-2.9	10.3	-19.6	19.3	27.5
HOEKVHLD	**0.2**	**3.8**	**1.0**	**5.7**	**5.5**	**10.1**	**6.3**	**10.1**	**11.9**
STAVNSE	0.5	3.9	0.5	5.0	-5.2	11.7	-14.7	14.3	20.5
BERGSDSWT	2.4	5.8	1.3	5.3	-6.9	15.6	-16.9	15.8	23.2
KRAMMSZWT	-2.1	4.7	1.1	5.4	-2.7	10.8	-16.0	15.0	22.0
SCHEVNGN	2.9	4.9	0.9	5.4	4.3	8.9	3.4	6.6	7.4
IJMDBTHVN	1.7	5.1	1.6	6.1	3.6	8.4	-4.2	11.0	11.8
Q1	-1.2	3.4	0.4	4.3	1.9	6.4	-3.9	9.6	10.3
DENHDR	**-1.1**	**3.6**	**0.5**	**4.9**	**-1.8**	**8.5**	**-11.1**	**11.3**	**15.9**
TEXNZE	-2.3	4.0	1.2	5.3	4.6	8.2	-8.4	9.0	12.2
K13APFM	0.7	2.7	0.4	4.1	1.4	5.6	-2.8	10.2	10.6
F16	-1.1	2.9	0.4	4.1	2.1	6.6	-1.5	4.8	5.0

Total	Tidal low water		Skew surge error (low water)						
	all		<99.0% skew surges		99.0% - 99.8% skew surges		>99.8% skew surges		
	bias (cm)	RMSE (cm)	bias (cm)	RMSE (cm)	bias (cm)	RMSE (cm)	Bias (cm)	Std (cm)	RMSE (cm)
OUDSD	-0.7	3.3	0.1	4.5	-3.5	8.3	-11.2	12.0	16.4
DENOVBTN	-5.0	7.1	-0.5	8.8	3.7	10.5	-5.2	14.5	15.4
TERSLNZE	-0.4	3.2	0.7	5.5	5.7	11.3	-5.2	10.0	11.3
VLIELHVN	-2.3	4.2	1.0	5.0	-3.7	11.2	-20.3	10.8	23.0
WESTTSLG	-0.5	4.0	-0.1	5.6	-9.7	15.3	-25.6	16.5	30.4
KORNWDZBTN	-0.7	3.1	0.1	6.3	2.1	10.6	-9.5	16.4	18.9
WIERMGDN	0.1	3.8	0.2	5.6	5.4	11.3	1.5	12.4	12.5
HUIBGT	2.9	5.3	0.3	5.8	4.2	9.6	1.2	10.4	10.5
HARLGN	**10.7**	**11.6**	**-0.1**	**7.5**	**-10.6**	**14.7**	**-25.5**	**19.5**	**32.1**
NES	17.6	19.7	-0.7	8.3	-26.0	28.4	-41.3	19.2	45.5
LAUWOG	7.3	9.5	0.3	6.4	-17.1	21.0	-25.4	20.8	32.9
SCHIERMNOG	20.7	22.9	-1.5	10.0	-32.3	35.3	-38.0	20.4	43.2
BORKUM_Sudstran.	7.1	9.0	0.4	6.1	-10.0	15.0	-14.0	11.7	18.2
BorkumFischerbalje	3.2	6.0	0.1	6.0	-7.5	12.5	-12.4	11.3	16.8
EMSHORN	7.3	9.0	0.7	6.8	-13.9	17.2	-22.0	11.4	24.8
EEMSHVN	4.9	7.4	1.1	6.7	-10.0	14.8	-17.3	10.3	20.1
DUKEGAT	7.2	9.2	1.4	7.4	-10.9	15.3	-16.0	10.1	18.9
DELFZL	**16.0**	**17.5**	**1.5**	**8.0**	**-16.6**	**20.7**	**-25.3**	**11.6**	**27.8**
KNOCK	12.3	13.9	0.5	7.5	-16.8	20.8	-25.8	12.4	28.6
Average (total)	**2.1**	**6.0**	**0.3**	**5.7**	**-2.8**	**12.0**	**-11.4**	**12.7**	**18.4**
Average (offshore)	**-0.4**	**3.5**	**0.4**	**4.4**	**2.2**	**7.1**	**-1.9**	**8.7**	**9.0**
Average (coast)	**1.0**	**4.6**	**0.4**	**5.4**	**1.9**	**10.1**	**-5.1**	**10.7**	**13.1**
Average (SWD)	**-0.5**	**4.9**	**0.1**	**5.2**	**-4.4**	**11.9**	**-17.6**	**16.3**	**24.0**
Average (WS)	**6.2**	**10.0**	**0.1**	**7.0**	**-11.2**	**17.3**	**-22.2**	**15.6**	**27.8**

B Use of external data sources

The DCSM-FM 0.5nm model was developed with the use of external data sources. The following data sources were used in this model. The user of the model may not distribute the model or any of its associated data files to third parties. Furthermore, the user of the model must use the Attribution Texts from this table when reporting on the use of the model to third parties.

Organization	Related data	Mandatory Attribution text
ECMWF	IFS	The model has been generated using ECMWF information. ECMWF is responsible for any use that may be made of the ECMWF data it contains.
EMODnet-Bathymetry	EMODnet	Data/information used in the model was made available by the EMODnet Bathymetry project, www.emodnet-bathmetry.eu, funded by the European Commission Directorate general for Maritime Affairs and Fisheries.
AVISO+	FES2014	The model is generated using AVISO+ Products.
NOAA	World vector shoreline	The model contains Global Self-consistent Hierarchical High-resolution Geography, GSHHG is released under the GNU Lesser General Public License, and is developed and maintained by Dr. Paul Wessel, SOEST, University of Hawaii, and Dr. Walter H. F. Smith, NOAA Laboratory for Satellite Altimetry. For further contributions please read https://www.ngdc.noaa.gov/mgg/shorelines/data/gshhg/latest/readme.txt

Deltares is een onafhankelijk kennisinstituut voor toegepast onderzoek op het gebied van water en ondergrond. Wereldwijd werken we aan slimme oplossingen voor mens, milieu en maatschappij.

Deltares

www.deltares.nl